

THE IMPACT OF AGING AND OVARECTOMY ON CARDIAC CONTRACTILE
FUNCTION IN ISOLATED VENTRICULAR MYOCYTES

by

Elias Fares

Submitted in partial fulfillment of the requirements
for the degree of Doctor of Philosophy

at

Dalhousie University
Halifax, Nova Scotia
August 2012

© Copyright by Elias Fares, 2012

DALHOUSIE UNIVERSITY
DEPARTMENT OF PHARMACOLOGY

The undersigned hereby certify that they have read and recommend to the Faculty of Graduate Studies for acceptance a thesis entitled “THE IMPACT OF AGING AND OVARECTOMY ON CARDIAC CONTRACTILE FUNCTION IN ISOLATED VENTRICULAR MYOCYTES” by Elias Fares in partial fulfillment of the requirements for the degree of Doctor of Philosophy.

Dated: August 10, 2012

External Examiner: _____

Research Supervisor: _____

Examining Committee: _____

Departmental Representative: _____

DALHOUSIE UNIVERSITY

DATE: August 10, 2012

AUTHOR: Elias Fares

TITLE: THE IMPACT OF AGING AND OVARECTOMY ON CARDIAC
CONTRACTILE FUNCTION IN ISOLATED VENTRICULAR
MYOCYTES

DEPARTMENT OR SCHOOL: Department of Pharmacology

DEGREE: PhD CONVOCATION: October YEAR: 2012

Permission is herewith granted to Dalhousie University to circulate and to have copied for non-commercial purposes, at its discretion, the above title upon the request of individuals or institutions. I understand that my thesis will be electronically available to the public.

The author reserves other publication rights, and neither the thesis nor extensive extracts from it may be printed or otherwise reproduced without the author's written permission.

The author attests that permission has been obtained for the use of any copyrighted material appearing in the thesis (other than the brief excerpts requiring only proper acknowledgement in scholarly writing), and that all such use is clearly acknowledged.

Signature of Author

TABLE OF CONTENTS

LIST OF TABLES	viii
LIST OF FIGURES	ix
ABSTRACT	xii
LIST OF ABBREVIATIONS AND SYMBOLS USED	xiii
ACKNOWLEDGMENTS	xv
CHAPTER 1 INTRODUCTION	1
1.1 Broad Overview	1
1.2 EC-coupling pathway	3
1.2.1 Cardiac EC-coupling	3
1.2.2 Modulation of the EC-coupling pathway by β -adrenergic signaling	8
1.2.3 Dysfunction of the EC-coupling pathway leads to triggered activity	10
1.3 Age-related changes in cardiac function	13
1.3.1 Structural changes in the aging heart	13
1.3.2 Impact of age on cardiac contractility	13
1.3.3 Contractile function in ventricular myocytes from aged animals	14
1.3.4 The EC-coupling pathway in the aging heart	15
1.4 Sex differences in cardiac function	24
1.4.1 Sex differences in the structure and function of the intact heart	24
1.4.2 Sex differences in cardiomyocyte function	26
1.4.3 Age-related differences in cardiac structure and function in males and females.....	29
1.5 Estrogen and the heart.....	32
1.5.1 Clinical studies of hormone replacement therapy.....	32
1.5.2 Sex steroid hormones and the cardiovascular system	38
1.5.3 Estrogen and the heart	41

1.6 Hypotheses.....	46
CHAPTER 2 MATERIALS AND METHODS	47
2.1 Materials	47
2.1.1 Animals	47
2.1.2 Chemicals	47
2.2 Methods	48
2.2.1 Survival curve	48
2.2.2 Ventricular myocyte isolation	48
2.2.3 Experimental apparatus	50
2.2.4 Field stimulation experiments	52
2.2.5 Current and voltage clamp experiments	55
2.2.6 Simultaneous measurement of intracellular Ca ²⁺ and cellular shortening	61
2.2.7 Measurement of spontaneous Ca ²⁺ sparks	65
2.2.8 <i>In vitro</i> myofilament Ca ²⁺ sensitivity assessment	66
2.2.9 Measurement of <i>in vivo</i> ventricular function through echocardiography	68
2.2.10 Data analysis and statistics.....	69
CHAPTER 3 RESULTS	70
3.1 The effects of extreme aging on cardiac contractile function in male and female mice.....	70
3.1.1 Survival in C57BL/6 mice	70
3.1.2 Phenotypic characteristics of young adult and senescent mice	70
3.1.3 Cardiac contractile function in young adult and senescent male and female mice.....	71
3.1.4 Changes in intracellular Ca ²⁺ stores in young adult and senescent male and female mice	73
3.1.5 Summary of Section 3.1	74
3.2 The effect of ovariectomy on cardiac contractile function in female mice	86
3.2.1 Physical characteristics of young adult sham and OVX mice.....	86

3.2.2 Field stimulation analysis of Ca ²⁺ transients in young adult sham and OVX mice	86
3.2.3. Voltage clamp assessment of Ca ²⁺ homeostasis in young adult sham and OVX mice	87
3.2.4 Investigation of SR Ca ²⁺ stores in young adult sham and OVX mice	89
3.2.5 Analysis of Ca ²⁺ spark parameters in young adult sham and OVX mice	90
3.2.6 Spontaneous Ca ²⁺ transients in young adult sham and OVX mice	91
3.2.7 Summary of Section 3.2	91
3.3 The impact of OVX and aging on cardiac contractile function in female mice	105
3.3.1 Physical characteristics of aged sham and OVX mice.....	105
3.3.2 Cardiac contractile function and Ca ²⁺ handling in field stimulated myocytes from aged sham and OVX mice.....	105
3.3.3 <i>In vivo</i> ventricular function in aged sham and OVX mice.....	106
3.3.4 Action potential properties in aged sham and OVX mice.....	107
3.3.5 Voltage clamp assessment of EC-coupling mechanisms in aged sham and OVX mice	108
3.3.6 Myofilament Ca ²⁺ sensitivity in aged sham and OVX hearts	109
3.3.7 Assessment of SR Ca ²⁺ stores in aged sham and OVX mice.....	111
3.3.8 Unitary Ca ²⁺ release properties in aged sham and OVX mice.....	112
3.3.9 Spontaneous Ca ²⁺ transients and triggered electrical activity in aged sham and OVX mice	113
3.3.10 Summary of Section 3.3.....	114
CHAPTER 4 DISCUSSION.....	134
4.1 The effect of extreme aging on sex differences in the heart	135

4.1.1	Summary of key findings	135
4.1.2	The effect of extreme old age on myocyte size and function	136
4.1.3	The effect of extreme old age on components of the EC-coupling pathway in male mice	138
4.1.4	The effect of extreme old age on components of the EC-coupling pathway in female mice	143
4.2	The impact of short term ovariectomy on cardiac contractile function	147
4.2.1	Summary of key findings	147
4.2.2	The effect of short term ovariectomy of Ca ²⁺ transients	148
4.2.3	The effect of short term ovariectomy on components of the EC-coupling pathway	149
4.2.4	The effect of short term ovariectomy on SR Ca ²⁺ content and spontaneous Ca ²⁺ release	151
4.3	The effect of long term ovariectomy on the aging female heart	154
4.3.1	Summary of key findings	154
4.3.2	Changes in Ca ²⁺ transients and contractile function with long term ovariectomy	155
4.3.3	Changes in components of the EC-coupling pathway with long term ovariectomy	158
4.3.4	Spontaneous Ca ²⁺ release and triggered activity with long term ovariectomy	160
4.4	Limitations	163
4.5	Significance of findings	164
	REFERENCES	166
	APPENDIX A: PUBLICATIONS	186
	APPENDIX B: COPYRIGHT PERMISSIONS	187

LIST OF TABLES

Table 1. Age-associated functional alterations to ventricular myocytes	21
Table 2. Age-associated modifications to components of the EC-coupling pathway	22
Table 3. Ages and weights of young adult and senescent male mice	76
Table 4. Ages and weights of young adult and senescent female mice	77
Table 5. Summary of responses from voltage clamp experiments in male myocytes	78
Table 6. Summary of responses from voltage clamp experiments in female myocytes	79
Table 7. Physical characteristics of animals and cells used in this study	92
Table 8. Summary of Ca ²⁺ handling responses from field stimulation experiments	93
Table 9. Ca ²⁺ handling parameters in voltage clamp experiments	94
Table 10. Characteristics of spontaneous Ca ²⁺ sparks	95
Table 11. Physical characteristics of animals and cells used in this study	115
Table 12. Summary of responses from field stimulation experiments	116
Table 13. Summary of responses from current clamp experiments	117
Table 14. Ca ²⁺ handling parameters in voltage clamp experiments	118
Table 15. Characteristics of spontaneous Ca ²⁺ sparks	119

LIST OF FIGURES

Figure 1	The excitation-contraction (EC) coupling pathway.....	12
Figure 2	Age-associated changes to the EC-coupling pathway.....	23
Figure 3	Schematic of field stimulation setup	54
Figure 4	Schematic of voltage clamp setup	60
Figure 5	<i>In vitro</i> calibration curve for Fura-2.....	64
Figure 6	Survival rates were similar between male and female mice.....	80
Figure 7	Myocytes length was significantly increased by age in male but not female mice	81
Figure 8	Cellular shortening declined with age in cells from male but not female mice	82
Figure 9	Ca ²⁺ transients declined with age in cells from both male and female mice.....	83
Figure 10	Ca ²⁺ current density declined with age in cells from males but not females.....	84
Figure 11	SR Ca ²⁺ stores were not affected by age, but fractional release significantly declined in both males and females.....	85
Figure 12	OVX amplified the size and speed of Ca ²⁺ transients in comparison to sham controls	96
Figure 13	Peak Ca ²⁺ transients were larger in OVX myocytes when compared to sham controls	97
Figure 14	EC-coupling gain was enhanced in OVX myocytes when compared to sham controls	98
Figure 15	OVX enhanced Ca ²⁺ transients across a range of membrane potentials.....	99
Figure 16	OVX increased EC-coupling gain at several membrane potentials.....	100
Figure 17	OVX significantly increased SR Ca ²⁺ content	101

Figure 18	Three dimensional representative plots of unitary Ca^{2+} release events.....	102
Figure 19	OVX enhanced Ca^{2+} spark frequency and amplitudes	103
Figure 20	Spontaneous Ca^{2+} transients were larger in OVX myocytes	104
Figure 21	Ca^{2+} transients were larger and faster in myocytes from OVX mice in comparison to sham controls.....	120
Figure 22	Cellular shortening was similar between myocytes from sham and OVX mice.....	121
Figure 23	<i>In vivo</i> ventricular function and heart rate were similar in sham and OVX mice.....	122
Figure 24	Action potentials and contractions were unaffected by OVX	123
Figure 25	OVX increased Ca^{2+} transients across several membrane potentials	124
Figure 26	Ca^{2+} current density was enhanced by OVX at membrane potentials near the peak of the IV curve	125
Figure 27	OVX reduced myofilament Ca^{2+} sensitivity.....	126
Figure 28	OVX reduced myofilament Ca^{2+} sensitivity as assessed by actomyosin MgATPase activity.....	127
Figure 29	Decreased myofilament Ca^{2+} sensitivity in OVX mice was not due to changes in phosphorylation of myofilament proteins.....	128
Figure 30	OVX greatly increased intracellular Ca^{2+} loads	129
Figure 31	Three dimensional representative plots of Ca^{2+} sparks from aged sham and OVX myocytes.....	130
Figure 32	Ca^{2+} spark frequency, amplitudes, and widths were significantly increased in myocytes from OVX mice when compared to sham controls.....	131
Figure 33	OVX increased the size of spontaneous Ca^{2+} transients.....	132
Figure 34	OVX promoted early afterdepolarizations	133
Figure 35	Summary of the effects of extreme old age on components of the EC-coupling pathway in male mice	142

Figure 36	Summary of the effects of extreme old age on components of the EC-coupling pathway in female mice	146
Figure 37	Summary of the effects of short term OVX on components of the EC-coupling pathway	153
Figure 38	Summary of the effects of long term OVX on components of the EC-coupling pathway	162

ABSTRACT

Previous studies have shown that cardiac contractile function declines with age in ventricular myocytes from 24 month old males but not females. As estrogen modulates cardiac contractile function, age-dependent changes in estrogen may help preserve contraction in the aging female heart. The present study examined the effects of extreme old age as well as short and long term estrogen deprivation on cardiac contractile function. Cardiomyocytes were isolated from young adult (~7 mos) and senescent (~32 mos) C57BL/6 male and female mice, or from young adult (~8 mos) and aged (~24 mos) ovariectomized or sham control female mice. Myocytes were loaded with Fura-2 and paced at 2 Hz (37°C). Results showed that while Ca^{2+} dysregulation occurred in both senescent male and female mice, contractile function was preserved in female myocytes, even with extreme old age. This suggests that while aging causes Ca^{2+} dysregulation in males and females, contractile function is preserved in females. In other experiments, the effect of short ovariectomy on the excitation-contraction (EC) coupling pathway was investigated. Short term ovariectomy enhanced sarcoplasmic reticulum (SR) Ca^{2+} storage and release, by augmenting SR Ca^{2+} content and by increasing Ca^{2+} transients, Ca^{2+} sparks and EC-coupling gain. These findings suggest that estrogen may play a role in limiting SR Ca^{2+} loading and Ca^{2+} release in the female heart. The present study also investigated the effect of long term ovariectomy on the aging female heart. The results showed that long term ovariectomy enhanced Ca^{2+} influx and increased SR Ca^{2+} storage and release, but did not affect contractile function. This was due to a decrease in myofilament Ca^{2+} sensitivity with long term ovariectomy. However, enhanced Ca^{2+} levels did lead to larger spontaneous Ca^{2+} transients and greater abnormal electrical activity in the form of early afterdepolarizations. Together, the results suggest that aging as well as short and long term estrogen deprivation leads to Ca^{2+} dysregulation and spontaneous SR Ca^{2+} release. In the aging female heart, this Ca^{2+} dysregulation may increase the susceptibility to cardiovascular disease and dysfunction.

LIST OF ABBREVIATIONS AND SYMBOLS USED

[Ca ²⁺] _i	Intracellular calcium concentration
%	Percentage
°C	Degrees Celsius
APD	Action potential duration
APD ₅₀	Action potential duration to 50% repolarization
APD ₉₀	Action potential duration to 90% repolarization
ATP	Adenosine triphosphate
Ca ²⁺	Calcium
CaMKII	Calcium/calmodulin-dependent protein kinase II
cAMP	Cyclic adenosine monophosphate
CICR	Calcium induced calcium release
cm	Centimeter
DAD	Delayed afterdepolarization
EAD	Early afterdepolarization
EC-coupling	Exciting contraction-coupling
EC ₅₀	Half maximal effective concentration
ER	Estrogen receptor
ER-α	Estrogen receptor alpha
ER-β	Estrogen receptor beta
ERE	Estrogen response elements
ERK	Extracellular signal-regulated kinase
F	Fluorescence intensity
F ₀	Background
FDHM	Full duration at half maximum
FKBP12.6	FK-506 binding protein
FWHM	Full width at half maximum
g	Gram
G _i	Inhibitory G-protein
G _s	Stimulatory G-protein
HERS	Heart and Estrogen Progestin Replacement Study
HRT	Hormone replacement therapy
Hz	Hertz
I _{CaL}	L-type calcium current
I _{Kur}	Delayed rectifier potassium current
I _{TI}	Transient inward current
I _{TO}	Transient outward current
IV	Current-voltage
K ⁺	Potassium
K _d	Dissociation constant
kDa	Kilodalton
KEEPS	Kronos Early Estrogen Prevention Study
kg	Kilogram
KHz	Kilo Hertz

LV	Left ventricle
M	Molar
mA	Milliamp
MAPK	Mitogen-activated protein kinase
MCIP1	Modulatory calcineurin-interacting protein 1
min	Minute
ml	Milliliter
mM	Millimolar
mm	Millimeter
mos	Months
ms	Millisecond
mV	Millivolts
MyBP-C	Myosin binding protein-C
MΩ	Megaohm
nA	Nanoamp
Na ⁺	Sodium
NCX	Sodium-calcium exchanger
Nm	Nanometer
NO	Nitric oxide
NOS	Nitric oxide synthase
OVX	Ovariectomized
PI3K	Phosphatidylinositol 3-kinase
PKA	Protein kinase A
PLB	Phospholamban
PP1	Protein phosphatase 1
PP2A	Protein phosphatase 2A
RMP	Resting membrane potential
RyR	Ryanodine receptor
s	Second
SEM	Standard error of the mean
SERCA	Sarco/endoplasmic reticulum calcium ATPase
SR	Sarcoplasmic reticulum
t-tubule	Transverse tubule
tau	Time constant of spark decay
Tm	Tropomyosin
TnC	Troponin-C
TnI	Troponin-I
TnT	Troponin-T
U	Units
UV	Ultra violet
WHI	Women's Health Initiative
α	Alpha
β	Beta
μm	Micrometer
μM	Micromolar

ACKNOWLEDGMENTS

First and foremost, I'd like to thank my supervisor Dr. Susan Howlett. Your insight, guidance, and support have helped shape me into a better graduate student and young scientist. You've also put up with my shenanigans over the years. Whether it was my classic "pressure makes diamonds" response, or the day you met your doppelganger, you have continuously been a great sport and I've always appreciated it. Most importantly, you've provided an environment where I was always free to learn and explore. You've helped me write better, think faster, and learn to assess things critically. For that, I will always be grateful.

Secondly, I'd like to thank my parents. The two people who have sacrificed and struggled to provide the best life they could for my brother and I. Though you are unable to read this, I dedicate it to you.

Lastly, my brother, my friends, my lab mates, and my love. Words cannot express what you mean to me. You have provided me with the two things a man really needs: friendship and love. While I may not say it enough, thank you.

CHAPTER 1 INTRODUCTION

1.1 BROAD OVERVIEW

The incidence of cardiovascular diseases, including congestive heart failure, left ventricular hypertrophy, and cardiac arrhythmias, significantly increases with age (Lakatta and Levy, 2003). In Canada, our population is inevitably aging. Individuals 65 years of age and over accounted for 14.8% of the total Canadian population in 2011, a rise of 14.1% from 2006 (Statistics Canada, 2011). In the near future, more “baby boomers” will reach 65 years of age and the proportion of older individuals in the population is expected to substantially increase (Statistics Canada, 2011). Overall, this will have an effect on both healthcare resources and the economy, as cardiovascular diseases currently cost Canadians approximately 21 billion dollars per year (Conference Board of Canada, 2010). Thus, the mechanisms that lead to age-associated changes in the cardiovascular system are critically important to improve our understanding of the pathophysiology of cardiovascular diseases.

Interestingly, cardiovascular diseases affect men and women differently. This is evident even in the oldest available mortality statistics from England and Wales that provide causes of death (Nikiforov and Mamaev, 1998). Beginning in the 1920s, it was reported that cardiovascular disease mortality in 25 to 74 year old males was higher than in females. However, the number of deaths from cardiovascular diseases was similar in men and women in individuals aged 75 years and older. Interestingly, data from the United States showed a similar trend. From the 1920s and onward, there was greater cardiovascular disease-related mortality in males than females (Nikiforov and Mamaev, 1998).

Several hypotheses that might help explain sex differences in cardiovascular disease have been proposed over the years. Differences in the social roles of men and women, where men tended to be employed in more difficult and demanding occupations, have been implicated (Lopez et al., 1995; Waldron, 1985). Also, it has been suggested that a more favourable female lifestyle, where women have a better diet, pay more attention to personal health, and smoke fewer cigarettes than men may also contribute to this difference (Lopez et al., 1995; Waldron, 1985). However, as time progressed gender equality in the workplace and changes in the lifestyles of both men and women have minimized these differences between the sexes, and clinical studies have not supported these theories (Nikiforov and Mamaev, 1998).

One hypothesis that emerged in 1957 highlighted the importance of biological differences between males and females with regards to mortality (Madigan, 1957). Madigan compared mortality between male and female teachers and administrative staff within the Roman Catholic Church in an attempt to minimize sociocultural factors that may influence mortality rate. Madigan's findings suggested that biological factors were more important than sociocultural factors, and contributed to the shorter life expectancy in men and longer life expectancy in women (Madigan, 1957). Over the years, investigators have hypothesized that female sex hormones, such as estrogen, may have a protective effect in women, particularly on cardiovascular function (Luczak and Leinwand, 2009; Murphy, 2011). This is supported by evidence that women are less likely to develop cardiovascular disease that impairs systolic function, such as congestive heart failure (Gottdiener et al., 2000). Further, men and women are susceptible to different types of cardiovascular diseases, and these tend to occur later in life in women

than in men (Czubryt et al., 2006; Huxley, 2007; Luczak and Leinwand, 2009; Yarnoz and Curtis, 2008). However, the extent of our knowledge regarding the effect of female sex hormones on cardiac function is limited because most basic science research has used hearts and cells from male animals. Further, the importance of both age and sex on cardiovascular function has only recently begun to be investigated. Therefore, the overall goal of this thesis was to examine aspects of the impact of age on cardiac contractile function in male and female mice, and to determine the effect of ovarian estrogen deprivation on cardiac function in female animals.

1.2 EC-COUPLING PATHWAY

1.2.1 Cardiac EC-coupling

Cardiac excitation contraction (EC) coupling refers to the process of myocardial electrical excitation and the resulting calcium (Ca^{2+})-mediated contraction. A schematic of the EC-coupling pathway is shown in figure 1. This process begins with the conduction of the cardiac action potential (Bers, 2001; Birkeland et al., 2005; Guatimosim et al., 2002). This four-phase action potential differs from the action potential in skeletal muscle and neurons because of its long duration and plateau phase (Birkeland et al., 2005). Beginning with Phase 0, the cardiac action potential causes depolarization of the sarcolemma resulting in entry of Na^+ ions through voltage-gated Na^+ channels (Bers, 2001; Birkeland et al., 2005). This alters the membrane potential from approximately -80 mV to a positive value. Phase 1, also known as early repolarization, follows with transient outward K^+ channels opening, giving rise to the transient outward K^+ current (I_{TO}) (Birkeland et al., 2005). Phase 2, the plateau phase,

results in the activation of voltage-gated L-type Ca^{2+} channels within transverse tubules (t-tubules) and gives rise to the L-type Ca^{2+} current (I_{CaL}), which subsequently triggers contraction (Birkeland et al., 2005). In Phases 3 and 4, repolarization occurs through outward K^+ currents, such as the delayed rectifier, returning the membrane potential to the resting value. Cells are maintained at -80 mV, via the inward rectifier K^+ channels, until another action potential occurs (Birkeland et al., 2005).

Ca^{2+} entering through L-type Ca^{2+} channels acts as the predominant trigger to amplify Ca^{2+} release from intracellular stores in the sarcoplasmic reticulum (SR; Bers, 2002). This gives rise to the Ca^{2+} transient, and leads to cellular contraction (Bers, 2002). Ca^{2+} entry through T-type Ca^{2+} channels and reverse mode Na^+ - Ca^{2+} exchange (NCX) is also thought to be a weak trigger of Ca^{2+} release in adult hearts (Sipido, 1998). This process by which Ca^{2+} influx triggers SR Ca^{2+} release is known as Ca^{2+} -induced Ca^{2+} release (CICR) (Fabiato, 1985a; Fabiato, 1985b; Fabiato, 1985c). To stimulate Ca^{2+} release from intracellular stores, this trigger Ca^{2+} binds to SR Ca^{2+} release channels known as ryanodine receptors (RyR), causing their activation and opening (Meissner, 2004).

RyR2, the main receptor isoform in the heart, is composed of four subunits that assemble to form a functional calcium release channel (Tunwell et al., 1996). This ligand gated channel is activated at low μM $[\text{Ca}^{2+}]$ and inhibited at high mM $[\text{Ca}^{2+}]$ (Marx, 2003). RyRs form a macromolecular complex by associating with proteins that modulate channel function. One protein associated with RyR2 is the FK-506 binding protein (FKBP12.6) (Marx, 2003). FKBP12.6 regulates function by enhancing the cooperativity of the four RyR2 subunits and the adjacent RyR2 channels (Brillantes et al., 1994; Marx

et al., 2001). Changes to the interaction between RyR2 and FKBP12.6 can occur via phosphorylation by protein kinase A (PKA) (Marx et al., 2000). PKA phosphorylation of RyR2 at Ser2808 causes dissociation of FKBP12.6. This results in an increased RyR2 channel opening probability and greater Ca^{2+} sensitivity for activation (Marx et al., 2000). Similarly, phosphorylation of the RyR2 complex by Ca^{2+} /calmodulin-dependent protein kinase II (CaMKII) at Ser2814 can enhance RyR2 activity and channel opening probability (Wehrens et al., 2004). Channel phosphorylation is counteracted by the protein phosphatases (PP1 and PP2A), which help modulate the phosphorylation status of the RyR2 (Zalk et al., 2007). Through the actions of these proteins, the activity of RyR2 can be modified to enhance SR Ca^{2+} release and cardiac contractile function within the myocyte.

SR Ca^{2+} release is thought to occur in distinct release units called Ca^{2+} sparks (Cheng et al., 1993; Lopez-Lopez et al., 1994; Santana et al., 1996). These Ca^{2+} sparks originate near specialized junctions between the sarcolemma (t-tubule or surface membrane) and the SR (Bootman et al., 2006; Inoue and Bridge, 2005; Scriven et al., 2002). At these junctions, L-type Ca^{2+} channels and RyR are located in close proximity and function as clusters known as release units or couplons, which generate Ca^{2+} sparks (Bootman et al., 2006; Inoue and Bridge, 2005; Scriven et al., 2002). Specifically, Ca^{2+} sparks are thought to represent coordinated Ca^{2+} release through RyR, which become activated by one or more L-type Ca^{2+} channels (Bers, 2008; Inoue and Bridge, 2005; Wang et al., 2001). Spontaneous Ca^{2+} sparks also can occur in quiescent cells, even in the absence of L-type Ca^{2+} channel openings (Cheng et al., 1993; Ferrier et al., 2003; Santana et al., 1996). Ca^{2+} spark frequency increases as SR Ca^{2+} load increases, which

suggests that spontaneous Ca^{2+} sparks may represent a leak pathway for Ca^{2+} that limits SR Ca^{2+} content (Sato et al., 1997). It is important to limit SR Ca^{2+} loading, as SR Ca^{2+} overload can lead to spontaneous SR Ca^{2+} release and in turn, triggered electrical activity (Guatimosim et al., 2002; Sato et al., 1997). Normally, Ca^{2+} release from one release unit does not activate neighbouring release units, as released Ca^{2+} diffuses away from adjacent couplons (Bers, 2008). However, upon depolarization several release units are activated simultaneously via CICR and individual Ca^{2+} sparks fuse to form the Ca^{2+} transient (Bers, 2008; Guatimosim et al., 2002).

Ca^{2+} release from the SR is proportional to the magnitude of the L-type Ca^{2+} current (I_{CaL}) and the degree to which this signal is amplified is known as the "gain" of CICR (Bers, 2008). Experimentally, gain is defined as the amount of SR Ca^{2+} release divided by the amount of trigger Ca^{2+} influx (total Ca^{2+} release/ I_{CaL} ; Bers, 2008). Gain, which is modulated by temperature and SR Ca^{2+} load (Ginsburg and Bers, 2004; Shutt and Howlett, 2008), is thought to play a role in the regulation of SR Ca^{2+} release and cardiac contraction (Altamirano and Bers, 2007). In the failing heart, impaired EC-coupling gain and SR Ca^{2+} release can compromise contractile function (Sjaastad et al., 2003).

Once Ca^{2+} is released from the SR, the Ca^{2+} ions interact with the troponin complex to initiate myofilament contraction. The troponin complex consists of three polypeptide chains: troponin-C (TnC), which contains the Ca^{2+} binding sites; troponin-I (TnI), which interacts with actin filaments and inhibits their ability to activate myosin ATPase, thus inhibiting the production of force; and troponin-T (TnT), which binds tropomyosin (Tm) and is thought to be responsible for attaching the troponin complex to

the thin filament in the proper configuration (Bers, 2001). Once Ca^{2+} binds to TnC, a conformational change occurs allowing TnC to bind TnI causing its dissociation from the actin filament. In turn, this causes a shift in the TnT-Tm complex and exposes myosin binding sites on the actin filament (Bers, 2008). Myosin heads can then strongly bind to actin filaments to form a cross-bridge. Intrinsic ATPases within myosin heads then utilize ATP to drive and cycle cross-bridges. This moves thin filaments along the thick filaments and causes the muscle to contract (Huxley, 1957). Another sarcomeric protein, cardiac myosin binding protein-C (MyBP-C), plays an important role in stabilizing this thick-thin filament interaction (Barefield and Sadayappan, 2010). In addition, phosphorylation of the myofilament proteins TnI, TnT, and MyBP-C, has been shown to modulate contractile function by decreasing the sensitivity of the myofilaments to Ca^{2+} , which enhances the speed of cardiomyocyte relaxation (Barefield and Sadayappan, 2010; Kobayashi and Solaro, 2005).

Relaxation occurs when cytosolic Ca^{2+} is removed from the cell. The majority of Ca^{2+} released from intracellular stores is transported back into the lumen of the SR (Bers, 2002). However, some Ca^{2+} is removed from the cell through the electrogenic NCX pump, which transports three Na^+ ions for every Ca^{2+} ion. The sarcolemmal Ca^{2+} ATPase also removes Ca^{2+} from the cell, although this is a fairly minor pathway for Ca^{2+} efflux (Bers, 2002). The amount of Ca^{2+} removed from the cell is proportional to the amount that enters via I_{CaL} , and thus the amount of Ca^{2+} that enters the cell equals the amount of Ca^{2+} removed from the cell during relaxation (Bers, 2008).

Ca^{2+} reuptake into the SR occurs primarily through the actions of the SR Ca^{2+} ATPase (SERCA). The primary isoform expressed in the heart, SERCA2a, is regulated

by the phosphoprotein phospholamban (PLB) (Rodriguez and Kranias, 2005). In its unphosphorylated state, PLB interacts with SERCA2a and decreases the affinity of this enzyme for Ca^{2+} (Janczewski and Lakatta, 2010; Rodriguez and Kranias, 2005). However, once PLB is phosphorylated by PKA and/or CaMKII, inhibition of SERCA2a is alleviated (Janczewski and Lakatta, 2010; Rodriguez and Kranias, 2005). Thus, modulators of the PKA and CaMKII pathways, such as β -adrenergic signaling, have been shown to alter SERCA2a activity (Li et al., 2000). Modulation of the EC-coupling pathway by β -adrenergic signaling is discussed in the next section.

1.2.2 Modulation of the EC-coupling pathway by β -adrenergic signaling

β -adrenergic signaling has been shown to regulate EC-coupling in the myocardium (Wallukat, 2002). The effects of β -adrenergic stimulation in the heart are mediated by the stimulation of a family of G-protein coupled receptors known as the β -adrenergic receptors. Three subtypes of these serpentine receptors have been discovered (β_1 , β_2 , and β_3), with the β_1 -adrenergic receptor predominating in the heart (Wallukat, 2002). In ventricular myocytes, binding of catecholamines to either β_1 - or β_2 -adrenergic receptors induces the activation of the stimulatory G-protein (Gs) (Wallukat, 2002). Active Gs subsequently activates adenylate cyclase, which increase the formation of intracellular cAMP (Wallukat, 2002). cAMP then activates PKA, which phosphorylates intracellular targets including L-type Ca^{2+} channels, RyR2, SERCA2a, PLB, and TnI (Cachelin et al., 1983; Li et al., 2000; Okazaki et al., 1990; Wallukat, 2002). This phosphorylation increases the open probability of L-type Ca^{2+} channels and RyR2, allowing greater Ca^{2+} influx upon depolarization and enhanced CICR resulting in larger

Ca²⁺ transients (Cachelin et al., 1983; Marx et al., 2000). PKA phosphorylation of SERCA2a and PLB increases the activity of SERCA2a, resulting in faster SR Ca²⁺ reuptake and myocyte relaxation (Li et al., 2000). Additionally, phosphorylation of TnI by PKA decreases myofilament Ca²⁺ sensitivity, which enhances relaxation by accelerating the dissociation of myosin from actin (Kentish et al., 2001; Okazaki et al., 1990). Overall, activation of PKA results in positive inotropy and enhanced relaxation. Interestingly, β 2-adrenergic receptors also couple to inhibitory G proteins (Gi) (Xiao et al., 1995). Gi counteracts the actions of Gs and cAMP, and thus activation of β 2-adrenergic receptors limits the positive inotropy activated by drugs that bind to β 1-adrenergic receptors (Xiao and Lakatta, 1993).

In addition to PKA regulation, CaMKII can modulate the EC-coupling pathway. The Ca²⁺/calmodulin complex activates CaMKII when there is a rise in intracellular Ca²⁺ levels, allowing phosphorylation of several intracellular targets (Maier and Bers, 2007). CaMKII phosphorylation occurs at sites distinct from PKA phosphorylation, but can enhance inotropy and relaxation in a manner similar to PKA. These include modulating the open probability of RyR2 and L-type Ca²⁺ channels and by increasing the speed of SR Ca²⁺ reuptake by phosphorylating SERCA2a and PLB (Maier and Bers, 2007).

Overall, phosphorylation of key proteins in the EC-coupling pathway by PKA or CaMKII results in positive inotropy and enhanced relaxation in ventricular myocytes. This modulation of the EC-coupling pathway is a highly regulated process. Electrical and contractile dysfunction in the heart can occur if these pathways become disrupted.

1.2.3 Dysfunction of the EC-coupling pathway leads to triggered activity

The cardiac action potential and EC-coupling pathway are tightly regulated processes. However, abnormal electrical activity and spontaneous SR Ca^{2+} release can occur when these pathways are disrupted. This can lead to triggered activity, which can be detrimental to cardiac function. Two specific types of triggered activity can occur within myocytes. These are known as early afterdepolarizations (EADs), and delayed afterdepolarizations (DADs) (Clusin, 2003). EADs occur prior to repolarization of the action potential, particularly if the action potential is abnormally prolonged (Clusin, 2003; January and Riddle, 1989). A prolonged action potential allows Ca^{2+} channels to recover from inactivation before full repolarization occurs. Ca^{2+} channels can then reopen, allow Ca^{2+} to enter from the extracellular space and trigger additional Ca^{2+} release from the SR (Clusin, 2003; January and Riddle, 1989). This results in triggered electrical activity in form of an EAD. Conversely, DADs occur after repolarization of the cardiac action potential is complete, but prior to the next stimulated beat (Ferrier and Moe, 1973). DADs are due to a large, spontaneous release of SR Ca^{2+} that leads to triggered activity (Ferrier and Moe, 1973). Spontaneous Ca^{2+} release tends to occur when the SR becomes overloaded with Ca^{2+} (Clusin, 2003; Ferrier and Moe, 1973). This released Ca^{2+} is removed from the cytosol by the NCX, which exchanges one Ca^{2+} ion for three Na^+ ions (Bers, 2001; Clusin, 2003). This generates a net inward current known as the transient inward current (I_{TI}) (Bers et al., 2002; Clusin, 2003). If Na^+ influx through NCX is large enough to reach threshold, a DAD can occur resulting in a full sized spontaneous action potential and associated contraction (Clusin, 2003; Ferrier and Moe, 1973). Since cells are electrically coupled in the intact heart, triggered activity in the

form of an EAD or DAD can propagate throughout the myocardium and lead to cardiac arrhythmias (Pogwizd et al., 1992).

In the normal heart, the cardiac action potential and the EC-coupling pathway work efficiently and contractile function occurs without disruption. However, when one or more aspects of the EC-coupling pathway are disrupted, cardiac electrical and contractile function can become impaired. Interestingly, the aging process is known to alter several biochemical and physiological components of the EC-coupling pathway, as well as cardiac structure, as discussed in detail in the next section.

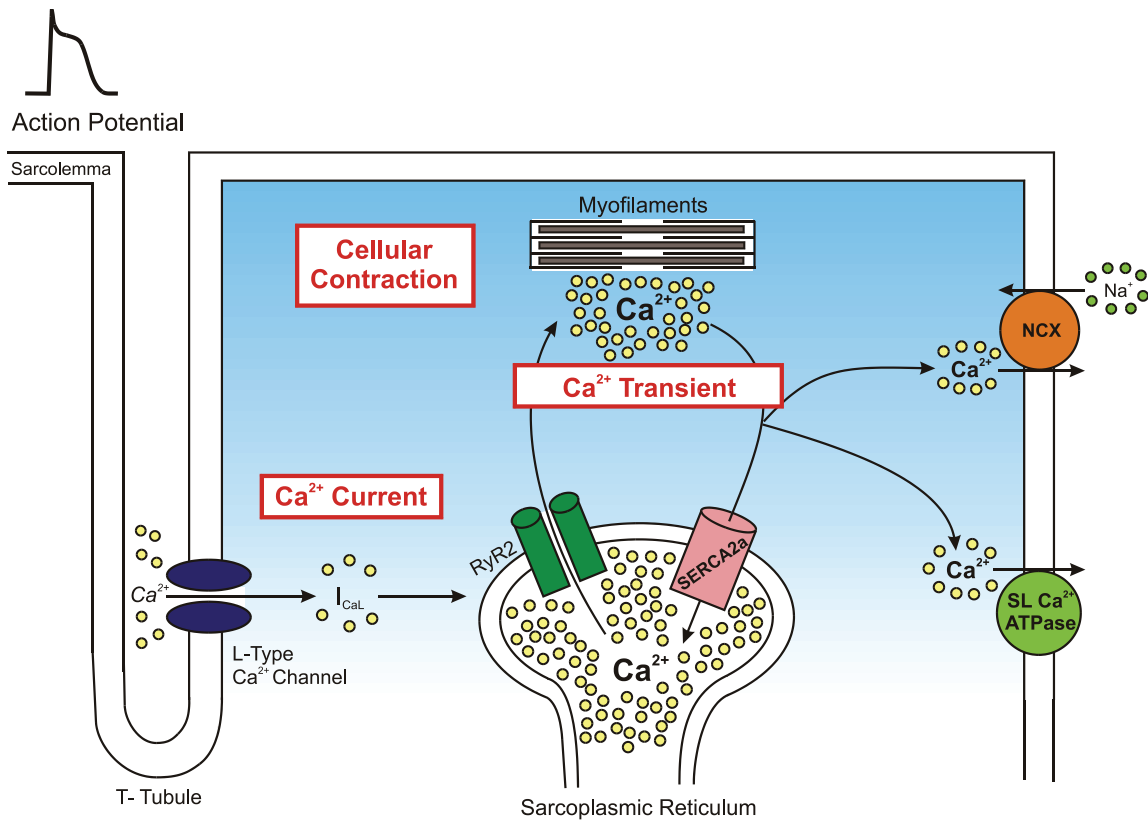


Figure 1. The excitation-contraction (EC) coupling pathway. Depolarization of the sarcolemma by the cardiac action potential causes L-type Ca²⁺ channels to open and gives rise to the L-type Ca²⁺ current (I_{CaL}). This trigger Ca²⁺ then binds to and activates ryanodine receptors (RyR2) on the sarcoplasmic reticulum (SR). This causes Ca²⁺-induced Ca²⁺-release (CICR), and allows Ca²⁺ from intracellular stores to enter the cytosol. This gives rise to the Ca²⁺ transient. The Ca²⁺ transient can then interact with myofilament proteins to cause a cellular contraction. Contraction is terminated when Ca²⁺ is removed from the cytosol. This occurs by either reuptake into the SR by sarco/endoplasmic reticulum ATPase (SERCA2a) or by efflux from the cell by the Na⁺/Ca²⁺ exchanger (NCX) and the sarcolemmal Ca²⁺ ATPase.

1.3 AGE-RELATED CHANGES IN CARDIAC FUNCTION

1.3.1 Structural changes in the aging heart

In humans, aging causes significant changes in the structure of the heart, even in the absence of overt cardiovascular disease (Lakatta and Levy, 2003). With increasing age, the number of viable ventricular myocytes declines (Lakatta and Levy, 2003). This causes the remaining myocytes to increase in size, and contributes to left ventricular hypertrophy (Lakatta and Levy, 2003). In addition to cellular hypertrophy, an increase in collagen deposition and fibrous tissue causes the left ventricular wall to thicken with age (Lakatta and Levy, 2003). Studies in aged rodent models have also shown age-associated changes in the structure of the heart. The total number of ventricular myocytes decreases with age in the rat heart, as a result of an increase in necrotic and apoptotic cell death (Hacker et al., 2006; Kajstura et al., 1996). However, individual ventricular myocytes are hypertrophied in many different species (Anversa et al., 1990; Dibb et al., 2004; Lim et al., 2000; Liu et al., 2000; Walker et al., 1993; Xiao et al., 1994). In addition, left ventricular mass and fibrous tissue content has been reported to increase in the hearts of older rats (Anversa et al., 1990; Buttrick et al., 1991; Hacker et al., 2006; Olivetti et al., 1991). These structural changes are thought to contribute to age-associated changes in cardiac contractility (Lakatta and Levy, 2003).

1.3.2 Impact of age on cardiac contractility

At rest, cardiac contractility does not appear to be influenced by age (Fleg et al., 1995; Najjar et al., 2004; Ruan and Nagueh, 2005). However, the capacity to increase ejection fraction in response to greater demand, such as during exercise, declines in older

individuals (Lakatta and Levy, 2003). In addition, cardiac contraction and relaxation are prolonged in the aged human heart when compared to younger adults (Lakatta and Levy, 2003; Lakatta and Sollott, 2002). In both intact hearts and isolated cardiac tissues, peak contractions are unaffected by age at low pacing rates, however, fractional shortening declines and the rates of contraction and relaxation become impaired at rapid pacing rates in older hearts (Assayag et al., 1998; Froehlich et al., 1978; Lakatta et al., 1975; Orchard and Lakatta, 1985; Rozenberg et al., 2006; Schmidt et al., 2000; Wei et al., 1984). Similar results are seen in *in vivo* studies where β -adrenergic receptors are stimulated to mimic the effects of exercise (Hacker et al., 2006; Lieber et al., 2008). Results showed that unlike younger rat hearts, aged hearts did not increase contractile force in response to β -adrenergic stimulation (Hacker et al., 2006; Lieber et al., 2008). Previous studies have shown that the decline in cardiac contractile function in the aging heart is due, in part, to the inability of individual ventricular myocytes to contract effectively (Isenberg et al., 2003; Lim et al., 2000; Xiao et al., 1994). This may be due to the marked changes in biochemical and physiological components of the EC-coupling pathway observed in the aging heart.

1.3.3 Contractile function in ventricular myocytes from aged animals

A decrease in the contractile function of individual cardiomyocytes may underlie the age-associated decline in cardiac function. When individual ventricular myocytes from rodents are paced at slow stimulation rates (< 1 Hz), the degree of cellular contraction is similar in young adult and aged animals (Capasso et al., 1992; Farrell and Howlett, 2007; Lim et al., 2000; Xiao et al., 1994). At rapid pacing rates (> 2 Hz),

myocytes from young adult animals exhibit an increase in the size and speed of cellular contractions (Lim et al., 2000). In addition, myocytes from younger animals have larger, faster underlying Ca^{2+} transients at higher stimulation frequencies (Isenberg et al., 2003; Lim et al., 2000). Conversely, cell shortening is impaired and relaxation is prolonged at rapid stimulation rates in myocytes from aged mice (Lim et al., 2000). Ca^{2+} transients are also much smaller and rates of decay are slower when compared to responses from younger animals (Isenberg et al., 2003; Lim et al., 2000). In addition, isolated myocytes from older animals do not exhibit an increase in contraction size and Ca^{2+} transient amplitude when β -adrenergic receptors are stimulated to mimic the effect of exercise (Farrell and Howlett, 2007; Farrell and Howlett, 2008; Xiao et al., 1994). The rates of relaxation of the contraction and decay of the Ca^{2+} transient also are slower in cells from older animals when compared to younger animals in the presence of β -adrenergic receptor stimulation (Xiao et al., 1994). These results suggest that the ability of individual ventricular myocytes to contract declines with age, in particular, under conditions of stress such as rapid pacing and β -adrenergic stimulation. This would be expected to decrease overall contractility of the aging heart. Table 1 summarizes the age-associated changes to ventricular myocyte function.

1.3.4 The EC-coupling pathway in the aging heart

To understand the mechanisms behind the decline in contractile function in the aging heart, studies have assessed whether there are age-related changes in components of the EC-coupling pathway. A schematic of the age-associated changes to the EC-coupling pathway are shown in figure 2. Studies have shown that the cardiac action

potential is prolonged in cells from older hearts (Liu et al., 2000; Walker et al., 1993; Wei et al., 1984). While resting membrane potentials are not affected by age, there is evidence that the increased action potential duration results from age-dependent changes in transmembrane currents (Liu et al., 2000; Walker et al., 1993; Wei et al., 1984). Aging is associated with a decrease in the peak density and rate of inactivation of the transient outward K^+ current (I_{TO}) (Liu et al., 2000; Walker et al., 1993). The inactivation of I_{CaL} is also slower in ventricular myocytes from older rats when compared to cells from younger animals (Josephson et al., 2002; Liu et al., 2000; Walker et al., 1993). This decrease in I_{TO} and slowed inactivation of I_{CaL} would increase action potential duration by prolonging depolarization. An increase in action potential duration would allow for greater Ca^{2+} influx, which would enhance SR Ca^{2+} release and cellular contractions. However, in the aging heart an increase in action potential duration does not result in larger contractions. This may be due to age-associated changes to L-type Ca^{2+} channels.

Some studies have suggested that peak I_{CaL} density declines with age in ventricular myocytes from rodents (Grandy and Howlett, 2006; Howlett, 2010; Liu et al., 2000), although this has not been seen in all studies (Walker et al., 1993; Xiao et al., 1994). Receptor binding studies have shown that the expression of L-type Ca^{2+} channels declines with age, although the properties of these channels do not change with age (Howlett and Nicholl, 1992). As I_{CaL} is the predominant trigger for CICR, a decrease in peak I_{CaL} may partially account for the reduction in Ca^{2+} transient amplitude and smaller contraction size reported in myocytes from aged hearts (Isenberg et al., 2003; Lim et al., 2000; Xiao et al., 1994).

The impact of the aging process on proteins involved in SR Ca^{2+} release in the heart has also been investigated. mRNA levels of the major SR Ca^{2+} binding protein, calsequestrin (CSQ), are similar in young adult and older hearts (Lim et al., 1999; Lompre et al., 1991). However, other proteins involved in SR Ca^{2+} release have been shown to change with age. Studies have shown that there is an age-associated decline in the protein levels of RyR2 (Assayag et al., 1998; Nicholl and Howlett, 2006), although this has not been reported in all models (Xu and Narayanan, 1998). In addition, phosphorylation of RyR2 by CaMKII is reduced in the aging heart (Xu and Narayanan, 1998). As phosphorylation of RyR2 is thought to increase Ca^{2+} release channel activity (Marx et al., 2000), an age-associated decrease in RyR2 phosphorylation might reduce SR Ca^{2+} release in older hearts. As reduced RyR2 channel density and decreased RyR2 phosphorylation may affect unitary SR Ca^{2+} release events, several studies have investigated the impact of age on Ca^{2+} sparks. Studies in mouse ventricular myocytes have shown that the frequency of spontaneous Ca^{2+} sparks increases with age, but the duration of individual Ca^{2+} sparks is reduced (Howlett et al., 2006). A similar increase in spark frequency and decrease in spark duration has been shown in hearts from aged rats (Zhu et al., 2005). However, aged rat myocytes also showed a decline in Ca^{2+} spark width and amplitude (Zhu et al., 2005). These findings suggest that an age-associated decline in unitary Ca^{2+} release events may decrease Ca^{2+} transient size in the aging heart. Increased Ca^{2+} spark activity may also reduce SR Ca^{2+} content and attenuate Ca^{2+} transients in older hearts.

Changes in myofilament proteins have been investigated to help explain the impact of age on cardiac contractile function. Studies have shown that there is an age-

associated decrease in the expression of the faster alpha myosin heavy chain, and an increase in the slower beta myosin heavy chain in the aged rat heart (Buttrick et al., 1991). This results in decreased myosin ATPase activity in the aging heart (Buttrick et al., 1991). This reduction in myocardial myosin ATPase activity may contribute to the age-dependent slowing of contractile responses.

Changes in Ca^{2+} removal mechanisms may also prolong relaxation in older hearts. Studies have shown that an age-associated decrease in SERCA2a activity may prolong Ca^{2+} transient decay and slow relaxation (Froehlich et al., 1978; Lompre et al., 1991; Wei et al., 1984). A decline in SERCA2a expression could also account for prolonged Ca^{2+} transients in aged myocytes (Lompre et al., 1991), although this has not been observed in all studies (Buttrick et al., 1991; Lim et al., 1999; Xu and Narayanan, 1998). Changes in the regulation of SERCA2a activity by the endogenous inhibitor phospholamban (PLB) also may slow contraction in the aging heart. PLB expression levels are elevated in hearts from older mice (Lim et al., 1999). This would be expected to slow Ca^{2+} reuptake in the aging heart. Additionally, phosphorylation of PLB by both PKA and CaMKII declines with age (Xu and Narayanan, 1998). As phosphorylation of PLB by PKA and CaMKII increases SERCA2a activity and speeds relaxation (Rodriguez and Kranias, 2005), reduced PLB phosphorylation may slow contraction in the aging heart. Thus, lower SERCA2a activity with aging may be due to both decreased pump density and greater inhibitory regulation of SERCA2a, which would prolong relaxation in older hearts.

Other studies have investigated the impact of age on cardiac NCX activity. Studies using membrane vesicles or cardiac muscles have reported that NCX activity is

either decreased (Heyliger et al., 1988; Lim et al., 1999) or unchanged (Abete et al., 1996) in the aging heart. By contrast, a more recent study in isolated ventricular myocytes has shown that NCX activity may actually increase with age (Mace et al., 2003). The reasons for these divergent results remain unclear, but may be due to differences in membrane preparations or experimental models. Still, these findings indicate that the activities of several key proteins in the EC-coupling pathway are reduced in the aging heart. Reduced myosin ATPase activity and lower SERCA2a activity would contribute to a decline in cardiac function and slowed contractile responses in older hearts. A decrease in the activity of other components of Ca^{2+} removal, such as NCX, may also slow the speed of contraction in the aging heart. Table 2 summarizes the age-associated changes to components of the EC-coupling pathway.

In summary, age-related changes in cardiac structure and molecular mechanisms are implicated in the decline in cardiac contractile function in older hearts. While this is not evident at rest, older hearts lose the ability to effectively increase contractile function in response to greater demand. At the cellular level, contractions and Ca^{2+} transients are smaller and slower in the aged heart during rapid pacing or β -adrenergic stimulation. This decline in contractile function may be due to changes in the expression, regulation, and function of several proteins within the EC-coupling pathway. Interestingly, almost all previous animal studies of the effect of age on cardiac contractile function have used male animals, so little is known about the impact of age on the female heart. However, as outlined in the next section, recent studies have shown that the age-associated decline in cardiac contractile function is much more prominent in myocytes from males than females. The next section will highlight the impact of biological sex on cardiac

contractile function in the young adult heart, and will outline what is known about differences in the effect of age on cardiac contractile function between the sexes.

TABLE 1**Age-associated functional alterations to ventricular myocytes**

Myocyte Physiology	Functional Change	Reference
Contraction	With β -adrenergic or rapid stimulation:	Xiao et al., 1994 Lim et al., 2000 Grandy et al., 2006 Farrell et al., 2007 Farrell et al., 2008 Howlett, 2010
	↓ Cell shortening ↓ Relaxation	
Ca ²⁺ Transient	With β -adrenergic or rapid stimulation:	Xiao et al., 1994 Lim et al., 2000 Isenberg et al., 2003 Grandy et al., 2006 Howlett, 2010
	↓ Peak amplitude ↓ Decay	
Ca ²⁺ Sparks	↑ Spontaneous sparks ↓ Spark duration	Howlett et al., 2006
	↓ Spark width ↓ Spark amplitude	Zhu et al., 2005
β -adrenergic signaling	↓ Adenylate cyclase activity ↓ cAMP production	Farrell et al., 2008

TABLE 2**Age-associated modifications to components of the EC-coupling pathway**

EC-coupling component	Modification	References
AP	↑ Duration	Wei et al., 1984 Walker et al., 1993 Liu et al., 2000
I _{CaL}	↓ Rate of inactivation ↓ Peak current density ↓ Channel density	Walker et al., 1993 Liu et al., 2000 Josephson et al., 2002 Grandy et al., 2006 Howlett, 2010 Howlett et al., 1992
I _{TO}	↓ Peak current density ↓ Rate of inactivation	Walker et al., 1993 Liu et al., 2000
RyR	↓ Receptor density ↓ Activation via phosphorylation	Assayag et al., 1998 Nicholl et al., 2006 Xu et al., 1998
SERCA2a	↓ Sequestration of Ca ²⁺ ↓ Channel expression ↓ Activation via phosphorylation	Froehlich et al., 1978 Wei et al., 1984 Lompré et al., 1991 Xu et al., 1998
PLB	↑ Protein expression ↓ Inactivation via phosphorylation	Lim et al., 1999 Xu et al., 1998
NCX	↑ Channel activity ↑ Forward mode current	Mace et al., 2003
Calsequestrin	↔	Lompré et al., 1991 Lim et al., 1999
Myosin ATPase	↓ ATPase activity Shift from α to β myosin heavy chain	Buttrick et al., 1991

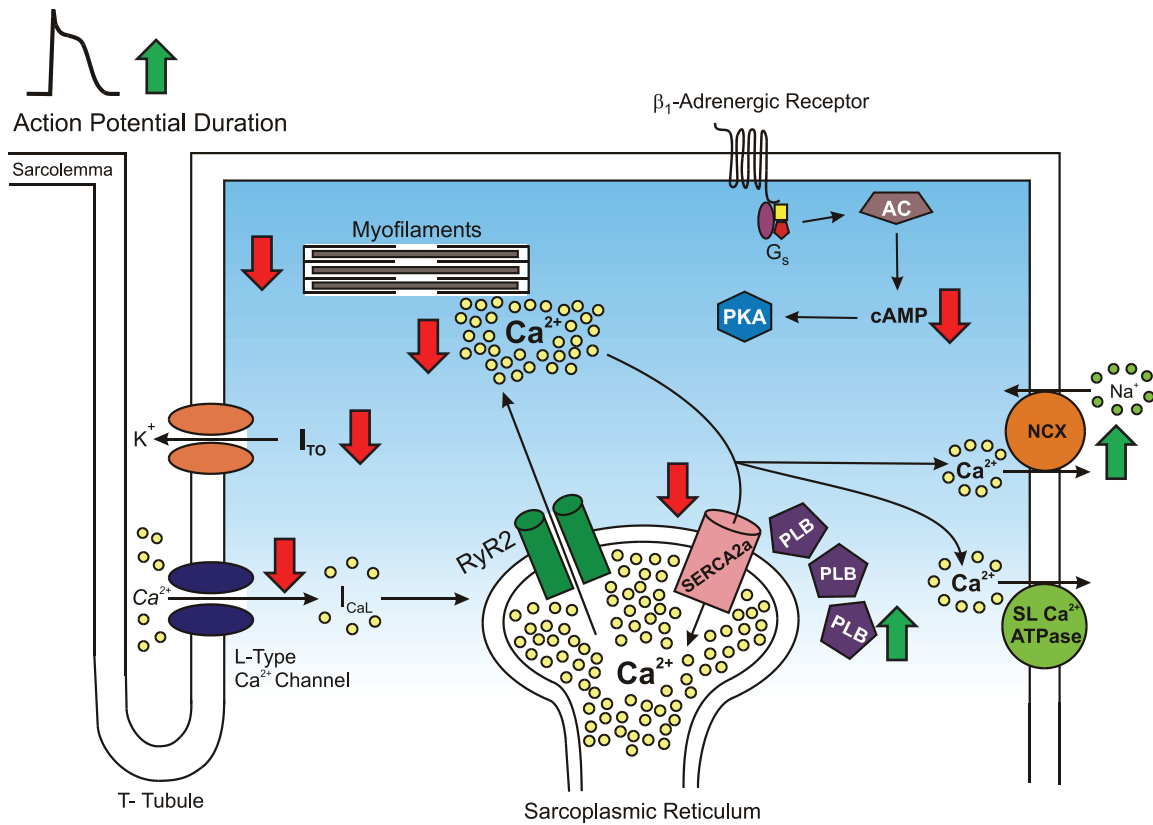


Figure 2. Age-associated changes to the EC-coupling pathway. In the aging heart, action potential duration increases, due to a decrease in the inactivation of L-type Ca²⁺ channels and transient outward current density (I_{TO}). Ca²⁺ current density (I_{CaL}) also decreases in the aging heart resulting in smaller Ca²⁺ transients and contractions. Ca²⁺ transients and contractions are prolonged in aged hearts due to a decline in SERCA2a activity and an increase in PLB expression. An age-related decrease in the effect of β-adrenergic stimulation also occurs, due to a reduction in cAMP production in older hearts. Changes in these mechanisms are thought to be responsible for the decline in cardiac contractile function in the aging heart.

1.4 SEX DIFFERENCES IN CARDIAC FUNCTION

1.4.1 Sex differences in the structure and function of the intact heart

Studies have shown that biological sex affects the normal structure of the human heart. While males and females are born with a similar number of equally sized myocytes, cells from males undergo a greater degree of hypertrophy after puberty (Luczak and Leinwand, 2009). In young adults, heart mass is 15-30% smaller in women and left ventricular chamber size is reduced when compared to men (Legato, 2000; Luczak and Leinwand, 2009; Vasan et al., 1997). With aging, both septal and wall thickness increases in males and females (Luczak and Leinwand, 2009). However, myocardial mass is only lost in older men (Grandi et al., 1992). With age, men lose more ventricular myocytes and the remaining cells exhibit a greater degree of hypertrophy in comparison to women (Olivetti et al., 1995). In women, the number and size of myocytes is preserved with aging (Olivetti et al., 1995). Thus, changes in cardiac structure are more prominent in the hearts of men than women.

Cardiac function also differs between the sexes. Women have higher ventricular ejection fraction at rest (Hanley et al., 1989; Merz et al., 1996), but men are able to increase ejection fraction to a larger extent in response to the greater demand, such as exercise (Hanley et al., 1989; Merz et al., 1996). Women also have higher resting heart rates than men (Hanley et al., 1989; Legato, 2000; Umetani et al., 1998). Prior to puberty, the QT interval is similar between males and females (Rautaharju et al., 1992). However, after puberty corrected QT intervals and action potential durations (APD) become longer in women (Yarnoz and Curtis, 2008). This is due to increasing androgen levels in men, which shorten the APD and the QT interval (Bidoggia et al., 2000). Age-

associated changes in cardiac function also differ between men and women. Left ventricular contractility is greater in older women when compared to older men in studies that have assessed function through echocardiography (Claessens et al., 2007) or cardiac catheterization (Hayward et al., 2001). These results show that there are inherent differences in cardiac function between men and women. Additionally, older women are better able to preserve cardiac contractility in comparison to men.

It is well established that the incidence of cardiovascular disease in premenopausal women is significantly lower than in age-matched men (Czubryt et al., 2006; Lloyd-Jones et al., 1999; Luczak and Leinwand, 2009). However, after menopause women exhibit an increase in the susceptibility to cardiovascular disease (Czubryt et al., 2006; Harman, 2006; Luczak and Leinwand, 2009). Moreover, there are differences in the type of cardiovascular diseases to which older men and women are susceptible (Czubryt et al., 2006; Huxley, 2007; Luczak and Leinwand, 2009; Yarnoz and Curtis, 2008). Men are at a greater risk than premenopausal women for developing hypertension, yet after menopause, this sex difference is lost (Messerli et al., 1987; Staessen et al., 1989). The incidence of specific arrhythmias also differs between men and women. The risk of developing atrial fibrillation is greater in men, while the incidence of arrhythmias associated with long QT syndrome, such as Torsades de Pointes, is higher in women (Yarnoz and Curtis, 2008). Women are also less likely to experience heart failure than men (Gottdiener et al., 2000), and the type of heart failure differs between the sexes. Heart failure with systolic dysfunction resulting in reduced ejection fraction is more common in older men, while heart failure with preserved ejection fraction but diastolic dysfunction occurs in older women (Regitz-Zagrosek et al.,

2007). These observations suggest that there are fundamental differences in cardiac function between men and women, and differences between the sexes influence the structure and function of the heart later in life. Given these observations, some recent studies have explored the cellular mechanisms underlying sex differences in cardiac function in the aging heart. However, our understanding of the impact of biological sex on the heart is far from complete.

1.4.2 Sex differences in cardiomyocyte function

While sex differences in the heart are apparent, information regarding electrical and contractile function in the hearts of males and females is limited. Studies in animal models have shown that, in intact hearts, responses are smaller and slower in female rats in comparison to males (Schaible and Scheuer, 1984). Similarly, studies in cardiac tissue have shown smaller, slower responses in female rats in comparison to males, and these differences are more apparent under conditions of higher demand, such as at faster stimulation frequencies (Leblanc et al., 1998; Petre et al., 2007). Within individual myocytes, peak contractions and Ca^{2+} transients are also smaller in individual myocytes from females than males (Curl et al., 2001; Farrell et al., 2010; Grandy and Howlett, 2006; Howlett, 2010). In addition, the rates of contraction and relaxation, as well as the decay of the Ca^{2+} transient are slower in female myocytes than male myocytes (Curl et al., 2001; Farrell et al., 2010; Grandy and Howlett, 2006; Howlett, 2010). This suggests that sex differences in cardiac contractile function may originate at the level of the myocyte. Various components of the EC-coupling pathway have been investigated to explain differences in responses between the sexes.

Action potentials and ionic currents have been investigated to determine whether they account for contractile differences between the sexes. Studies have shown that the APD is longer in cells from females when compared to cells from males (Brouillette et al., 2005; Trepanier-Boulay et al., 2001; Xiao et al., 2006), although this is not observed in all models (Brouillette et al., 2007; James et al., 2004). Higher androgen levels in male animals have been shown to contribute to abbreviation of the APD (Brouillette et al., 2003). In addition, prolonged APD in females may be due to a decrease in K^+ channel expression and a reduction in K^+ current density (Brouillette et al., 2005; James et al., 2004; Trepanier-Boulay et al., 2001). There is evidence that the ultra-rapid delayed rectifier, the delayed rectifier, and the inward rectifier currents are reduced in female mice and guinea pigs when compared to age-matched males (Brouillette et al., 2005; James et al., 2004; Trepanier-Boulay et al., 2001), although this remains controversial (Brouillette et al., 2007). Sex differences in the Na^+ currents have also been reported. In the canine heart, Na^+ current amplitude is higher in males than females on both the endocardial and epicardial surfaces, but not in the mid-myocardium (Barajas-Martinez et al., 2009). This suggests that biological sex may also affect the dispersion of ionic currents in the heart (Barajas-Martinez et al., 2009). Interestingly, the impact of sex on I_{CaL} remains unclear. Several studies have reported that peak I_{CaL} density is not influenced by biological sex (Brouillette et al., 2007; Farrell et al., 2010; Grandy and Howlett, 2006; Howlett, 2010; LeBlanc et al., 1998; Trepanier-Boulay et al., 2001), but some studies have shown that I_{CaL} is smaller (James et al., 2004; Liew et al., 2004) or larger (Vizgirda et al., 2002; Xiao et al., 2006) in cells from females in comparison to males. This may be due to variance in L-type Ca^{2+} current density in the different layers

of the heart in females and males (Pham et al., 2002; Xiao et al., 2006). Taken together these findings suggest that biological sex affects ion channels and can modulate cardiac action potential duration.

Intracellular Ca^{2+} handling mechanisms have also been compared in males and females, but to a limited extent. SR Ca^{2+} content does not appear to differ between the sexes under basal conditions (Chen et al., 2003; Curl et al., 2001; Farrell et al., 2010; Grandy and Howlett, 2006; Howlett, 2010). However, EC-coupling gain is reported to be less in females than in males (Farrell et al., 2010; Howlett, 2010). This may contribute to smaller Ca^{2+} transients and contractions observed in cells from females when compared to males (Farrell et al., 2010; Howlett, 2010). Further, Ca^{2+} sparks may differ between the sexes. Only one study has examined the impact of biological sex on Ca^{2+} sparks and has shown that Ca^{2+} sparks are smaller and slower in cells from females in comparison to males, even though the occurrence of spontaneous sparks is similar between the sexes (Farrell et al., 2010). Reduced gain and unitary Ca^{2+} release in females suggest that there is a difference in the modulation of RyR between the sexes. This may explain the smaller Ca^{2+} transients and contractile responses in cells from female animals. One possibility is that the female sex hormone estrogen may modulate Ca^{2+} handling. However, whether estrogen plays a role in suppressing SR Ca^{2+} release has yet to be determined.

While sex differences in cardiac function in young adult hearts are evident, an understanding of the underlying mechanisms is incomplete. Further, very few animal studies of aging have considered sex as a variable, and most studies have examined only male animals or have not identified sex when investigating cardiac aging. Thus, little is known about the effect of age on cardiac contractile function in hearts from females. The

following section outlines current knowledge of the impact of age on the heart in males and females.

1.4.3 Age-related differences in cardiac structure and function in males and females

Biological sex can have an impact on age-associated changes that occur in the heart. Similar to observations in older men and women (Olivetti et al., 1995), cellular hypertrophy differs between the sexes in animal models. Age-associated cellular hypertrophy is much more prominent in myocytes from males than females in both aged rodents and monkeys (Forman et al., 1997; Grandy and Howlett, 2006; Howlett, 2010; Zhang et al., 2007). Age-related changes in cardiac function are also influenced by the sex of the animal. *In vivo* assessment of ventricular function via echocardiography shows that left ventricular (LV) fractional shortening is significantly lower in aged male than aged female rats (Forman et al., 1997). In addition, studies in intact monkey hearts show that contractile responses to β -adrenergic stimulation are preserved with age in females, but the ability of β -adrenergic stimulation to increase contractility is impaired in older males when compared to young adult males (Takagi et al., 2003).

Sex differences are also present in cardiomyocytes from aging hearts. Although contractions are significantly larger in cells from young animals, the size of responses declines with age in cells from males (Grandy and Howlett, 2006; Howlett, 2010; Lim et al., 2000; Xiao et al., 1994). Conversely, while contractile responses in myocytes from younger female animals are smaller than those from males, females do not show an age-associated decline in cardiac contractile function (Dibb et al., 2004; Farrell et al., 2010;

Grandy and Howlett, 2006; Howlett, 2010). There is evidence that these differences are attributable to age- and sex-dependent changes in Ca^{2+} transients. Peak Ca^{2+} transients are larger in young adult males than in females, but Ca^{2+} transient size declines in older males (Grandy and Howlett, 2006; Howlett, 2010; Isenberg et al., 2003; Lim et al., 2000). By contrast, Ca^{2+} transient amplitudes do not decline with age in females (Dibb et al., 2004; Grandy and Howlett, 2006; Howlett, 2010). Previous studies have also shown that the time course of contractions and Ca^{2+} transients is modified by age and sex. Contractile responses and Ca^{2+} transients are faster in younger male animals than in females, but these responses become prolonged in cells from aged males (Grandy and Howlett, 2006; Lim et al., 2000; Xiao et al., 1994). Conversely, the speed of contractions and Ca^{2+} transients are not affected by age in female hearts (Grandy and Howlett, 2006; Howlett, 2010). These findings suggest that a decline in cardiac contractile function is more pronounced in males than females. However, previous rodent studies have only compared responses in cells from 3-6 month old animals with responses in 24 month old animals. As females age, there is a greater susceptibility to cardiovascular dysfunction. However, whether cardiac contractile function and Ca^{2+} handling deteriorates in myocytes from females later in life has not been investigated.

Although limited information is available, some studies have compared components of the EC-coupling pathway in myocytes from older male and female animals. Whether peak I_{CaL} density differs between the sexes in the aging heart remains controversial. Some studies have shown that I_{CaL} density declines significantly with age in males (Grandy and Howlett, 2006; Howlett, 2010; Liu et al., 2000), but others have shown no change with age (Walker et al., 1993; Xiao et al., 1994). I_{CaL} does not decline

with age in cells from female mice and sheep (Dibb et al., 2004; Grandy and Howlett, 2006), but this may depend on the model as a decrease in I_{CaL} does occur in cardiomyocytes from female rats (Howlett, 2010). Similarly, whether intracellular Ca^{2+} content changes with age depends on the sex of the animal. SR Ca^{2+} stores decrease with age in male rodents (Grandy and Howlett, 2006; Howlett, 2010). By contrast, SR Ca^{2+} stores actually increase with age in myocytes from female rats, mice and sheep (Dibb et al., 2004; Grandy and Howlett, 2006; Howlett, 2010). In addition to these findings, EC-coupling gain has been shown to decline with age in myocytes from male rats, but not in cells from female rats or sheep (Dibb et al., 2004; Howlett, 2010). Changes in gain may underlie the age-associated decline in Ca^{2+} transients and contractions in cells from the aging male heart. However, the mechanisms responsible for preserving contractile function in the aging female heart have not been investigated. If estrogen suppresses Ca^{2+} release in younger females, an age-associated decline in estrogen levels may alleviate contractile suppression to maintain cardiac function. However, it is not known whether contractile function and Ca^{2+} handling is preserved in the female heart later in life. In addition, the effect of long-term estrogen reduction on Ca^{2+} handling mechanisms such as I_{CaL} , EC-coupling gain, and SR Ca^{2+} stores in myocytes from aged females has not been determined. Also, it remains unknown whether long-term estrogen deprivation impairs Ca^{2+} homeostasis and leads to a deterioration in contractile function, like in older males.

Thus, our understanding of the impact of age on the hearts of male and female animals is incomplete. Yet, the investigation of sex differences in animal models have stemmed from observations of differences in heart function and cardiovascular disease in men and women. We know that the incidence of cardiovascular dysfunction is lower in

premenopausal women than age-matched men (Czubryt et al., 2006; Lloyd-Jones et al., 1999; Luczak and Leinwand, 2009). However, as women undergo menopause, the incidence of cardiovascular disease significantly increases (Czubryt et al., 2006; Huxley, 2007; Luczak and Leinwand, 2009; Yarnoz and Curtis, 2008). These observations suggest that estrogen may play a cardioprotective role in the aging female heart. However, the protective effects of estrogen on the cardiovascular system remain controversial (Hulley et al., 1998; Anderson et al., 2004). As detailed in the section below, investigations in the clinic and within the laboratory have explored the effects of estrogen on the female heart.

1.5 ESTROGEN AND THE HEART

1.5.1 Clinical studies of hormone replacement therapy

The incidence of cardiovascular disease in women significantly rises after the onset of menopause (Harman, 2006; Luczak and Leinwand, 2009). Since the levels of estrogen and progesterone decline during menopause, it has been speculated that female sex steroids play a role in cardioprotection in the female heart (Luczak and Leinwand, 2009). Thus, clinical and basic research studies have investigated whether hormone replacement therapy (HRT) in post-menopausal women and in animal models of menopause would restore the cardioprotection observed in pre-menopausal women.

Clinical studies of the benefits of HRT have yielded mixed results. More than 50 observational studies have reported that HRT reduces cardiovascular incidents (Hodis et al., 2002). An early study examined HRT in women between 45 and 69 years of age and reported that long term HRT did not cause stroke or myocardial infarction (Thompson et

al., 1989). Another early observational study showed that HRT actually decreases mortality in postmenopausal women (Henderson et al., 1991). In assessing women who had been taking HRT for more than 15 years, it was reported that there was a 40% reduction in overall mortality in those taking HRT in comparison to untreated women (Henderson et al., 1991). Further, women treated with HRT were shown to have a 20% decrease in the risk of lung and breast cancer in this early study, although an increase in the risk of endometrial cancer was also noted (Henderson et al., 1991).

In addition to these early findings, larger observational studies have reached similar conclusions regarding HRT. The Iowa Women's Health Study, which examined more than 40,000 women between 55 and 69 years of age, assessed the effect of HRT on the risk of various diseases and mortality (Folsom et al., 1995). This study showed that women treated with HRT had a 20% decrease in the risk of coronary heart disease, cancer, and death. The risk for other cardiovascular diseases was also decreased more than 50%. However, there was a 24% increase in the risk of breast cancer and a 30% increase in the risk of stroke for women treated with HRT. Further, the risk of endometrial cancer was substantially higher in women with an intact uterus taking HRT when compared to untreated patients (Folsom et al., 1995). While HRT did increase the risk of developing several types of cancer, this study concluded that HRT decreased cardiovascular events and increased longevity in older women (Folsom et al., 1995).

The largest observational study, the Nurses' Health Study, examined the effects of HRT on cardiovascular events in over 120,000 female nurses. Subjects were 30 to 55 years of age and were followed for up to 20 years (Grodstein et al., 2000). Subjects with an intact uterus were treated with a combination of estrogen and progestin, and those

without a uterus were treated with estrogen alone. The results showed that women treated with HRT showed a 40% decrease in the incidence of major coronary events (Grodstein et al., 2000; Grodstein et al., 1996). Additionally, subjects taking HRT observed a 37% and 50% reduction in the risks of overall mortality and mortality from coronary heart disease, respectively, when compared to untreated women (Grodstein et al., 1997). However, the incidence of stroke was higher in subjects taking a higher dose of estrogen (0.625 mg vs. 0.3 mg), or in subjects taking the combined estrogen and progestin therapy. In addition, the risk of developing breast cancer increased by at least 30% in women taking HRT (Grodstein et al., 1996). Overall, the vast sample size and duration of this study provides convincing evidence that HRT is protective against cardiovascular events in older women.

The Nurses' Health Study also showed that HRT could benefit patients with established cardiovascular disease (Grodstein et al., 2001). Studies in 2489 postmenopausal women with previously diagnosed coronary heart disease were assessed as part of the Nurses' Health Study. The results showed that an initial non-significant increase in the risk of recurrent major coronary events was present in patients within the year following initiation of HRT, but a significant decrease in the risk of cardiovascular events occurred with longer term HRT (Grodstein et al., 2001). Another observational study also showed that HRT was beneficial in postmenopausal women that previously had a myocardial infarction. Over 114,000 women that were 55 years of age or older with confirmed myocardial infarction were assessed when presented at hospitals participating in the National Registry of Myocardial Infarction-3 (Shlipak et al., 2001). At the time of hospitalization, mortality was evaluated in women currently using HRT

versus non-users. Unadjusted mortality was 7.4% in patients taking HRT, and 16.2% in non-users. After adjustments were made, patients treated with HRT maintained an improved rate of survival (Shlipak et al., 2001). Both of these observational studies suggest that HRT may benefit postmenopausal women with established cardiovascular conditions by reducing recurrent adverse cardiovascular events and increasing survival after myocardial insult.

While many observational studies have shown that HRT lowers the risk for coronary heart disease and provides cardioprotection in older women, other studies have reported that HRT may be detrimental. Studies suggest that if HRT is given for over 10 years, the risk of breast cancer increases by 20-30% (Colditz et al., 1995; Schairer et al., 2000). HRT is also associated with a slight increase in the risk of venous thromboembolism (Harman, 2006). Furthermore, even observational studies that showed cardioprotection indicate that susceptibility to several types of cancer and stroke increases in patients treated with HRT. As variability and biases in observational studies can skew the results (Harman, 2006), randomized clinical trials have been conducted to control for these factors. However, findings from these randomized clinical trials have conflicted with those of observational studies.

The two major randomized clinical trials that investigated the effects of HRT on coronary heart disease were the Heart and Estrogen Progestin Replacement Study (HERS) and the Women's Health Initiative (WHI). The HERS study was a randomized, blinded clinical trial conducted prior to the WHI (Hulley et al., 1998). Studies in 2763 postmenopausal women between 55-79 years of age with documented coronary heart disease were randomized and treated with either a combined estrogen and progestin HRT

or a placebo. Subjects were followed for a mean time of 4.1 years. The results showed that HRT increased the risk of venous thromboembolism and gallbladder disease, but had no significant effect on the incidence of stroke, cancer or mortality (Hulley et al., 1998). Importantly, HERS also showed that HRT provided no cardiovascular benefit to patients with established coronary heart disease. In fact, HRT resulted in an increase in the risk of cardiovascular events in the early years of treatment, but this decreased over time. Thus, the HERS trial concluded that HRT was not cardioprotective in women with coronary heart disease (Hulley et al., 1998).

To date, the Women's Health Initiative (WHI) has been the largest clinical trial to assess the effects of HRT on the heart (Rossouw et al., 2002). Over 26,000 postmenopausal women between 50-79 years of age were treated with HRT (either a combination of estrogen and progestin, or estrogen alone) or a placebo. While the duration of this randomized, double-blinded clinical trial was set for 8.5 years, the study was terminated early (after 5.2 years) in women being treated with combined estrogen and progestin. Surprisingly, the study reported that the risk of coronary heart disease actually increased by 29% and the incidence of total cardiovascular disease increased by 22% in women taking estrogen and progestin in comparison to placebo. The study also showed that there was a 26% increase in the risk of breast cancer and a 40% increase in the risk of stroke (Rossouw et al., 2002). There was also an increase in the risk of pulmonary embolism in the treatment group. It is important to note that some benefits were shown in women taking HRT, such as a 24% decrease in the risk of fractures and a 37% decrease in the risk of colon cancer (Rossouw et al., 2002).

The WHI trial was allowed to continue in subjects treated with estrogen alone, as no detrimental effects were initially observed. Unfortunately, the estrogen only arm of the study was also prematurely halted after 6.8 years (Anderson et al., 2004). While patients treated with estrogen as a HRT showed a 23% decrease in the risk of breast cancer, the risk of stroke rose by 40% and the risk of thromboembolic disease increased by 30%. Additionally, subjects taking HRT did not benefit from any additional cardiovascular protection when compared to placebo controls (Anderson et al., 2004). In light of these findings, the WHI concluded that HRT should not be recommended to postmenopausal women due to the increased risk of adverse events and lack of cardiovascular benefits (Anderson et al., 2004).

One of the main criticisms of the HERS and WHI trials were the age of the women enrolled in the studies. The mean age of patients in the HERS trial was 67 years and those in the WHI trial were 63 years (Harman, 2006). Overall, this means that HRT was being reintroduced to women who had been postmenopausal for approximately a decade. This has prompted a new study designed to determine whether the timing of HRT is important. This study is called the Kronos Early Estrogen Prevention Study (KEEPS) (Harman et al., 2005). The focus of KEEPS will be to assess estrogen HRT in 720 women between the ages of 42 and 58 years, and are between 6 to 36 months post menses. Treating patients early in menopause may provide more beneficial cardiovascular results. In the WHI, women 50–59 years of age that were treated with estrogen as a HRT had a lower risk of cardiovascular disease events than women randomized to placebo (Anderson et al., 2004). This suggests that women treated with

estrogen at an early age may gain the most benefit from HRT (Harman et al., 2005). KEEPS was set to conclude in 2010, and the results are yet to be published.

These controversial findings of HRT from observation studies and clinical trials have led to considerable interest in exploring the effects of estrogen on the cardiovascular system. Animal models have been used to identify the specific receptors and effects of estrogen in the heart. The sections below describe our current knowledge of the signaling pathways by which estrogen exerts its biological effects on the heart and the mechanisms by which estrogen may affect cardiac function.

1.5.2 Sex steroid hormones and the cardiovascular system

Given the differences in cardiovascular disease between the sexes and potential protective effect of estrogen on the cardiovascular system, there is considerable interest in understanding the effects of sex steroid hormones on the cardiovascular system. The primary sex steroid hormones are estrogen, progesterone, and testosterone. These hormones are produced from cholesterol and play critical roles in the development and maturation of males and females, and in regulation of the menstrual cycle in women (Czubryt et al., 2006). The major receptors for these hormones are present in several organs and tissues. Interestingly, the two forms of the estrogen receptor (ER- α and ER- β), progesterone receptors A and B, and the androgen receptor are present within cardiomyocytes and the vasculature (Goldstein et al., 2004; Grohe et al., 1997; Lizotte et al., 2009; Marsh et al., 1998). These receptors have been shown to signal via both genomic and non-genomic pathways (Czubryt et al., 2006). There is also evidence that a G-protein coupled receptor with a high affinity for estrogen (known as GPER or GPR30)

is present in the heart, and may modulate rapid signaling events (Deschamps and Murphy, 2009).

The primary estrogens in humans are estrone, estrinol, and the most active form 17 β -estradiol (Czubryt et al., 2006). All three estrogens are synthesized from precursor steroid hormones. The hormone 17 β -estradiol is generated from testosterone by the actions of the aromatase enzyme. In premenopausal women, estrogen is predominately synthesized in the ovaries. However, after menopause peripheral tissues with aromatase activity, such as adipose tissue, become a significant source of estrogen as ovarian-derived hormone production ceases (Purohit and Reed, 2002; Simpson, 2003). While all three estrogens may affect cardiovascular function, most studies have focused on the actions of 17 β -estradiol on the heart and vasculature.

The effects of estrogen on heart are primarily mediated by the estrogen receptor (ER) (Murphy, 2011). This nuclear hormone receptor has two forms, the 67 kDa ER- α and the 59 kDa ER- β . ER- α and ER- β are highly homologous. The ligand-binding and DNA-binding domains are highly conserved between ER- α and ER- β (Murphy, 2011). However, ER- α and ER- β differ at their transcriptional control domains, the region where co-regulators associate with the receptor (Murphy, 2011). Variation at this domain is thought to be responsible for the differing effects of ER- α and ER- β . Levels of ER- α and ER- β also vary depending on tissue, and are influenced by age and gender. For instance, ER levels in the vasculature differ between premenopausal and postmenopausal women. ER- α levels are 33% lower in postmenopausal women than in premenopausal women (Gavin et al., 2009). Interestingly, there is also evidence that ER levels fluctuate in relation to the menstrual cycle (Gavin et al., 2009). In cardiac myocytes, ER- β

expression is similar in male and female rats, but ER- α levels are greater in females (Grohe et al., 1998). ER levels also change in conjunction with cardiovascular disease; ER- α and ER- β expression increases in men and women with aortic valve stenosis (Nordmeyer et al., 2004). Unfortunately, the importance of differential ER expression and signaling in the heart has yet to be fully clarified (Murphy, 2011).

Estrogen has been shown to act via genomic and non-genomic signaling pathways. This mechanism of action is similar for both ER- α and ER- β isoforms. To initiate genomic signaling, estrogen binds to the ligand-binding domain of the ERs (Czubryt et al., 2006; Murphy, 2011). In the absence of hormone, the ERs are localized in the cytosol. Estrogen binding causes a conformational change in the ERs, leading to their dimerization and translocation to the nucleus (Czubryt et al., 2006; Murphy, 2011). Once in the nucleus, the ERs bind to estrogen response elements (EREs) on DNA. In turn, ERs recruit the transcriptional machinery, coactivators and corepressors resulting in an increase or decrease in gene expression (Czubryt et al., 2006; Murphy, 2011). In genes that are regulated by the ER but do not contain an ERE, ER can bind to DNA indirectly via transcription factors (Murphy, 2011). The ER can also be phosphorylated allowing it to bind to ERE or bind DNA indirectly via transcription factors to regulate gene transcription even in the absence of ligand binding (Murphy, 2011).

Nuclear ER- α and ER- β can also signal in a non-genomic manner. This mechanism of action is similar in ER- α and ER- β isoforms. Estrogen can bind to ERs localized to the plasma membrane and activate the phosphatidylinositol 3-kinase (PI3K) signaling pathway (Simoncini et al., 2000). In brief, PI3K activates protein kinase B (Akt). Akt can subsequently activate nitric oxide synthase (NOS) to produce nitric oxide

(NO) (Furukawa and Kurokawa, 2008; Murphy, 2011). NO can then modulate components of the EC-coupling pathway, such as ion channels (Furukawa and Kurokawa, 2008). PI3K has also been shown to regulate cAMP levels, which would modulate PKA activity within ventricular myocytes (Kerfant et al., 2005; Kerfant et al., 2006).

Estrogen can also bind to ERs to activate a second non-genomic signaling pathway that acts through mitogen-activated protein kinases (MAPK), specifically the extracellular signal-regulated kinases (ERK) (Endoh et al., 1997; Watters et al., 1997). When ERK becomes activated, it translocates to the nucleus and activates transcription factors required for gene expression (Furukawa and Kurokawa, 2008). Recently, it has been shown that estrogen also binds to an orphan G-protein-coupled receptor known as GPER (Revankar et al., 2005), and that GPER is expressed in cardiac tissue (Deschamps and Murphy, 2009). When estrogen binds to GPER, it can also activate the PI3K and MAPK non-genomic signaling pathways (Murphy, 2011). The binding of estrogen to the various ERs in the heart is thought to have important effects on cardiac function as outlined in the next section.

1.5.3 Estrogen and the heart

Many studies have shown that estrogen has important effects on the structure and function of the heart in the setting of cardiovascular disease. Estrogen has been shown to decrease apoptosis and prevent cardiac remodeling in myocardial infarction (Murphy, 2011). Adult myocytes isolated from infarcted rat hearts showed less apoptosis and greater survival in culture when treated with estrogen when compared to untreated

controls (Brinckmann et al., 2009). Other studies have shown that 17 β -estradiol treatment of ovariectomized (OVX) mice reduces cardiomyocyte apoptosis following coronary artery-ligation induced myocardial infarction (Patten et al., 2004). Further, studies in OVX rabbits have shown that *in vivo* administration of estrogen prior to coronary artery-ligation induced myocardial infarction can reduce infarct size (Booth et al., 2003). This may be due to the ability of estrogen to activate survival signals within cardiomyocytes. Pressure overload in OVX rats results in a significant decrease in the prosurvival kinase, Akt, when compared to sham controls (Bhuiyan et al., 2007). Conversely, treatment of cultured neonatal rat cardiomyocytes with 17 β -estradiol has been shown to rapidly increase the activation of Akt (Patten et al., 2004). Increased activation of Akt also occurs *in vivo* in mice supplemented with 17 β -estradiol prior to coronary artery ligation (Patten et al., 2004). Further, premenopausal women have greater Akt activity in their cardiac myocytes when compared to men or to postmenopausal women (Camper-Kirby et al., 2001). Together, these studies suggest that the increased expression of the prosurvival kinase Akt in the female heart may contribute to the cardioprotection observed in cardiovascular disease models.

Estrogen has also been shown to prevent cardiac hypertrophy. In female mice, less cardiac hypertrophy occurs in comparison to males after transaortic constriction, which induces pressure overload (Fliegner et al., 2010; Skavdahl et al., 2005). Interestingly, studies also show that knockout of ER- β , but not ER- α , in female mice abolishes the protective effects of female sex on cardiac hypertrophy (Fliegner et al., 2010; Skavdahl et al., 2005). Similarly, OVX and ER- α knockout female mice treated with 17 β -estradiol showed reduced cardiac hypertrophy after transaortic constriction in

comparison to untreated controls (Babiker et al., 2006; Donaldson et al., 2009; van Eickels et al., 2001). However, 17 β -estradiol had no effect on cardiac hypertrophy in ER- β knockout mice (Babiker et al., 2006). It has been suggested that estrogen may prevent induction of the calcineurin stress response pathway that leads to a hypertrophic response. Studies have shown that 17 β -estradiol activates the calcineurin antagonist known as the modulatory calcineurin-interacting protein 1 (MCIP1) (Pedram et al., 2005; Pedram et al., 2008). Additionally, OVX mice treated with 17 β -estradiol showed a reduction in calcineurin A levels in comparison to placebo-treated females (Donaldson et al., 2009). Treatment with an ER antagonist or knockout of ER- β prevented 17 β -estradiol mediated decreases in calcineurin levels and activity (Donaldson et al., 2009; Pedram et al., 2008). Overall, these findings suggest that 17 β -estradiol acts through the estrogen receptor to prevent cardiomyocyte apoptosis and hypertrophy. This likely occurs by activating anti-apoptotic Akt signaling and inhibiting stress response signaling through the calcineurin pathway.

Estrogen has also been shown to affect cardiac function. As mentioned above, contractile function in intact hearts and cardiac tissue is greater in male than in female rats (Curl et al., 2008; Leblanc et al., 1998; Petre et al., 2007; Schaible and Scheuer, 1984). Interestingly, a recent study also showed that the degree of left ventricular fractional shortening as determined by echocardiography is greater in rats subjected to OVX than in controls (Stice et al., 2011). These findings suggest estrogen may suppress contractility. Similar effects are evident at the level of the individual myocyte. Cellular contractions from OVX animals are significantly larger when compared to sham-controls (Curl et al., 2003; Wu et al., 2008). OVX has also been shown to increase the size of

Ca²⁺ transients (Curl et al., 2003; Kravtsov et al., 2007; Ma et al., 2009; Wu et al., 2008). In addition, the speed of contractile responses is faster in myocytes from OVX animals (Curl et al., 2003). OVX also increases the rates of rise and decay of the Ca²⁺ transient when compared to sham (Curl et al., 2003; Kravtsov et al., 2007). Interestingly, the enhanced responses observed with OVX are reversed with estrogen replacement (Curl et al., 2003; Kravtsov et al., 2007; Wu et al., 2008). Taken together, these findings suggest that removal of ovarian-derived estrogen increases the speed and size of contractile responses and Ca²⁺ transients in the female heart.

Estrogen may affect cardiac contractile function by modulating the underlying EC-coupling pathway. Estrogen has been shown to affect ion channels in the heart. Acute application of estrogen to isolated ventricular myocytes from guinea pigs has been shown to reduce I_{CaL} (Jiang et al., 1992). Studies of chronic estrogen reduction have shown that I_{CaL} and L-type Ca²⁺ channel density is increased in ER knockout mice in comparison to control (Johnson et al., 1997). Further, OVX increases the expression of Cav1.2, the main L-type Ca²⁺ channel subunit in rat ventricular myocytes (Chu et al., 2006). Estrogen may also affect potassium channels. ER knockout mice show an increase in APD and a prolongation of the QT interval without significant changes in PQ or QRS intervals (Johnson et al., 1997). Estrogen has also been shown to downregulate Kv1.5 and Kv4.3 subunits resulting in smaller transient outward (I_{TO}) and delayed rectifier (I_{Kur}) potassium currents (Saito et al., 2009; Trepanier-Boulay et al., 2001), which would prolong APD. Taken together these finding suggest that estrogen may regulate Ca²⁺ and K⁺ channels by decreasing channel expression and ionic current density in the female heart.

Estrogen may also affect Ca^{2+} storage and Ca^{2+} removal mechanisms. One study has shown that OVX significantly increased the size of intracellular Ca^{2+} stores in the SR (Kravtsov et al., 2007). This suggests that reduced estrogen levels may promote SR Ca^{2+} loading. Investigation of proteins involved in Ca^{2+} removal have shown that while SERCA2a, PLB, and NCX expression are unchanged or in some instances reduced with OVX, the activity of the NCX may be elevated (Bupha-Intr et al., 2009; Bupha-Intr and Wattanapermpool, 2006; Chu et al., 2006; Kravtsov et al., 2007). As responses become faster when estrogen is removed, changes in NCX activity may contribute to enhanced decay rates observed in OVX animals.

Taken together, these findings suggest that estrogen suppresses cardiac contractile function at the level of the individual cardiomyocyte by modulating components of the EC-coupling pathway. However, our knowledge of the effects of estrogen on specific EC-coupling mechanisms in cardiomyocytes is still limited. As premenopausal women have a lower incidence of cardiovascular disease in comparison to postmenopausal women (Czubryt et al., 2006; Luczak and Leinwand, 2009), female sex steroids may play a role in protecting the aging heart. One possibility is that estrogen suppresses Ca^{2+} release, which prevents Ca^{2+} overload and Ca^{2+} dysregulation in the setting of cardiovascular disease. Yet, the effects of estrogen reduction on specific aspects of the EC-coupling pathway such as the relationship between I_{CaL} , EC-coupling gain, Ca^{2+} sparks and SR Ca^{2+} content have not been assessed. It is also possible that estrogen deprivation impairs Ca^{2+} homeostasis and causes contractile deficits, leaving the aging female heart vulnerable to cardiovascular dysfunction. However, the impact of both short and long term estrogen reduction on cardiac contractile function in the female heart has

not been compared. In addition, it is unknown whether short and long term estrogen deprivation lead to detrimental electrical and contractile abnormalities in cells from female hearts. The overall goal of this thesis was to investigate the effects of both natural aging and estrogen deprivation in the female myocardium to improve our understanding of the role of female sex hormones in the adult and aging heart.

1.6 HYPOTHESES

This thesis will evaluate these specific hypotheses:

- 1) Extreme old age results in deterioration of cardiac contractile function in the female heart, as estrogen levels have naturally declined with age. These responses mirror those observed in age-matched males.
- 2) Short term OVX enhances cardiac contractile function by effects on specific components of the EC-coupling pathway.
- 3) Long term OVX impairs cardiac contractile function and disrupts Ca^{2+} handling in the aging female heart.

CHAPTER 2 MATERIALS AND METHODS

2.1 MATERIALS

2.1.1 Animals

All experimental protocols involving animals were approved by the Dalhousie University Committee on Laboratory Animals and conformed to the guidelines published by the Canadian Council on Animal Care (CCAC; Ottawa, ON: Vol. 1, 2nd edition, 1993; Vol. 2, 1984). Male and female C57BL/6 mice were obtained from Charles River Laboratories (St. Constant, QC). For experiments investigating the effect of ovariectomy (OVX), female mice were subjected to either a bilateral OVX or control-sham surgery at Charles River Laboratories approximately one month after birth. In male and female experiments, animals were investigated at two ages: young adults (~7 mos) or senescent (~32 mos). For experiments investigating sham and OVX animals, mice were aged to either young adult (~8 mos) or old (~24 mos). Animals were group housed in micro-isolator cages at the Carleton Campus Animal Care facility at Dalhousie University. All mice were allowed a minimum of 24 hours to acclimatize to the animal care facility before use in experiments. Mice were maintained on a 12-hour light/dark cycle and had free access to food and water. At all times a sentinel mouse was present in the housing area to confirm the health of the environment within the facility. On experimental days, one mouse was selected at random, placed in a clean cage in the animal care facility, and transported to the laboratory.

2.1.2 Chemicals

Lidocaine, HEPES buffer, EGTA, MgCl₂, anhydrous DMSO, 4-aminopyridine

and caffeine were purchased from Sigma-Aldrich Canada Ltd. (Oakville, ON, Canada). Fura-2 AM and fluo-4 AM were obtained from Invitrogen Inc. (Burlington, ON, Canada). All other chemicals were purchased from BDH Inc (Toronto, ON, Canada). Stock solutions of Fura-2 AM were prepared in anhydrous DMSO, with a final concentration of 0.2% DMSO. Fluo-4 AM was prepared as a stock solution in fetal bovine serum supplemented with Pluronic® F-127 in anhydrous DMSO, with a final DMSO concentration of 2.4%. Fura-2 AM and fluo-4 AM were stored at -20°C until use. All other chemicals were dissolved in deionized water.

2.2 METHODS

2.2.1 Survival curve

Survival data was collected from male and female C57BL/6 mice housed in the aged mouse colony at Dalhousie University. Mortality was recorded as sudden death or when animals had to be euthanized as a humane endpoint, such as in cases of illness as determined by the university veterinarian. Mice were followed over a period of approximately 1100 days and Kaplan–Meier survival curves were generated from mortality data. Mice that were used in experiments were censored and included in the analysis as censored data. Statistical differences in survival were compared using a log-rank test in SigmaStat (version 3.1; Systat Software, Inc., Point Richmond, CA).

2.2.2 Ventricular myocyte isolation

To anaesthetize mice and prevent blood coagulation during myocyte isolation,

sodium pentobarbital (220 mg/kg; Pharmaceutical Partners of Canada, Richmond, ON) and heparin (3000 U/kg; CDMV, Saint-Hyacinthe, QC) were co-administered via intraperitoneal injection. Mice were maintained in a covered cage until the induction of anaesthesia (2-5 minutes). Anaesthesia was determined by absence of pedal withdrawal and corneal reflexes.

Following anaesthesia, the animal was weighed, and then placed on a surgical table in a supine position. Forelimbs were secured with clamps to maintain animal position. The thoracic cavity was opened with an incision between the diaphragm and the ribs. The rib cage was cut laterally on both the left and right side, then folded back and clamped to expose the heart. A silk suture (A-55, Ethicon Inc., Somerville, NJ) was placed around the aorta and positioned near the aortic trunk. The aorta was cannulated *in situ* and the silk suture was used to secure the heart. The cannulated heart was removed from the thoracic cavity and attached to the perfusion apparatus.

The hearts were retrogradely perfused at 2 ml/min for 10 minutes with a nominally Ca^{2+} -free perfusion buffer that contained (mM): 105 NaCl, 5 KCl, 25 HEPES, 20 glucose, 0.33 NaH_2PO_4 , 1.0 MgCl_2 , 3.0 Na-pyruvate, 1.0 lactic acid (pH 7.4 with NaOH). Hearts were then enzymatically digested by perfusing with the same buffer supplemented with 50 μM Ca^{2+} , protease dispase II (0.10-0.15 mg/ml; Roche Diagnostics, Laval, QC), collagenase type 1 (0.3-0.5 mg/ml; 250 U/mg, Worthington, Lakewood, NJ) and trypsin (0.01-0.02 mg/ml; Sigma Aldrich, Oakville, ON) for 8-10 minutes. All solutions were oxygenated (100% O_2 ; Praxair, Halifax, NS) and warmed to 37°C by a water bath (Isotemp 3016H; Fisher Scientific, Ottawa, ON). A Piper model P peristaltic pump (Fred A. Dungey Inc., Agincourt, ON) was used to deliver solutions

through the perfusion apparatus. Solutions passed through a water-jacketed heating coil (Radnotia Glass Technology Inc., Monrovia, CA) containing a bubble trap, to maintain solution temperature at 37°C and collect any bubbles that formed in the solution. Following enzymatic digestion, the ventricles were isolated from the atria and were minced into small pieces. The minced tissue was stored in a high potassium buffer of the following composition (mM): 80 KOH, 30 KCl, 3 MgSO₄·7H₂O, 30 KH₂PO₄, 50 L-glutamic acid, 20 taurine, 0.5 EGTA, 10 HEPES, 10 glucose (pH 7.4 with KOH). Individual ventricular myocytes were dissociated from the minced tissue by gentle agitation, and the cell suspension was passed through a 225 μm polyethylene filter to remove large particles of undissociated tissue.

2.2.3 Experimental apparatus

A custom designed plexi-glass experimental chamber was mounted on the stage on an inverted microscope (Nikon Eclipse TE200, Nikon Canada Inc., Mississauga, ON). The bottom of the chamber consisted of a 1 cm by 2 cm optical grade glass coverslip (No. 1, 22 x 40 mm, VWR International, Montreal, QC). An outflow channel allowed solution to flow across the myocytes at a constant rate, and a small well to hold 2.7 M KCl to ground the bath was utilized during voltage clamp experiments (described in section 2.2.4). Solution was pumped through the setup using a Gilson Minipuls 3 peristaltic pump (3 mL/min, Mandel scientific, Guelph ON) and was coupled to drip chambers on both the inflow and outflow to reduce electrical noise conduction. All solutions were warmed to 37°C by a heat exchanger positioned at the inflow of the bath. The water within the heat exchanger was warmed and circulated by an immersion circulator

(Polystat 12112-10, Cole Parmer, Vernon Hills, IL).

The inverted microscope (Nikon Eclipse TE200, Nikon Canada Inc., Mississauga, ON) was placed within a Faraday cage on top of a custom-made anti-vibration table. An external DC power source (3-14V, Model 1686A, B+K Precision, Yorba Linda, CA) powered the microscope light, which passed through a filter (> 600 nm, red filter, Nikon Canada Inc.) to minimize interference with fluorescence recordings. Experiments were performed using a 40x objective (Nikon S-Fluor, numerical aperture 1.30, Nikon Canada Inc.) under oil immersion (Immersion 518F, Carl Zeiss Canada Ltd., Toronto, ON). A closed circuit video camera (Model TM-640, Pulnix America Inc., CA) was attached to the base of the inverted microscope, and connected to a television monitor (OPC, Model OVM-12E12, Korea) to display an image of the myocyte in the field of view. The signal from this camera was also coupled to a video edge detector (Model 105, Crescent Electronics, Sandy, UT) to measure cell shortening (contraction) of the myocyte of interest. A micromanipulator (Fine Science Tools Inc., North Vancouver, BC) was mounted to the microscope stage and controlled the positioning of the platinum electrodes for field stimulation or the microelectrode headstage for voltage clamp experiments. To minimize electrical interference, all components were grounded by attachment to a common ground panel, which was grounded to the voltage clamp amplifier.

Intracellular Ca^{2+} levels ($[\text{Ca}^{2+}]_i$) were visualized using a PTI (Photon Technology International, Birmingham, NJ) fluorescence imaging system. A xenon arc lamp (75 W LPS-220B power supply, PTI) was the source of UV light for excitation of the fluorescent dye. A DeltaRam high speed wavelength illuminator (PTI) was used to

rapidly select and switch between excitation wavelengths. A dichroic cube (Chroma Technology Corp., Rockingham, VT) was used to split the microscope light between the video camera (Model TM-640, Pulnix America Inc., CA) and the photomultiplier tube (PMT; Model D-104, PTI), which was used to measure emitted photons. This system is described in greater detail in section 2.2.5. To minimize interference in fluorescence recordings, the Faraday cage was covered in a dark fabric to reduce the entrance of ambient light. All remaining components of the experimental setup will be described in the appropriate sections.

2.2.4 Field stimulation experiments

A schematic of the field stimulation setup is shown in figure 3. In field stimulation experiments, myocytes were superfused at 3 ml/min with a buffer solution of the following composition (mM): 135 NaCl; 10 glucose; 10 HEPES; 4 KCl; 1 CaCl₂; 1 MgCl₂ (pH 7.4 with NaOH). A micromanipulator (Fine Science Tools Inc., North Vancouver, BC) was used to position two custom-designed platinum electrodes near the field of view of the microscope. pClamp software (version 8.2; Molecular Devices, Sunnyvale, CA) was used to set the myocyte pacing rate at 2 Hz, and a stimulus isolation unit (SIU- 102; Warner Instruments, Hamden, CT) delivered 3 ms bipolar pulses (15-30 mA; 1.5-2.0x threshold) to stimulate the cells. When a myocyte was selected, the closed circuit video camera (Model TM-640, Pulnix America Inc., CA) was used to record and orient the live image of the cell on the television monitor. The signal from this camera was also coupled to a video edge detector (sampling rate of 120 Hz; Model 105, Crescent Electronics, Sandy, UT) to detect changes in cell length. This allowed unloaded cell

shortening to be measured with each stimulated beat. Analog signals from the video edge detector were converted to digital signals using a 16-bit Digidata acquisition system (Model 1322A, Axon Instruments Inc., Foster City, CA). pClamp software (version 8.2; Molecular Devices, Sunnyvale, CA) was used to collect the data, which was stored on a computer hard drive. Cellular shortening was recorded in 10-second intervals. $[Ca^{2+}]_i$ was recorded simultaneously with cellular shortening (described in section 2.2.5). Contraction size was measured as the difference between cell length at rest and during peak contraction. Experiments used only quiescent, rod-shaped myocytes with clear striations and no visible membrane damage.

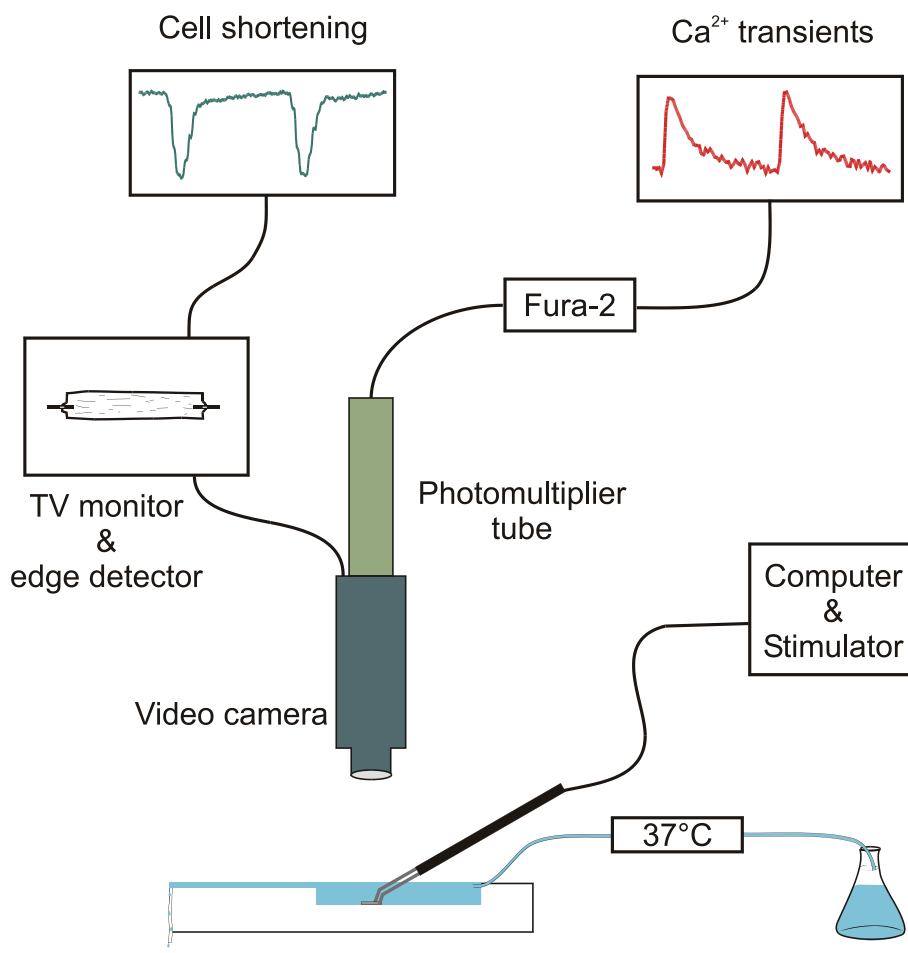


Figure 3. Schematic of field stimulation setup. In field stimulation experiments, myocytes in the experimental chamber were superfused with buffer solution at 37 C. pClamp computer software was used to set the myocyte pacing rate (2 Hz) and a stimulation unit attached to two platinum electrodes was used to stimulate the myocytes. A closed circuit video camera was used to display a live image of the cell on the television monitor. A video edge detector was used to detect cellular shortening. Ca²⁺ transients were recorded simultaneously with cellular shortening using the ratiometric Ca²⁺ sensitive dye, Fura-2 (described in section 2.2.5).

2.2.5 Current and voltage clamp experiments

A schematic of the voltage clamp setup is shown in figure 4. To measure membrane potentials and transmembrane currents, myocytes were impaled with high resistance (15-25 M Ω) microelectrodes. Borosilicate glass capillary tubes (Outer diameter 1.2 mm, inner diameter 0.6 mm; Sutter Instruments Co., Novato, CA) were pulled with a Flaming/Brown Micropipette Puller (Model P-97, Sutter Instruments Co., Novato, CA) to make microelectrodes on each experimental day. Prior to assessing each myocyte, the microelectrodes were filled with filtered 2.7 M KCl from a 1 mL syringe attached to a 30-gauge needle attached to a filter (pore size 0.22 μ m; Millex-GV, Millipore, Cambridge, ON). Microelectrodes were then placed in a microelectrode holder (Model MEH1S, World Precision Instruments, Sarasota, FL). The microelectrode holder contained a silver wire that was treated with 5% sodium hypochlorite prior to experiments. This coated the silver wire in silver chloride, producing a reversible electron donor/acceptor system (silver/silver chloride electrode) that allowed for bidirectional movement of charge. Microelectrodes were placed in the microelectrode holder so that the tip of the silver wire was immersed in 2.7 M KCl. The holder was then inserted into the amplifier headstage (Axon HS-2A Headstage, Gain x 0.1, Molecular Devices), which was attached to the micromanipulator. A ground wire was also attached to the amplifier headstage. This electrical ground was composed of a coiled silver wire, and like the microelectrode holder, was treated with 5% sodium hypochlorite prior to experimentation. The coiled silver wire component of the ground wire was submerged in a small well of 2.7 M KCl in the experimental chamber, while a brass pin soldered to the other end of the ground wire was attached to the headstage. To complete the electrical

circuit, the well containing 2.7 M KCl was connected to the bath using an agar bridge (1% agar in 2.7 M KCl).

When a myocyte of interest was identified, the microelectrode was lowered into the bath and positioned near the cell using the micromanipulator. Prior to impaling the myocyte, the junction potentials, resistance of the electrode, and the microelectrode capacitance were all compensated using adjustments on the Axoclamp 2B amplifier (Molecular Devices, Sunnyvale, CA). Using bridge mode of the amplifier, junction potentials in the electrical circuit were neutralized by adjusting the input voltage offset dial. Next, the resistance of the microelectrode (15-25 M Ω) was determined by passing 1 nA of current through the electrode. This resistance was compensated by adjusting the bridge control on the amplifier. Discontinuous current-clamp mode was used to observe the rate of microelectrode capacitance charging and decay. This voltage waveform (capacitance charging and decay) was visualized on an oscilloscope (Model COR5541U, Kikusui Electronic Corp., Japan). The rates of capacitive charging and decay were maximized by using the capacitance compensation dial on the amplifier. Once these neutralizations were completed, the myocyte of interest was impaled.

To impale myocytes, the microelectrode was lowered to the cell membrane until the tip made a clear indentation on the surface of the cell. The electrode was then inserted into the cell using a technique known as “buzzing”, where overcompensation of the electrode capacitance using high frequency current is injected through the microelectrode. This aids in electrode penetration through the cell membrane. Once the cell was impaled, the resting membrane potential (RMP) was measured. A small negative current was applied to the cell until the RMP stabilized near -80 mV. This

current was removed prior to recording action potentials from cell.

Action potentials were measured using bridge mode with the Axoclamp amplifier. Current was injected through the microelectrodes to trigger action potentials (2-4 nA; pulse duration = 3 ms). Action potentials were initiated at a rate of 2 Hz. Action potential data was collected using pClamp software (version 8.2; Molecular Devices). RMP was measured as the membrane voltage prior to the upstroke of the action potential. Action potential duration was measured from the time of the action potential overshoot to the time where repolarization reached 50% (APD₅₀) and 90% completion (APD₉₀). Contractions elicited by action potentials were also collected with pClamp software (version 8.2; Molecular Devices). As in field stimulation experiments, myocytes were visualized on the television monitor and cell shortening was measured using the video edge detector.

Transmembrane currents were measured using discontinuous single-electrode voltage clamp techniques. With this technique, a single electrode is used to both measure membrane voltage and inject current. To achieve this, the Axoclamp amplifier sampled the membrane potential of the impaled myocyte. This potential was then compared to a command voltage. If the sampled potential was not equivalent the command voltage, current was injected to bring the membrane potential closer to that of the command voltage. Once the membrane potential reached the command voltage, current injection ceased and voltage was recorded. For this to occur with a single electrode, the microelectrode rapidly cycled between sampling membrane potential and injecting current (5-8 KHz).

Voltage protocols were generated using pClamp software (version 8.2; Molecular

Devices). In all voltage clamp experiments, myocytes were initially held at -80 mV and a train of 5-10 conditioning pulses (voltage steps from -80 mV to 0 mV; 50 ms pulse duration) were delivered at a rate of 2 Hz. Conditioning pulses provided myocytes with a consistent activation history prior to eliciting test steps.

Test steps were designed to activate specific transmembrane currents. To measure L-type Ca^{2+} current (I_{CaL}), the membrane potential of the myocyte was held at -40 mV after the last conditioning pulse. This potential was used to facilitate voltage-dependent inactivation of Na^+ channels (Bers, 2001). In some experiments, 300 μM lidocaine was added to further ensure blockade of Na^+ current. The buffer solution used in voltage clamp experiments was also supplemented with 4 mM 4-aminopyridine to block outward K^+ current (I_{TO}). By disabling I_{Na} and I_{TO} currents, interference with I_{CaL} was minimized. In some experiments, a single test step from -40 mV to 0 mV was used to activate I_{CaL} . In other experiments, test steps were initiated from -40 mV to potentials between -30 and +80 mV in 10 mV increments. This protocol was used to activate I_{CaL} across a range of membrane potentials to construct current-voltage (IV) relationships.

A voltage clamp protocol was also used to measure SR Ca^{2+} stores. Through rapid application of caffeine (10 mM), ryanodine receptors were activated to allow the release of SR Ca^{2+} (Bers, 2001). This caffeine-induced Ca^{2+} transient was measured in cells loaded with Fura-2. In these experiments, ten conditioning pulses were delivered to the cell at a frequency of 2 Hz as described above. Following the last conditioning pulse, the membrane voltage was held at -60 mV, and after 500 ms, caffeine was applied for 1 s to assess SR Ca^{2+} content. A custom designed rapid solution switcher was used to deliver the caffeine solution (control valves: LFAA1201710H; The Lee Company Westbrook,

CT). The timing of caffeine application and activation of the rapid switcher was controlled using pClamp software (version 8.2; Molecular Devices). Solution was applied in direct proximity to the cell, and all solutions were maintained at 37°C. These experiments used a Na⁺/Ca²⁺-free buffer solution of the following composition (in mM): 10 caffeine; 140 LiCl; 4 KCl; 10 glucose; 5 HEPES; 4 MgCl₂; 4 4-aminopyridine; 0.3 lidocaine. Under these experimental conditions, caffeine application did not induce inward Na⁺-Ca²⁺ exchange current so caffeine was not removed from the cell during the caffeine switch (Delbridge et al., 1996; Katoh et al., 2000).

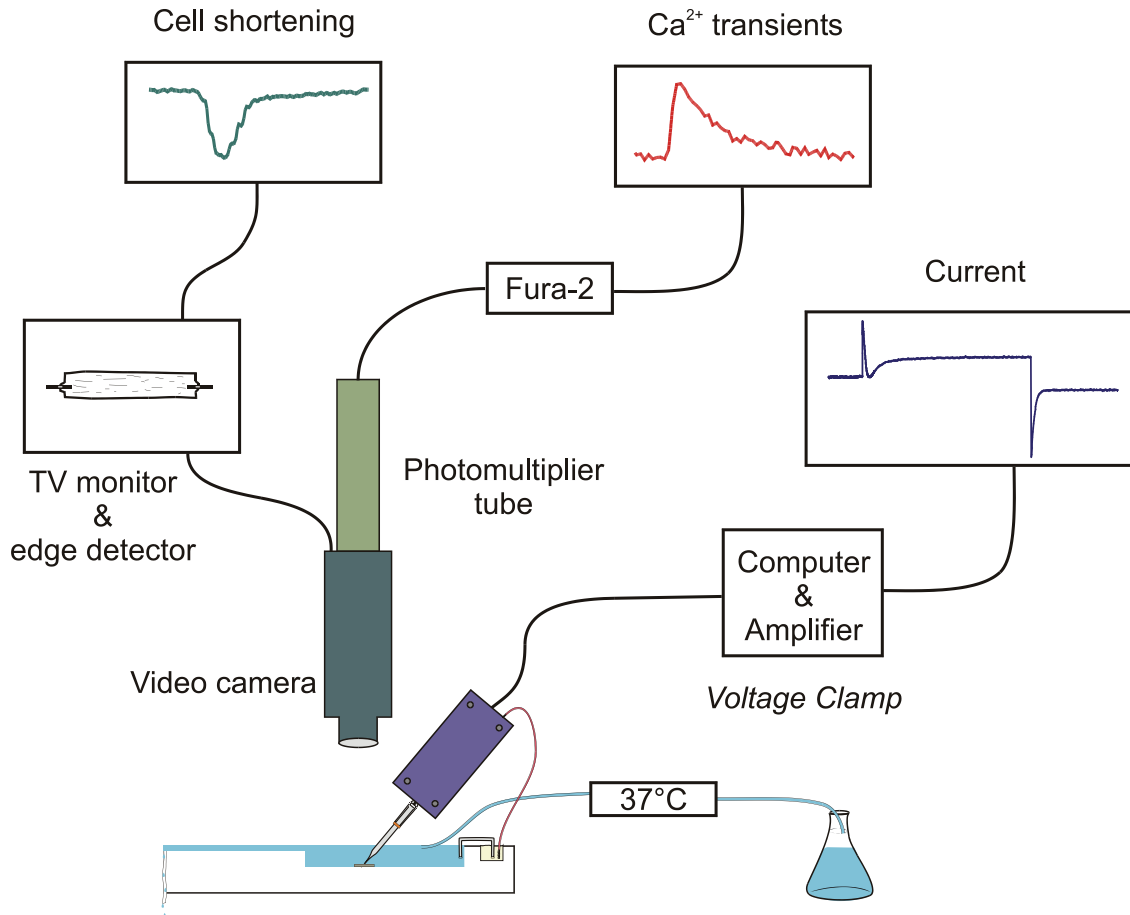


Figure 4. Schematic of voltage clamp setup. In voltage clamp experiments, myocytes in the experimental chamber were superfused with buffer solution at 37°C . High resistance microelectrodes were embedded into ventricular myocytes to manipulate membrane voltage and measure transmembrane current. pClamp computer software was used to design the voltage clamp protocol and record cellular data. A closed circuit video camera was used to display a live image of the cell on the television monitor. A video edge detector was used to detect cellular shortening. Ca^{2+} transients were recorded simultaneously with current and cellular shortening using the ratiometric Ca^{2+} sensitive dye, Fura-2 (described in section 2.2.5).

2.2.6 Simultaneous measurement of intracellular Ca^{2+} and cellular shortening

In some experiments, intracellular Ca^{2+} ($[\text{Ca}^{2+}]_i$) and cellular shortening were measured simultaneously. An *in vitro* fura-2 calibration was performed on the experimental apparatus prior to collection of fluorescence data. The calibration curve is shown in figure 5. This calibration curve was used to convert the ratio of fluorescence recordings (340/380 nm; discussed below) into Ca^{2+} concentrations. Using a cell impermeable fura-2 potassium salt (Invitrogen), the emission ratios (340/380 nm; discussed below) of several known Ca^{2+} concentrations were measured to generate a calibration curve. Prior to performing this calibration, all surfaces and glassware were washed with 1 M HCl to remove any residual Ca^{2+} that may be present. Two solutions were prepared, a Ca^{2+} -free EGTA buffer containing (in mM): 10 EGTA; 100 KCl; 10 K-MOPS; 1.0 μM fura-2 (pH 7.0 with KOH), and a Ca^{2+} containing EGTA buffer containing (mM): 10 EGTA; 100 KCl; 10 K-MOPS; 10 CaCl_2 ; 1.0 μM fura-2 (pH with 7.0 with KOH). An initial fura-2 fluorescence recording with Ca^{2+} -free EGTA buffer was performed to obtain a zero Ca^{2+} measure. Following this recording, an aliquot of Ca^{2+} -free EGTA buffer was removed, and an equal volume of Ca^{2+} containing EGTA buffer was added to the chamber. Fluorescence measurements were performed after each addition of Ca^{2+} -containing EGTA buffer, and this continued until a maximum Ca^{2+} concentration was reached. The free Ca^{2+} concentrations for each recording were determined using the equilibrium equation for Ca^{2+} binding to EGTA ($K_d = [\text{Ca}^{2+}][\text{EGTA}]/[\text{Ca}^{2+}\text{-EGTA}]$; K_d for $\text{Ca}^{2+}\text{-EGTA} = 380$ nM; Photon Technologies International (PTI), Birmingham, NJ). Solutions were warmed to 37°C during this calibration. These recordings were used to generate a calibration curve. A linear

regression was fit to the linear portion of the calibration curve, and the resulting equation of the line was used to convert fura-2 emission ratios to $[Ca^{2+}]_i$ in all experiments.

Myocytes were loaded with fura-2 AM (acetoxymethyl ester; 5 μ M with 0.2% anhydrous DMSO in suspension; Invitrogen, Burlington, ON) and incubated in the dark for 20 minutes at room temperature prior to experimentation. Fura-2 AM enters the cytosol of myocytes by crossing the sarcolemmal membrane. This is facilitated by the acetoxymethyl ester functional group, which allows the fluorephore to cross cell membranes (Tsien, 1981). Once within the cell, the AM group of fura-2 is cleaved by endogenous esterases. This renders fura-2 impermeable to cell membranes and sequesters the fluorephore to the cytosol. Fura-2 is a ratiometric Ca^{2+} dye. When fura-2 interacts with Ca^{2+} , its excitation wavelength is shifted. In a Ca^{2+} -unbound state fura-2 absorbs light at 380 nm, however when fura-2 is bound to Ca^{2+} , light is absorbed at 340 nm. This does not alter the Fura-2 emission wavelength, which remains constant at 510 nm. By determining the ratio of fura-2 emission from the fluorephore in a Ca^{2+} -bound and Ca^{2+} -unbound states (340/380 nm), changes in $[Ca^{2+}]_i$ within the cell can be calculated. Ratiometric measurements also minimize the effects of "photobleaching", where the fluorescent molecule becomes inactive due to excess excitation (Takahashi et al., 1999).

UV light was generated from a xenon arc lamp (75 W LPS-220B power supply, PTI) to excite fura-2. Using a DeltaRam high speed wavelength illuminator (PTI) to control a monochromator, excitation wavelengths were rapidly selected to an accuracy of ± 1 nm. By quickly switching between wavelengths, myocytes were alternatively excited at 340 nm and 380 nm. This light was delivered using a liquid light guide (PTI). A dichroic cube (Chroma Technology Corp., Rockingham, VT) was used to split the

microscope light between the video camera (Model TM-640, Pulnix America Inc., CA) and the photomultiplier tube (Model D-104, PTI). Light with longer wavelengths (>600 nm) was directed to the video camera to display the image of the cell and capture cell shortening; fura-2 emitted light (510 nm) was directed toward the photomultiplier tube. To specifically capture light emitted from the myocyte of interest, an aperture below the photomultiplier tube was closed to surround the length and width of the cell in the viewing window. Additionally, a barrier filter (80 nm) was placed between the aperture and photomultiplier tube to exclude light that did not have a wavelength between 470 and 550 nm. Fura-2 emissions (510 nm) were recorded for both excitation wavelengths (340 and 380 nm) at a rate of 200 samples/s using Felix software (PTI). Following each experimental protocol, a background recording was collected and was used to correct for any auto-fluorescence. An area adjacent to the cell that did not contain any cells or cell fragments was selected for the background recording. The background fluorescence values were subtracted from each emission recording (340 and 380 nm) before the emission ratio (340/380 nm) was calculated with Felix software (PTI). This new emission ratio was then used in the calculation of $[Ca^{2+}]_i$ from the regression obtained from the calibration curve (described above). Fura-2 Ca^{2+} transients were measured as the difference between the diastolic and systolic Ca^{2+} levels. Properties of Ca^{2+} transient decay were determined by fitting the decay portion of the Ca^{2+} transient with a standard exponential regression $(f(t) = \sum_{i=1}^n A_i e^{-t/\tau_i} + C)$ prior to measuring parameters.

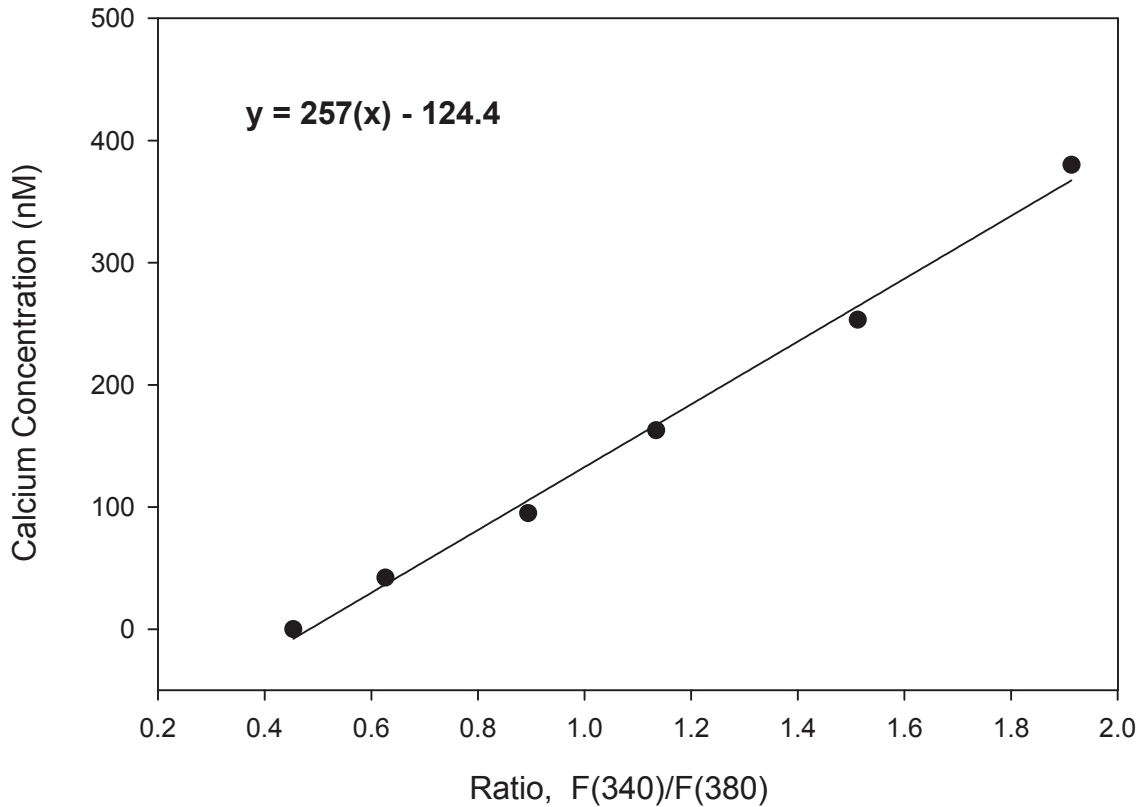


Figure 5. *In vitro* calibration curve for Fura-2. A calibration curve for Fura-2 was generated using several known Ca^{2+} concentrations and a cell impermeable Fura-2 fluophore. A regression line was fit to the calibration curve ($r^2 = 0.9950$). The resulting equation of the line was used to convert the ratio of fluorescence recordings (340/380 nm) into intracellular Ca^{2+} concentrations in all experiments.

2.2.7 Measurement of spontaneous Ca²⁺ sparks

In some experiments, myocytes were incubated with fluo-4 AM (Invitrogen) to examine spontaneous Ca²⁺ sparks in quiescent myocytes. Fluo-4 AM was used to visualize sparks, as it has faster Ca²⁺ binding kinetics in comparison to fura-2 (K_d of Ca²⁺ binding = 145 nM (fura-2) vs. 345 nM (fluo-4); Molecular Probes Inc., Eugene, OR). Unlike fura-2, fluo-4 is not a ratiometric Ca²⁺ sensitive dye, thus fluo-4 fluorescence emission was recorded only at 525 nm.

A 0.1 mM stock solution of Fluo-4 AM was prepared in fetal bovine serum supplemented with Pluronic® F-127 (20%, Sigma-Aldrich, Oakville, ON) to yield a final concentration of 20 µM fluo-4 AM in the myocyte suspension. Cells were incubated with fluo-4 for 30-35 minutes. The fluo-4 loaded myocytes then were placed in a mouse laminin coated experimental chamber (1 mg laminin/100 ml M199 medium), which was mounted on the stage of a laser scanning confocal microscope (Zeiss LSM 510-Meta, Carl Zeiss Canada Ltd, Toronto, ON). Myocytes were allowed to settle for 15 minutes prior to superfusion with buffer containing (mM): 135.5 NaCl, 4 KCl, 10 HEPES, 1 MgCl₂, 10 glucose, 1 CaCl₂, 2 probenecid, (pH 7.4 with NaOH). Buffer was heated to 37°C using a water bath and was maintained at this temperature using a stage heater (delta-T4 open dish system, Biopetech, Butler, PA) mounted on the stage of the confocal microscope. Cells were superfused with buffer using a peristaltic pump (4 mL/min; Minipuls 3, Mandel Scientific). A 63x oil immersion lens (Plan-Apochromat DIC objective, NA 1.40, Immersol 518N oil, Carl Zeiss Canada Ltd.) was used to perform the sparks experiments. Once a myocyte was selected for examination, an x-y scan was performed to visualize the cell. A laser scan line was drawn across the length of the cell

at a site that appeared uniformly loaded with fluo-4. LSM software (version 3.2, Carl Zeiss Canada Ltd) was used to control the argon laser (488 nm) and collect the line scan images (525 nm, pinhole size=98 μm , scan speed=649.35 lines/s, 512 pixels/line, laser intensity=20%). The argon laser repeatedly scanned quiescent myocytes and fluo-4 fluorescence was recorded for six seconds.

Line scan images were analyzed for spontaneous Ca^{2+} sparks using the SparkMaster plug-in (Picht et al., 2007) for ImageJ software (v1.34, NIH, Bethesda, MD). Sparkmaster was set to the following parameters: scanning speed=649.35 lines/s; pixel size (μm)=cell length/512 pixels; background=10; criteria=3.8; number of intervals=1; output=F/F0 + sparks, extended kinetics (where F=fluorescence intensity, F0=background). Under these conditions, SparkMaster identified Ca^{2+} sparks as areas of fluorescence intensity (F) greater than 3.8 times the standard deviation above background (F0). Subsequent to the automated analysis, each image was inspected manually. This was to exclude any anomalies detected by the program such as extended bright lines in the image that were detected as sparks, or clusters of multiple sparks that were perceived as a single unitary release.

2.2.8 *In vitro* myofilament Ca^{2+} sensitivity assessment

In some experiments, myofilaments were isolated from ventricular tissue to assess Ca^{2+} sensitivity. Mice were anaesthetized and the thoracic cavity was opened as described above. A butterfly needle (25 gauge; BD Biosciences, Mississauga, ON) attached to a 30 mL syringe containing ice-cold saline (0.9% saline; Hospira Healthcare Corp., Montreal, QC) was used to perfuse the heart. The butterfly needle was inserted

into the left ventricle. After slightly depressing the plunger of the syringe to enlarge the tissue, the right atrium was gently opened to allow both blood and perfusate to clear the heart. Once perfusion was complete, the heart was excised from the chest cavity and the ventricles were dissected from the rest of the organ. Ventricles were then rapidly frozen and stored at -80°C . Subsequently, ventricles were sent to Dr. W. Glen Pyle (University of Guelph, Guelph, ON). Dr. Pyle has expertise in examining myofilament Ca^{2+} sensitivity, and this aspect of the project was conducted in collaboration.

Ventricular samples were homogenized in ice-cold standard buffer containing (mM): 60 KCl, 30 imidazole (pH 7.0), 2 MgCl_2 , 0.01 leupeptin, 0.1 PMSF, 0.2 benzamidine, 0.1 cantharidin. Samples were centrifuged at 14,100g for 15 minutes at 4°C . The resulting pellets were resuspended in ice-cold standard buffer with 1% Triton X-100 for 45 minutes to remove cell membranes. Samples were then centrifuged at 1,100g for 15 minutes at 4°C . These pellets were washed three times in ice-cold standard buffer, and purified myofilaments were stored on ice for up to 2 hours or frozen for gel electrophoresis.

Myofilament function was assessed using a spectrophotometric actomyosin MgATPase assay. Purified myofilaments (25 mg) were incubated in activating solutions containing varying levels of free Ca^{2+} . Free Ca^{2+} was calculated using the program from Patton *et al.* (Patton et al., 2004). Myofilaments were incubated in activating buffers for 10 minutes at 32°C , then reactions were quenched using 10% trichloroacetic acid. MgATPase enzymatic activity was assessed by the production of inorganic phosphate from ATP hydrolysis. This was measured by reading the absorbance at 630 nm after adding an equal volume of 0.5% FeSO_4 and 0.5% ammonium molybdate in 0.5 M H_2SO_4 .

Purified myofilament proteins (10 mg) were separated using SDS-PAGE (12% separating gel). Total protein phosphorylation was assessed by staining gels with ProQ Diamond stain (Invitrogen, Burlington, ON) according to the manufacturer's instructions. Gels were scanned using a Typhoon gel scanner (GE Healthcare, Baie, Quebec), and analysis was done using Image J software (NIH, Bethesda, MD). Protein loading was assessed by Coomassie staining of gels after imaging.

2.2.9 Measurement of *in vivo* ventricular function through echocardiography

Two-dimensional guided M-mode echocardiography was performed on aged OVX and sham mice. A high-resolution linear transducer (i13L, GE ultrasound, Horten, Norway) connected to a Vivid 7 imaging system (GE Medical Systems, Horten, Norway) was used to collect images of the intact mouse heart. All experiments were performed with the mice anesthetized under 2% isoflurane in oxygen. Mice were placed in the supine position on a heated platform (37°C). The chest area of each mouse was shaved to minimize interference with the transducer, and ultrasound transmission gel (Parker Laboratories Inc., NJ, USA) was used to maximize image quality. ECG electrodes (Grass technologies, RI, USA) were placed subcutaneously to obtain electrocardiographic signals. M-mode in the short axis orientation was used to generate images. Measurements of diastolic and systolic ventricular dimensions were used to generate functional parameters. Ejection fraction (EF), which represents the volumetric fraction of blood pumped from the heart with each beat, was calculated using the equation: $EF = \frac{[(\text{end-diastolic}^3 - \text{end-systolic}^3) / \text{end-diastolic}^3] \times 100\%}{}$. Fractional shortening (FS),

which is the percentage change in ventricular diameter from diastole to systole and represents myocardial function, was calculated using the equation: $FS = [(end\text{-}diastolic - end\text{-}systolic) / end\text{-}diastolic] \times 100\%$. ECG traces were used to determine heart rate.

2.2.10 Data analysis and statistics

Data analysis was performed using pClamp software (version 8.2; Molecular Devices). All graphs were constructed with Sigmaplot (version 8.0; Systat Software, Inc., Point Richmond, CA). Statistical analyses were performed using SigmaStat (version 3.1; Systat Software, Inc.). Unpaired Student's *t*-tests were performed for comparison of single parameter means. Differences between means were also evaluated by two-way and two-way repeated-measures analysis of variance (ANOVA), as noted in the relevant results section. All pair-wise multiple comparisons were performed using Student-Newman-Keuls post-hoc test. Differences were considered significant if $p < 0.05$. Data are presented as means \pm SEM.

CHAPTER 3 RESULTS

3.1 THE EFFECTS OF EXTREME AGING ON CARDIAC CONTRACTILE FUNCTION IN MALE AND FEMALE MICE

3.1.1 Survival in C57BL/6 mice

To quantify the lifespan of male and female C57BL/6 mice, animal survival was followed and Kaplan-Meier analysis was used to assess this relationship. Overall, a total of 230 male mice and 190 female mice were followed over a period of approximately 1100 days and data collected were used to generate a survival curve. Figure 6 shows the resulting survival curves generated for male (black) and female (red) mice. These data showed that survival rates did not differ between male and female mice. The 50% survival was measured at approximately 900 days (29 mos) in both male and female mice. Arrows in Figure 6 indicate the relative ages of the young adult (~210 days) and senescent (~980 days) mice used in this study.

3.1.2 Phenotypic characteristics of young adult and senescent mice

Phenotypic characteristics of young adult and senescent male and female mice used in this study were also investigated. Tables 3 and 4 show mean values for the ages and body weights of mice used in this study. Results show that 32 month old male and female mice were significantly older than young adult mice (6.8 ± 0.2 vs. 32.1 ± 0.6 mos for male mice; 7.0 ± 0.5 vs. 32.5 ± 0.6 mos for female mice). In addition, body weight was significantly increased in both older male and female mice in comparison to young adult mice (34.2 ± 0.6 to 39.2 ± 1.6 g for male mice; 24.5 ± 0.7 to 32.1 ± 2.1 g for female mice). Myocyte length was compared between young adult and senescent mice. Figure 7

shows that mean cell length was significantly larger in cells from senescent mice in comparison to cells from young adult male and senescent female mice (Figure 7). Interestingly, myocyte length was not affected by age in female mice (Figure 7). These findings indicate that senescent mice of both sexes were significantly older and weighed significantly more than young adult mice. Interestingly, cellular hypertrophy was only observed in cells from male, but not female mice in extreme old age.

3.1.3 Cardiac contractile function in young adult and senescent male and female mice

To assess age-related changes in cardiac contractile function, myocytes from young adult and extremely old mice were incubated with fura-2 and examined under voltage clamp conditions using high resistance microelectrodes (37°C). The voltage clamp protocol is shown at the top of Figure 8A. Myocytes were stimulated with a train of ten conditioning pulses from -80 mV to 0 mV at a rate of 2 Hz, followed by a test step from -40 mV to 0 mV. Cell shortening, Ca²⁺ transients, and Ca²⁺ currents (I_{CaL}) were measured simultaneously. Figure 8A also depicts representative cellular shortening traces from young adult male and female mice (middle left and right, respectively) and senescent male and female mice (bottom left and right, respectively). As illustrated in these representative traces, contractile responses in cells from young adult male mice were larger than those in cells from senescent male mice. Contractile responses from female cells however, did not decline with age. Mean data showed that cell shortening significantly declined by 80% in cells from senescent males in comparison to young adult males (Figure 8B; left). In contrast, mean cell shortening was similar in cells from young

adult and 32 month old female mice (Figure 8B; right). Comparison of mean contractions from young adult male and young adult female mice also showed that responses were significantly larger in males than females. These data show that while responses are larger in young adult males in comparison to females, an age-related decline in contractile function only occurred in myocytes from male mice and not female mice in extreme old age.

As contractions are activated by a rise in intracellular Ca^{2+} levels, Ca^{2+} transient amplitudes were compared in myocytes from young adult and aged mice. Figure 9A shows representative Ca^{2+} transients activated by a test step from -40 mV to 0 mV (voltage clamp protocol shown in top panel). As seen in these examples, Ca^{2+} transient amplitudes were larger in myocytes from younger mice (young male, middle left; young female, middle right) in comparison to senescent mice (senescent male, bottom left; senescent female, bottom right). Mean responses showed that peak amplitudes declined by 65% in cells from senescent males when compared to cells from young males (Figure 9B; left). Interestingly, the size of Ca^{2+} transients was also 35% smaller in myocytes from senescent females in comparison young females (Figure 9B; right). Comparison of Ca^{2+} transients in young adult male and female myocytes also showed that mean amplitudes were significantly larger in cells from male mice. Resting Ca^{2+} levels were also assessed by measuring diastolic Ca^{2+} at -80 mV, prior to the last conditioning pulse. Diastolic Ca^{2+} levels were not affected by age or sex (Figure 9C). Hence, contractile function and Ca^{2+} transients both declined with age in males. In contrast, while contractile function was preserved in females at the extremes of life, there was a modest decrease in the size of the underlying Ca^{2+} transient.

Ca^{2+} transient size may decline with age due to a decrease in peak I_{CaL} . To investigate this, I_{CaL} was recorded using voltage clamp techniques in myocytes from males and females at different ages. The voltage clamp protocol used is shown at the top of Figure 10A. Representative examples of I_{CaL} recorded in myocytes from young adult and 32 month old male and female mice are shown in Figure 10A. These traces show that I_{CaL} was larger in cells from young males than cells from senescent males. However, peak I_{CaL} was not affected by age in female mice. Indeed, mean data show that peak I_{CaL} density was decreased by 61% in cells from older male mice (Figure 10B), but I_{CaL} did not decline with age in females (Figure 10B). To assess the impact on SR Ca^{2+} release, the effect of age on EC-coupling gain was compared. EC-coupling gain represents the amount of SR Ca^{2+} released in response to the amount of trigger Ca^{2+} that enters the cell (Ca^{2+} transient/ Ca^{2+} current density). Mean values indicate that EC-coupling gain declined by 57% in cells from senescent males (Figure 10C; left) and 46% in cells from senescent females (Figure 10C; right) when compared to values calculated for younger mice. These results show that peak I_{CaL} density declines in cells from males, but not females in extreme old age. However, EC-coupling gain is reduced in both males and females, which may explain the smaller Ca^{2+} transients observed in cells from these older animals.

3.1.4 Changes in intracellular Ca^{2+} stores in young adult and senescent male and female mice

To determine whether age- and sex-dependent changes in SR Ca^{2+} load influenced SR Ca^{2+} release, intracellular Ca^{2+} stores were measured. The voltage clamp

protocol used is shown in Figure 11A (top center). Myocytes were stimulated with a train of ten conditioning pulses from -80 mV to 0 mV at a rate of 2 Hz. Following the last conditioning pulse, myocytes were held at -60 mV and caffeine (10 mM) was applied for 1 s, 500 ms after the last conditioning pulse, using a rapid solution switcher. Figure 11A illustrates caffeine-induced Ca^{2+} transients from young adult and extremely old male and female mice. These examples show that peak caffeine transients were similar in young adult and senescent myocytes, regardless of sex. Mean data showed that caffeine-stimulated Ca^{2+} transients were similar in magnitude in cells from younger and older male (Figure 11B; left) and female mice (Figure 11B; right). As SR Ca^{2+} stores did not change with advanced age, fractional SR Ca^{2+} release was evaluated. Fractional SR Ca^{2+} release represents the amount of Ca^{2+} released from the SR in relation to the total amount of Ca^{2+} present within the SR. Fractional release was the ratio of the stimulated Ca^{2+} transient to the caffeine-induced transient for each cell. Averaged values showed that fractional release was significantly reduced by 57% in senescent males (Figure 11C; left) and 36% in senescent females (Figure 11C; right) when compared to cells from younger animals. These findings indicate that at extreme ages, SR Ca^{2+} stores do not decline in male and female mice. However, the fraction of Ca^{2+} released from the SR to form the Ca^{2+} transient was significantly reduced by age in cells from both males and females.

3.1.5 Summary of Section 3.1

In summary, myocytes from male and female mice exhibit significant changes in intracellular Ca^{2+} regulation with extreme old age. Cells from both 32 month old male and female mice had smaller Ca^{2+} transients in comparison to younger animals. This was

not due to a decrease in SR Ca^{2+} stores, but rather due to reduced EC-coupling gain and lower fractional release of SR Ca^{2+} in cells from males and females. Peak I_{CaL} density however, only declined in older males. In addition, contractile responses declined in myocytes from senescent males, but were preserved in cells from senescent females. Marked cellular hypertrophy was also observed in males, but not females with extreme aging. These findings suggest that biological sex continues to have an effect on the aging heart, even at the extremes of life. Tables 5 and 6 summarize the mean \pm SEM data in this study.

TABLE 3**Ages and Weights of Young Adult and Senescent Male Mice**

Parameter	Young Male	Senescent Male
Age (mos)	6.8 ± 0.2 (5)	32.1 ± 0.6† (7)
Body Weight (g)	34.2 ± 0.6 (5)	39.2 ± 1.6† (7)

Numbers represent mean ± SEM; values in brackets represent the number animals in this study. The † denotes significantly different from young adult values as tested by two-way ANOVA, p<0.05.

TABLE 4**Ages and Weights of Young Adult and Senescent Female Mice**

Parameter	Young Female	Senescent Female
Age (mos)	7.0 ± 0.5 (5)	32.5 ± 0.6† (8)
Body Weight (g)	24.5 ± 0.7* (5)	32.1 ± 2.1*† (8)

Numbers represent mean ± SEM; values in brackets represent the number animals in this study. The † denotes significantly different from young adult values. The * denotes significantly different from males. Tested by two-way ANOVA, $p < 0.05$.

TABLE 5**Summary of Responses from Voltage Clamp Experiments in Male Myocytes**

Parameter	Young Male	Senescent Male
Cell Shortening (%)	8.0 ± 2.2 (8)	1.6 ± 0.3† (6)
Ca ²⁺ transient (nM)	69.2 ± 9.8 (11)	21.0 ± 2.1† (9)
Diastolic Ca ²⁺ (nM)	60.3 ± 7.5 (11)	48.1 ± 4.3 (9)
Ca ²⁺ current (pA/pF)	-4.9 ± 0.6 (11)	-3.0 ± 0.3† (9)
Gain (nM pA/pF ⁻¹)	18.0 ± 4.2 (11)	7.8 ± 1.2† (9)
SR Ca ²⁺ stores (nM)	143.9 ± 34.1 (7)	135.0 ± 38.2 (6)
Fractional release (%)	59.0 ± 5.8 (7)	25.2 ± 6.9† (6)

Numbers represent mean ± SEM; values in brackets represent the number of cells. Mean parameters were calculated for responses activated by a test step to 0 mV. The † denotes significantly different from young adult values as tested by two-way ANOVA, p<0.05.

TABLE 6**Summary of Responses from Voltage Clamp Experiments in Female Myocytes**

Parameter	Young Female	Senescent Female
Cell Shortening (%)	4.0 ± 0.7* (10)	2.3 ± 0.6 (7)
Ca ²⁺ transient (nM)	41.8 ± 3.4* (12)	25.2 ± 2.9† (17)
Diastolic Ca ²⁺ (nM)	60.5 ± 6.7 (12)	62.5 ± 6.0 (17)
Ca ²⁺ current (pA/pF)	-4.6 ± 0.5 (12)	-4.7 ± 0.5* (17)
Gain (nM pA/pF ⁻¹)	11.5 ± 2.9 (12)	6.2 ± 0.8† (17)
SR Ca ²⁺ stores (nM)	102.3 ± 11.5 (6)	108.5 ± 19.3 (11)
Fractional release (%)	40.6 ± 5.6* (6)	26.1 ± 3.0† (11)

Numbers represent mean ± SEM; values in brackets represent the number of cells. Mean parameters were calculated for responses activated by a test step to 0 mV. The † denotes significantly different from young adult values. The * denotes significantly different from males. Tested by two-way ANOVA, p<0.05.

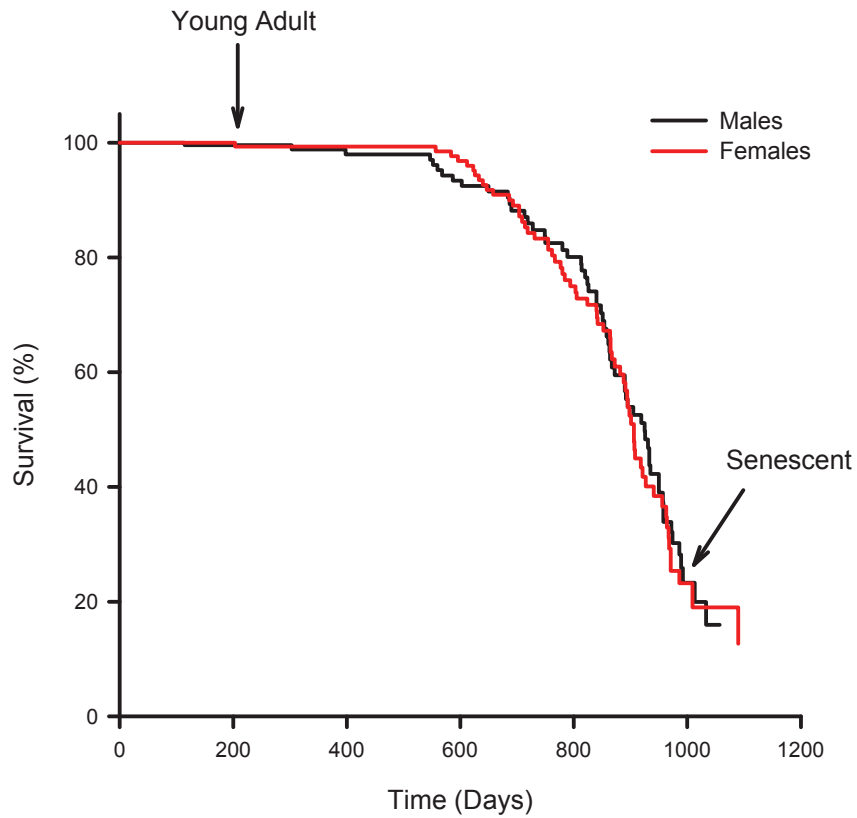


Figure 6. Survival rates were similar between male and female mice. Survival rates were compared between male and female mice using Kaplan-Meier analysis. Overall, survival did not differ between males and females, with 50% mortality occurring at approximately 900 days in both groups. Arrows above indicate the average ages of "young adult" and "senescent" mice used in this study. (n=230 male and n=191 female mice)

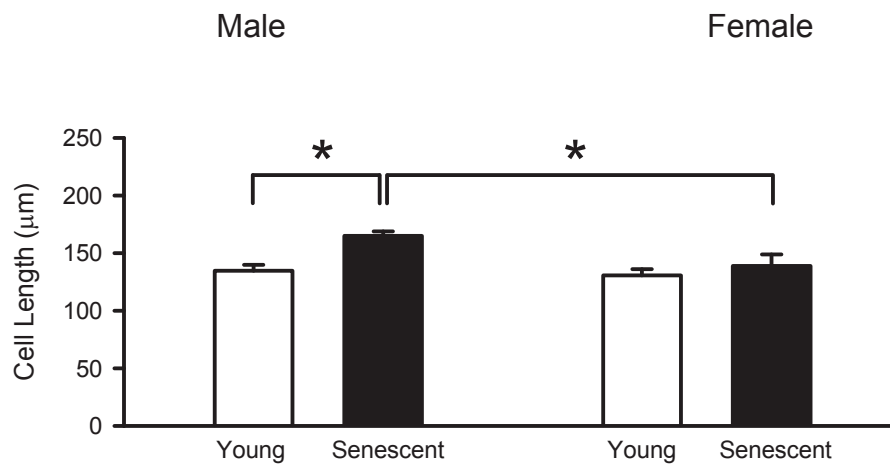


Figure 7. Myocyte length was significantly increased by age in male but not female mice. Cell length was significantly greater in senescent male myocytes when compared to young adult male or senescent female myocytes. Cell length did not differ between young and senescent female myocytes. (n=17 young male, n=17 senescent male, n=19 young female, n=17 senescent female myocytes; * denotes $p < 0.05$).

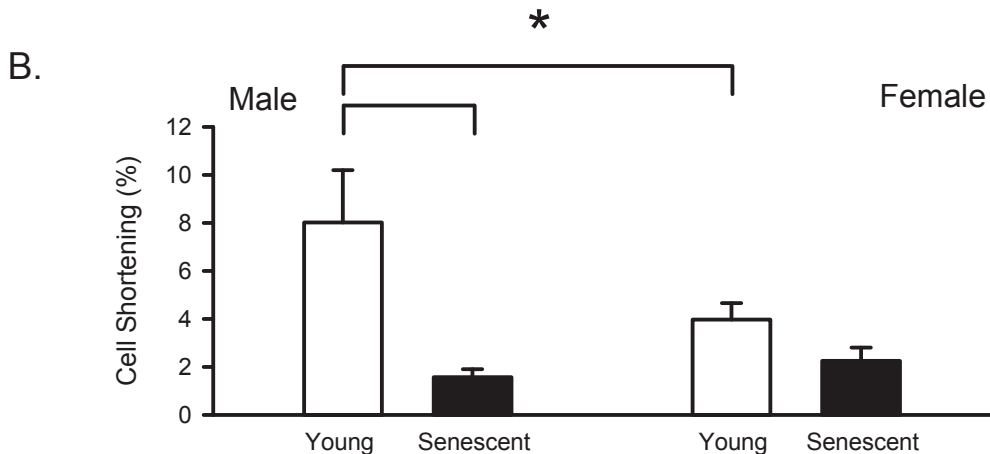
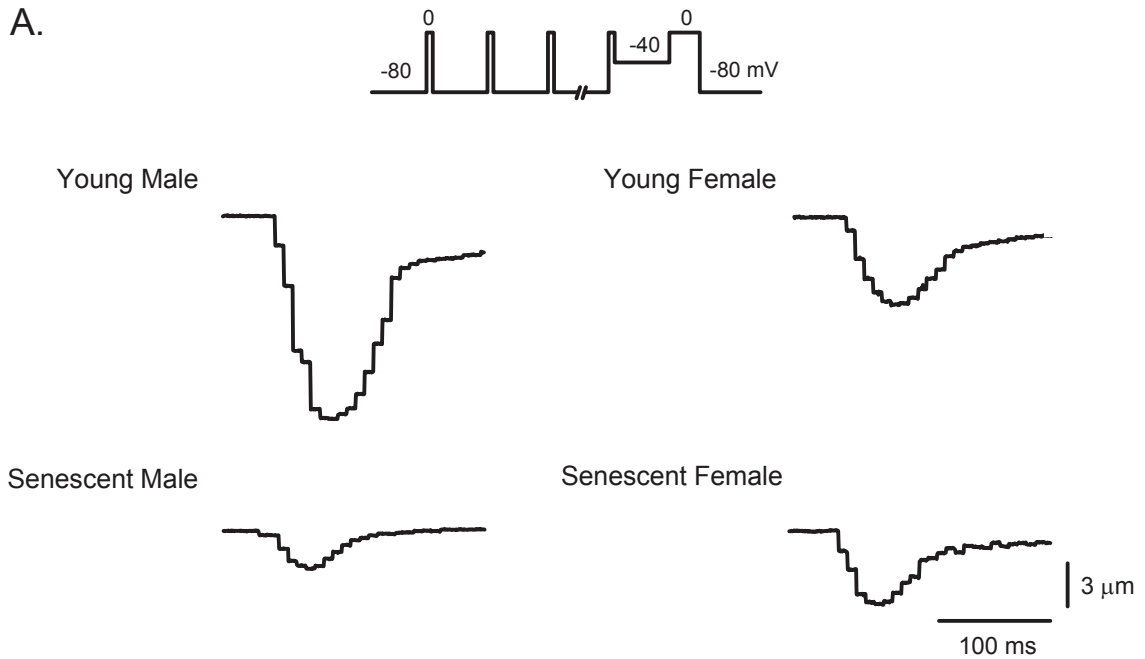


Figure 8. Cellular shortening declined with age in cells from male but not female mice. **A.** Representative examples of cellular contractions from young adult male (top left) and female (top right) myocytes, and senescent male (bottom left) and female (bottom right) myocytes. **B.** Mean cellular shortening significantly declined in cells from senescent males in comparison to young adult males. Mean cellular shortening was also significantly smaller in cells from young adult females in comparison to young adult males. Young adult and senescent female myocytes showed a similar degree of shortening. (n=8 young male, n=6 senescent male, n=10 young female, n=7 senescent female myocytes; * denotes $p < 0.05$).

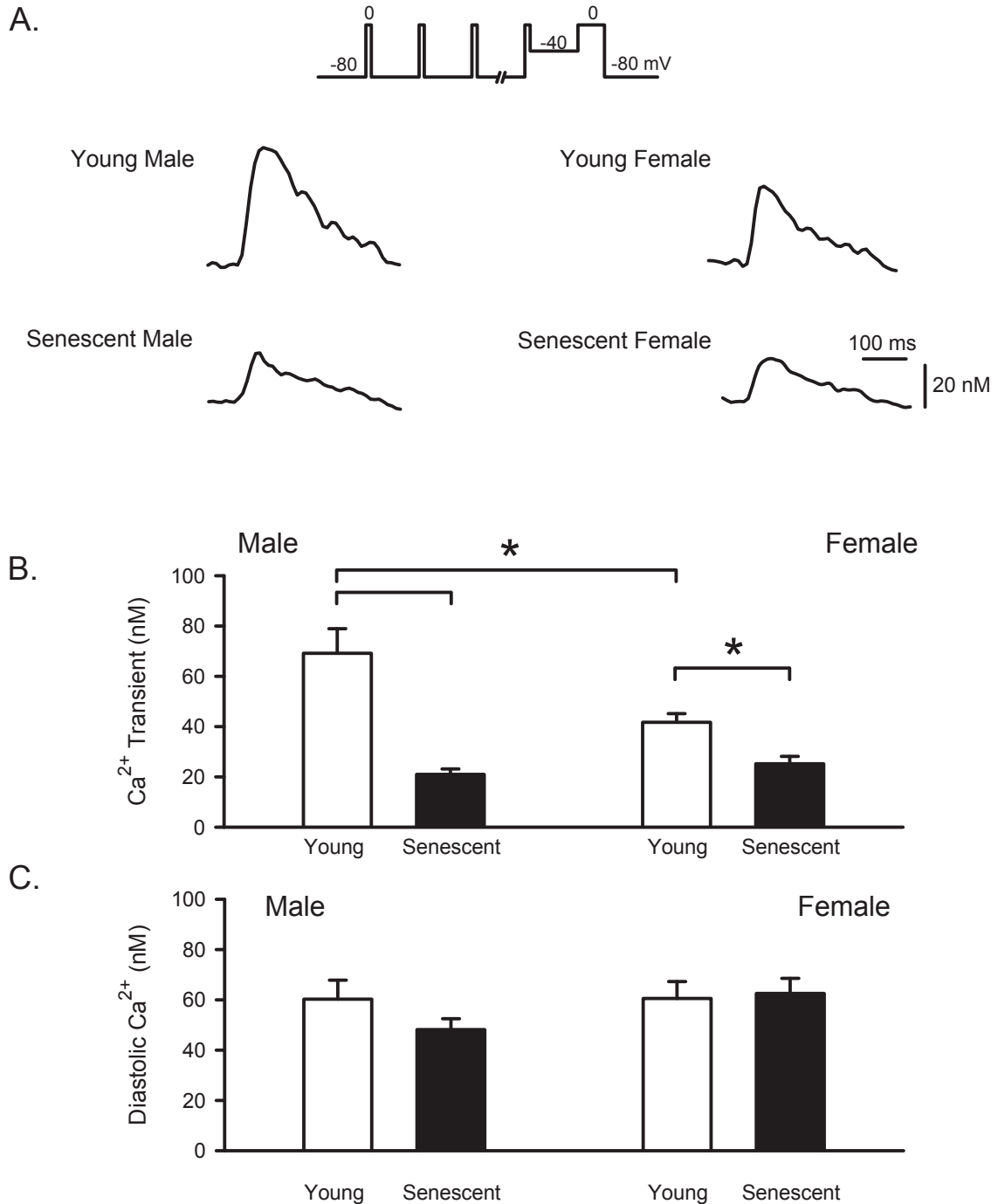


Figure 9. Ca^{2+} transients declined with age in cells from both male and female mice. **A.** Representative examples of Ca^{2+} transients from young adult male (top left) and female (top right) myocytes, and senescent male (bottom left) and female (bottom right) myocytes. **B.** Mean values for Ca^{2+} transients were significantly smaller in myocytes from senescent male and female mice in comparison to young adults. Young males also larger Ca^{2+} transients than young females. **C.** Mean diastolic Ca^{2+} levels were similar in myocytes from young adult and senescent mice (males, left; females, right). (n=11 young male, n=9 senescent male, n=12 young female, n=17 senescent female myocytes; * denotes $p < 0.05$).

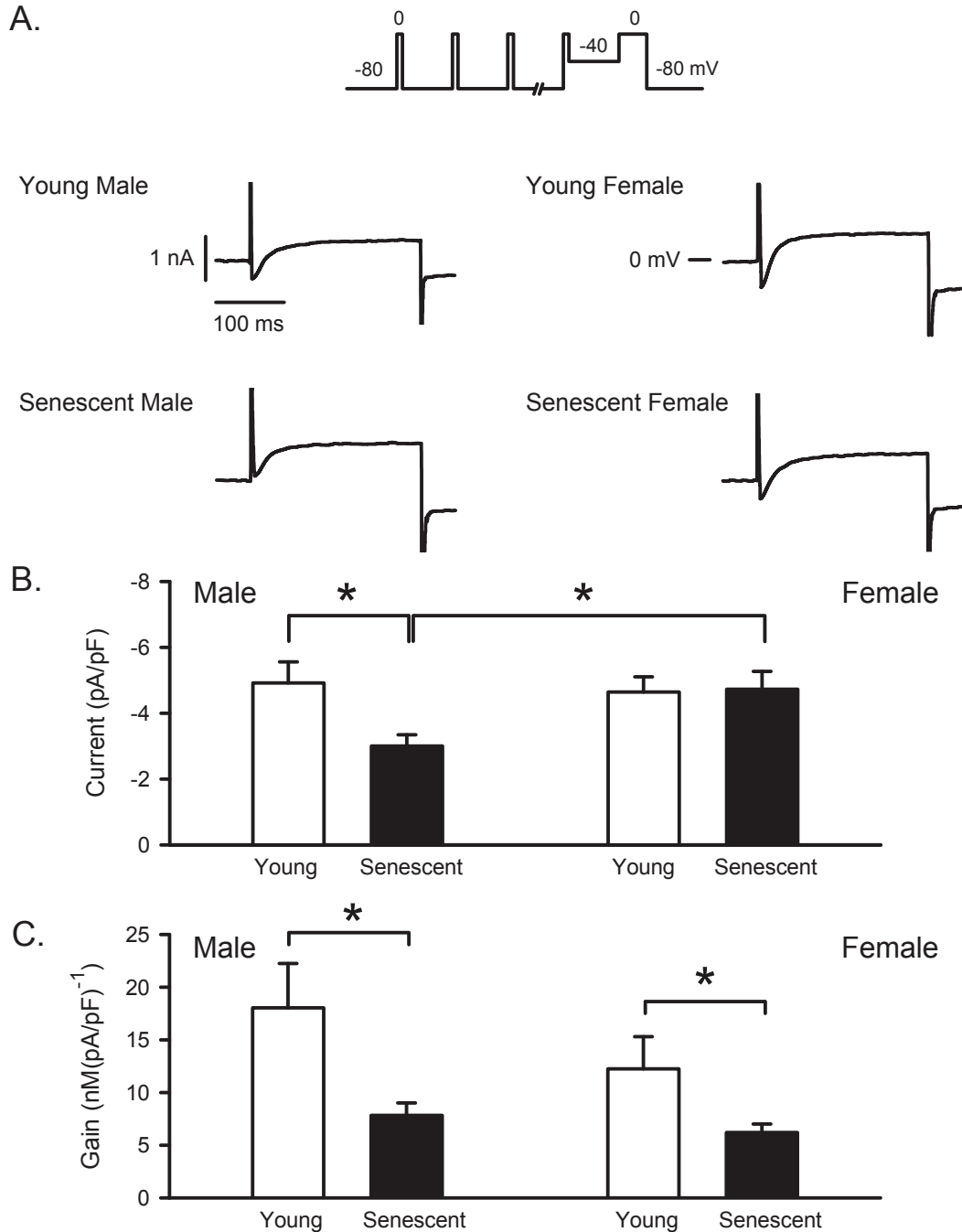


Figure 10. Ca²⁺ current density was declined with age in cells from males but not females. **A.** Representative examples of Ca²⁺ currents from young adult male (top left) and female (top right) cells, and senescent male (bottom left) and female (bottom right) myocytes. **B.** Mean Ca²⁺ current density was significantly smaller in myocytes from senescent males in comparison to young adult males and senescent females. Ca²⁺ current density was similar in young adult and senescent female mice. **C.** Average EC-coupling gain values declined in both senescent males (left) and females (right) when compared to young adult mice. (n=11 young male, n=9 senescent male, n=12 young female, n=17 senescent female myocytes; * denotes p<0.05).

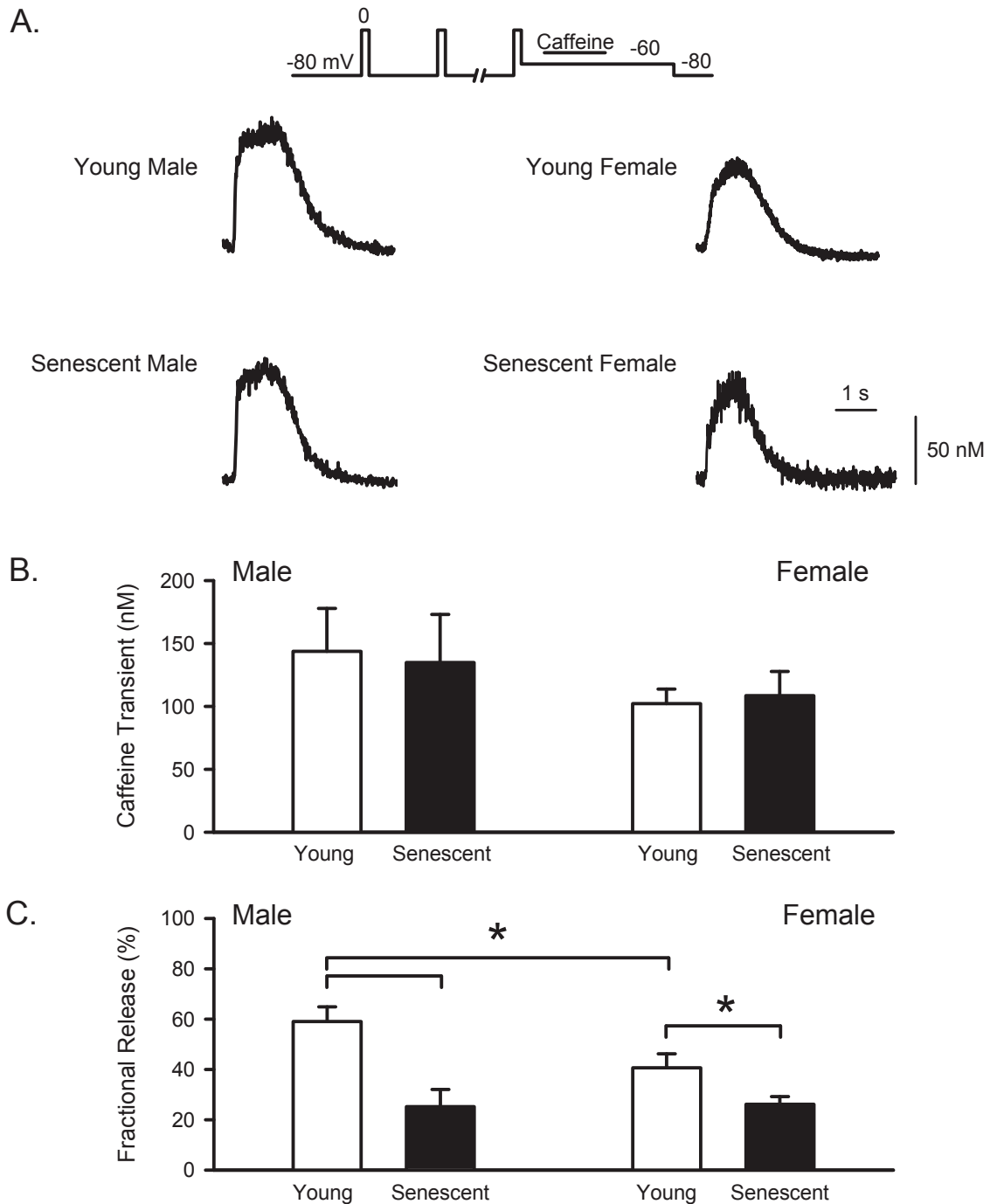


Figure 11. SR Ca^{2+} stores were not affected by age, but fractional release significantly declined in both males and females. **A.** Representative examples of caffeine-induced transients from young adult male (top left) and female (top right) cells, and senescent male (bottom left) and female (bottom right) myocytes. **B.** Mean amplitudes of caffeine transients did not differ between myocytes from young adult and senescent males (left) or females (right). **C.** Fractional release significantly declined in cells from older males and females when compared to young adults. Young males had greater fractional release than young females. (n=7 young male, n= 6 senescent male, n= 6 young female, n=11 senescent female myocytes; * denotes $p < 0.05$).

3.2 THE EFFECT OF OVARIECTOMY ON CARDIAC CONTRACTILE FUNCTION IN FEMALE MICE

3.2.1 Physical characteristics of young adult sham and OVX mice

The physical characteristics of young adult sham and OVX mice used in this study are shown in Table 7. Both sham and OVX animals were similar in age (8.7 ± 0.4 mos for sham and 8.5 ± 0.4 mos for OVX), but OVX mice weighed significantly more than sham animals (34.8 ± 1.4 g for sham and 42.0 ± 1.4 g for OVX). OVX resulted in marked uterine atrophy in comparison to sham mice (21.40 ± 0.22 μ g for sham and 3.51 ± 0.06 μ g for OVX). Myocyte characteristics were also assessed between the two groups to determine whether OVX impacted cell size. Mean cell length was similar in sham and OVX cells (128.7 ± 3.5 μ m for sham and 129.9 ± 3.6 μ m for OVX). Membrane capacitance, which provides an estimate of cell membrane area, was also similar between sham and OVX myocytes (206.4 ± 12.1 pF for sham and 216.7 ± 9.6 pF for OVX). These findings indicate that short term OVX significantly increased animal body weight and caused uterine atrophy in comparison to sham controls.

3.2.2 Field stimulation analysis of Ca²⁺ transients in young adult sham and OVX mice

To determine the impact of short term OVX on Ca²⁺ homeostasis in the young adult mouse heart, myocytes were investigated using field stimulation techniques. Myocytes were paced at 2 Hz using bipolar pulses (3 ms) to compare Ca²⁺ transient amplitudes and time courses between sham and OVX myocytes. Figure 12A shows representative Ca²⁺ transients recorded from a sham (left) and OVX (right) myocyte. As shown in these examples, Ca²⁺ transients were larger and faster in OVX cells. Mean data

show that peak Ca^{2+} transients were 83% larger in cells from OVX when compared to sham control (Figure 12B), but average diastolic Ca^{2+} levels were similar in the two groups (Figure 12C). The rates of rise (Figure 12D) and decay to 50% (Figure 12E) of the Ca^{2+} transient were determined by calculating the changes in intracellular Ca^{2+} concentration as a function of time. The results show that both the mean rate of rise of the Ca^{2+} transient and the average velocity to 50% decay were 54% and 112% faster in myocytes from OVX mice when compared to myocytes from sham controls. These results indicate that OVX increased the magnitude and velocity of Ca^{2+} transients in comparison to sham controls. Table 8 summarizes these key findings.

3.2.3. Voltage clamp assessment of Ca^{2+} homeostasis in young adult sham and OVX mice

To investigate the effect of short term OVX on specific mechanisms of EC-coupling, Ca^{2+} currents and Ca^{2+} transients were recorded simultaneously under voltage-clamp conditions. Myocytes were stimulated by a series of ten conditioning pulses from -80 to 0 mV at a frequency of 2 Hz, followed by a single test step from -40 to 0 mV as shown in Figure 13A. Representative Ca^{2+} transients are shown in Figure 13B for responses from sham (left) and OVX (right) mice. As shown, cells from OVX mice had larger Ca^{2+} transients in comparison to sham controls. Indeed, mean data show that OVX increased Ca^{2+} transient amplitude by 107% (Figure 13C) in comparison to sham. Diastolic Ca^{2+} concentrations were similar between the two groups under these experimental conditions (Figure 13D). Ca^{2+} current densities were also examined under voltage clamp conditions and compared between sham and OVX myocytes. Figure 14A

shows representative recordings of I_{CaL} from sham (top) and OVX (bottom) myocytes. As depicted in these traces, I_{CaL} was similar between cells from sham and OVX mice. Mean data show that peak I_{CaL} density was nearly identical in cells from sham and OVX mice (Figure 14B). As Ca^{2+} transients were larger but peak I_{CaL} density was unchanged with OVX, the effect of OVX on EC-coupling gain was determined. Mean values of EC-coupling gain (calculated as Ca^{2+} transient amplitude/ Ca^{2+} current density) show that OVX significantly increased gain by 112% in comparison to sham controls (Figure 14C). These findings show that short term OVX has no effect on I_{CaL} density, but instead amplifies EC-coupling gain and increases peak Ca^{2+} transients. This may explain augmented cellular shortening in OVX animal models. Table 9 summarizes findings from these experiments.

To examine whether OVX altered the voltage dependent activation of the EC-coupling pathway, Ca^{2+} transients, Ca^{2+} currents and EC-coupling gain were assessed over a wide range of membrane potentials. Sham and OVX myocytes were paced at 2 Hz with a series of five conditioning pulses prior to a test step from -40 to membrane potentials between -30 and +80 mV as shown in the voltage clamp protocol in Figure 15A. Figure 15B shows the Ca^{2+} transient-voltage relationship for cells from sham and OVX mice. Ca^{2+} transients were significantly larger in cells from OVX when compared to cells from sham at membrane potentials between -30 and +50 mV. Diastolic Ca^{2+} levels however, were similar between the two groups at all the membrane potentials tested (Figure 15C). In assessing the current-voltage (IV) relationship between sham and OVX myocytes, Ca^{2+} current density was identical between the two groups across all membrane voltages examined (Figure 16A). Activation of the Ca^{2+} current also showed

no differences between sham and OVX myocytes (Figure 16B). Since Ca^{2+} currents were similar, but Ca^{2+} transients were larger at several membrane potentials in cells from OVX mice, the EC-coupling gain was calculated for the two groups. The gain of SR Ca^{2+} release was significantly greater in myocytes from OVX mice in comparison to sham at -20 mV and at membrane potentials from +20 to +50 mV (Figure 16C). Thus, short term OVX did not affect the voltage dependent activation or density of Ca^{2+} currents, but did increase Ca^{2+} transient amplitudes and EC-coupling gain.

3.2.4 Investigation of SR Ca^{2+} stores in young adult sham and OVX mice

An increase in SR Ca^{2+} stores could help explain the increased gain observed in myocytes from mice subjected to short term OVX. To determine whether changes in SR Ca^{2+} load occurred with OVX, SR Ca^{2+} release was induced by the rapid application of 10 mM caffeine. Figure 17A shows the voltage protocol used in these experiments. Myocytes were stimulated with ten conditioning pulses at 2 Hz before being repolarized to -60 mV. Caffeine was applied for 1 s, 500 ms after the last conditioning pulse. Representative traces of caffeine-induced Ca^{2+} transients from a sham (left) and OVX (right) myocyte are shown in Figure 17B. As seen in these traces, OVX myocytes had larger caffeine-induced Ca^{2+} transients when compared to those from sham. Mean data show that SR Ca^{2+} loads were 83% larger in myocytes from OVX mice when compared to sham controls (Figure 17C). The fractional release of SR Ca^{2+} (calculated as the ratio of the peak Ca^{2+} transient and peak caffeine-induced transient) was also determined. Mean fractional release was similar between cells from OVX and sham mice (Figure

17D). These results show that OVX increased SR Ca^{2+} stores. This increase in SR Ca^{2+} may underlie the enhanced Ca^{2+} transient amplitude in cells from OVX mice. These findings are summarized in Table 9.

3.2.5 Analysis of Ca^{2+} spark parameters in young adult sham and OVX mice

To determine whether short term OVX affected unitary Ca^{2+} release from the SR, spontaneous Ca^{2+} sparks were measured in quiescent sham and OVX myocytes. Ventricular myocytes from sham and OVX mice were loaded with Fluo-4 and placed in a laminin coated chamber mounted on the stage of a laser scanning confocal microscope (Zeiss LSM 510-Meta, Carl Zeiss Canada Ltd, Toronto, ON). Examples of Ca^{2+} sparks recorded from sham and OVX myocytes are shown in Figure 18. In these examples, Ca^{2+} sparks appeared larger and occurred more frequently in OVX (right) than in sham myocytes (left). Mean data show that OVX significantly increased the frequency of spontaneous Ca^{2+} sparks in comparison to sham (Figure 19A). Average Ca^{2+} spark amplitudes were also significantly increased in OVX when compared to sham (Figure 19B). The time courses of Ca^{2+} sparks were also compared between sham and OVX myocytes. Results showed that the mean values for the time-to-peak and time constant of spark decay (τ) were similar in cells from sham and OVX mice (Figure 19C and D). In assessing the full duration at half maximum (FDHM) and full width at half maximum (FWHM) parameters, it was seen that mean values were similar in both groups (Figure 19E and F). These findings indicate that cells from mice subjected to short term OVX exhibit larger, more frequent Ca^{2+} sparks when compared to sham controls. Table 10 summarizes these results.

3.2.6 Spontaneous Ca²⁺ transients in young adult sham and OVX mice

Increased SR Ca²⁺ levels in OVX myocytes might also promote spontaneous SR Ca²⁺ release. To determine whether higher SR Ca²⁺ levels led to spontaneous SR Ca²⁺ release, we compared the incidence and magnitude of spontaneous Ca²⁺ transients in sham and OVX cells. Spontaneous Ca²⁺ release was measured in voltage clamped myocytes after the test step, during repolarization to -80 mV. Figure 20A shows a representative recording of a stimulated Ca²⁺ transient followed by two spontaneous Ca²⁺ transients in an OVX myocyte. Mean data showed that the incidence of spontaneous Ca²⁺ release was only slightly higher in OVX cells than in sham cells (Figure 20B). However, the average size of spontaneous Ca²⁺ transients was 87% larger in OVX cells compared to sham controls (Figure 20C). These results showed that short term OVX increased the magnitude of spontaneous SR Ca²⁺ release.

3.2.7 Summary of Section 3.2

In summary, short term OVX causes intracellular Ca²⁺ dysregulation in individual ventricular myocytes. Short term OVX did not impact I_{CaL}. However, EC-coupling gain, peak Ca²⁺ transients, and Ca²⁺ spark amplitudes were enhanced by OVX. Increased SR Ca²⁺ loading in OVX led to larger SR Ca²⁺ stores and an increase in Ca²⁺ spark frequency. In addition, short term OVX promoted larger spontaneous Ca²⁺ transients in comparison to sham controls. These findings suggest that enhanced Ca²⁺ homeostasis may contribute to augmented contractile function observed in OVX animal models.

TABLE 7**Physical Characteristics of Animals and Cells Used in this Study**

Parameter	Sham	OVX	p value
Age (months)	8.7 ± 0.4 (8)	8.5 ± 0.4 (10)	p=0.813
Body weight (g)	34.8 ± 1.4 (8)	42.0 ± 1.4* (10)	p=0.002
Uterine dry wt. (µg)	21.4 ± 0.22 (13)	3.51 ± 0.06* (16)	p=0.001
Cell length (µm)	128.7 ± 3.5 (31)	129.9 ± 3.6 (31)	p=0.818
Cell capacitance (pF)	206.4 ± 12.1 (23)	216.7 ± 9.6 (27)	p=0.503

Numbers represent mean ± SEM; values in brackets represent the number of cells/animals. The * denotes significantly different from sham values as determined by unpaired Student's *t*-tests, $p < 0.05$.

TABLE 8**Summary of Ca²⁺ Handling Responses from Field Stimulation Experiments**

Parameter	Sham	OVX	p value
Ca ²⁺ transient (nM)	61.7 ± 4.7 (19)	112.9 ± 11.5* (16)	p<0.001
Diastolic Ca ²⁺ (nM)	178.9 ± 9.4 (19)	208.6 ± 13.2 (16)	p=0.070
Rate of Ca ²⁺ transient rise (nM/msec)	3.03 ± 0.31 (19)	4.67 ± 0.36* (16)	p=0.002
Velocity to 50% transient decay (nM/msec)	0.62 ± 0.09 (19)	1.32 ± 0.14* (16)	p<0.001

Numbers represent mean ± SEM; values in brackets represent the number of cells. The * denotes significantly different from sham values as determined by unpaired Student's *t*-tests, p<0.05.

TABLE 9**Ca²⁺ Handling Parameters in Voltage Clamp Experiments**

Parameter	Sham	OVX	p value
Ca ²⁺ transient (nM)	24.9 ± 5.7 (8)	51.5 ± 1.8* (10)	p=0.002
Ca ²⁺ current (pA/pF)	-3.7 ± 0.5 (8)	-3.5 ± 0.3 (10)	p=0.682
Gain (nM pA/pF ⁻¹)	7.7 ± 2.0 (8)	16.3 ± 2.5* (10)	p=0.011
Diastolic Ca ²⁺ (nM)	101.7 ± 6.1 (8)	113.5 ± 7.8 (10)	p=0.271
SR Ca ²⁺ stores (nM)	61.2 ± 10.4 (8)	111.7 ± 11.9* (10)	p=0.011
Fractional release (%)	44.9 ± 7.2 (8)	49.5 ± 4.5 (10)	p=0.577

Numbers represent mean ± SEM; values in brackets represent the number of cells. Mean values were calculated for responses activated by a single test step to 0 mV. The * denotes significantly different from sham values as determined by unpaired Student's *t*-tests, *p*<0.05.

TABLE 10
Characteristics of Spontaneous Ca²⁺ Sparks

Parameter	Sham	OVX	p value
Spark Frequency (sparks/100 μ m/sec)	1.92 \pm 0.20 (130)	2.4 \pm 0.20* (142)	p=0.034
Spark Amplitude (Δ F/F ₀)	0.342 \pm 0.006 (894)	0.379 \pm 0.006* (1255)	p<0.001
Spark time-to-peak (TTP, msec)	13.53 \pm 0.46 (894)	13.9 \pm 0.51 (1255)	p=0.151
Tau for spark decay (msec)	35.01 \pm 4.5 (894)	40.53 \pm 4.3 (1255)	p=0.502
Full duration at half maximum (FDHM, msec)	21.23 \pm 0.40 (894)	22.13 \pm 0.48 (1255)	p=0.715
Full width at half maximum (FWHM, μ m)	1.71 \pm 0.03 (894)	1.67 \pm 0.02 (1255)	p=0.364

Numbers represent mean \pm SEM. The numbers in brackets denote the value of n. For spark frequency, n= number of cells; for all other spark parameters, n= the total number of sparks analyzed. In these experiments, cells from 6 sham animals and 7 OVX animals were used. The * denotes significantly different from sham values as determined by unpaired Student's *t*-tests, p<0.05.

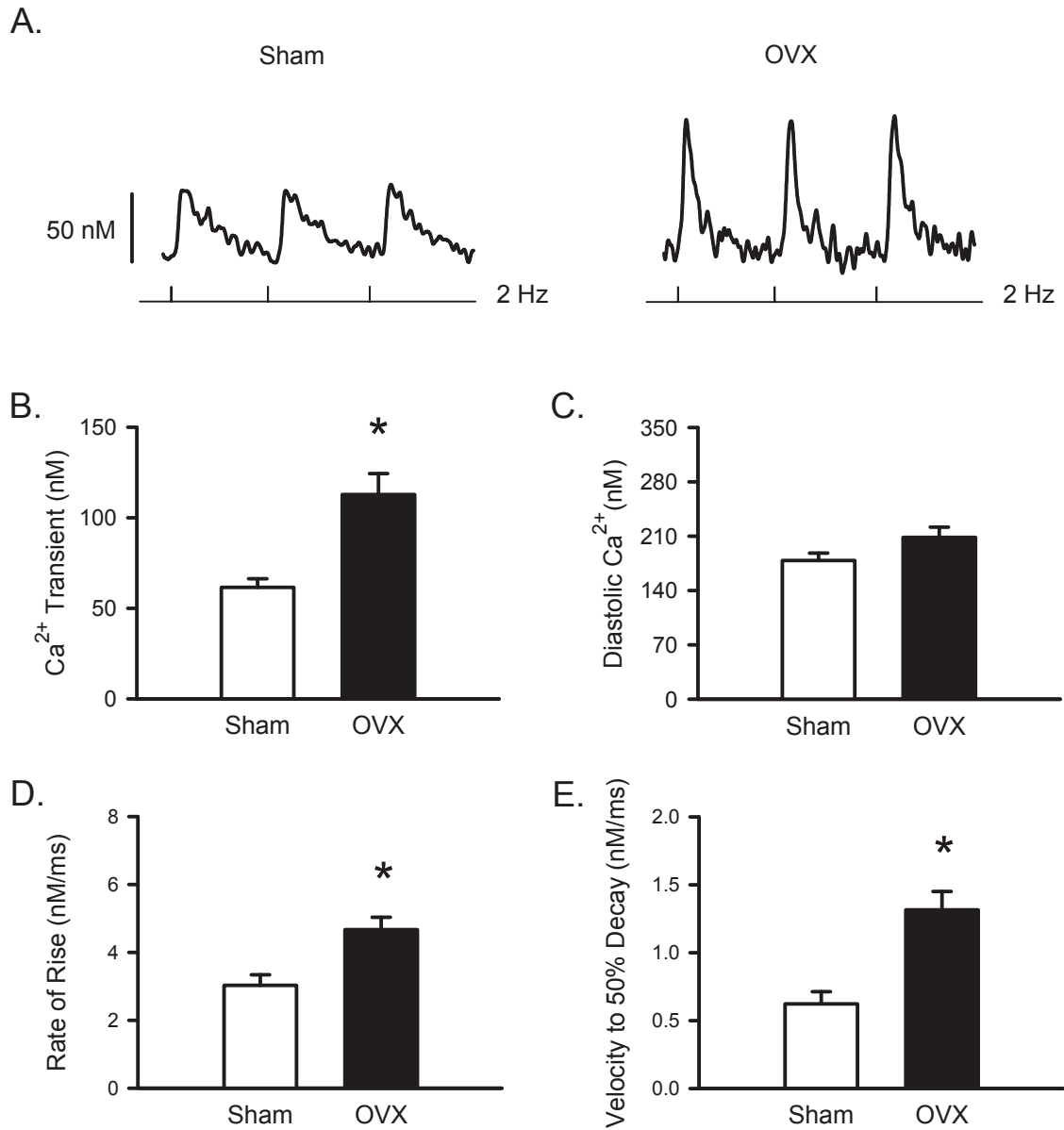


Figure 12. OVX amplified the size and speed of Ca²⁺ transients in comparison to sham controls. **A.** Representative Ca²⁺ transients from sham (left) and OVX (right) myocytes field stimulated at 2 Hz. **B.** OVX increased peak Ca²⁺ transients when compared to sham control. **C.** Diastolic Ca²⁺ levels were similar between sham and OVX myocytes. **D,E.** OVX increased the rate-of-rise and the velocity to 50% decay of the Ca²⁺ transient in comparison to sham controls. (n=19 sham and n=16 OVX myocytes; * denotes p<0.05).

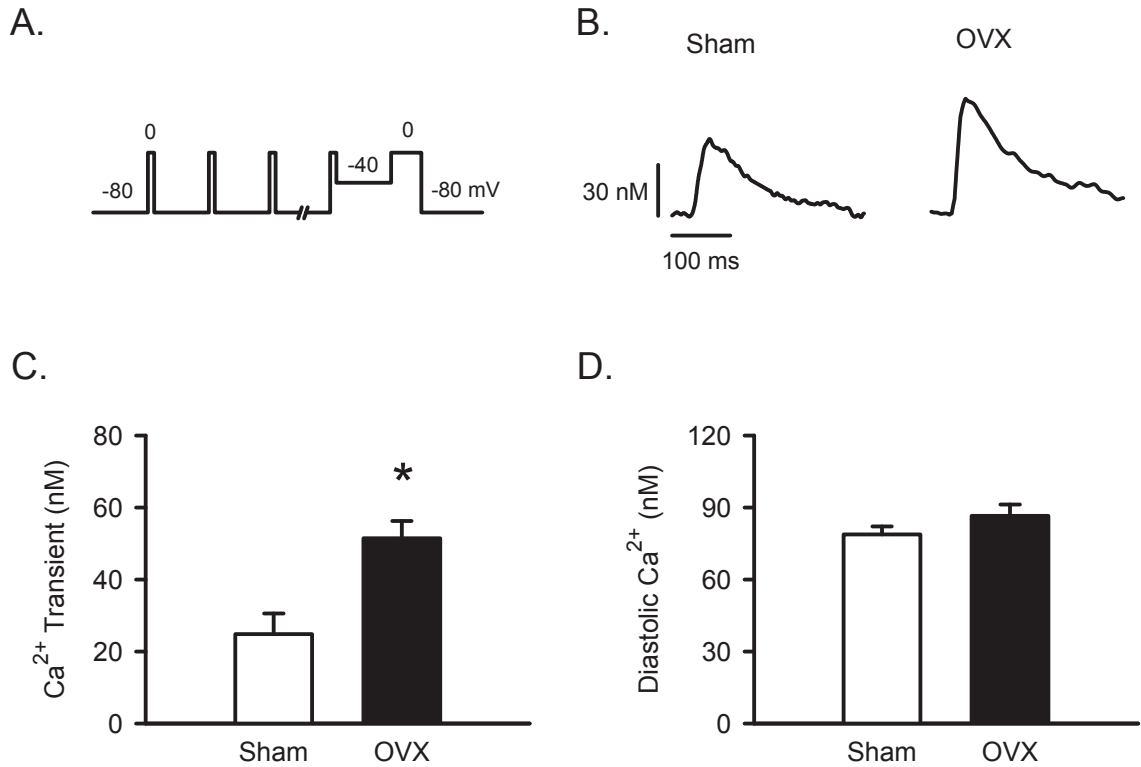


Figure 13. Peak Ca^{2+} transients were larger in OVX myocytes when compared to sham controls. **A.** The voltage clamp protocol used is shown above. Myocytes were stimulated with a train of conditioning pulses at 2 Hz prior to a single test step from -40 mV. **B.** Representative Ca^{2+} transients from a sham (left) and OVX (right) myocyte activated by the test step to 0 mV. **C.** Mean Ca^{2+} transients were significantly larger in OVX myocytes in comparison to sham controls. **D.** Average diastolic Ca^{2+} values were similar between the two groups. (n=8 sham and n=10 OVX myocytes; * denotes $p < 0.05$).

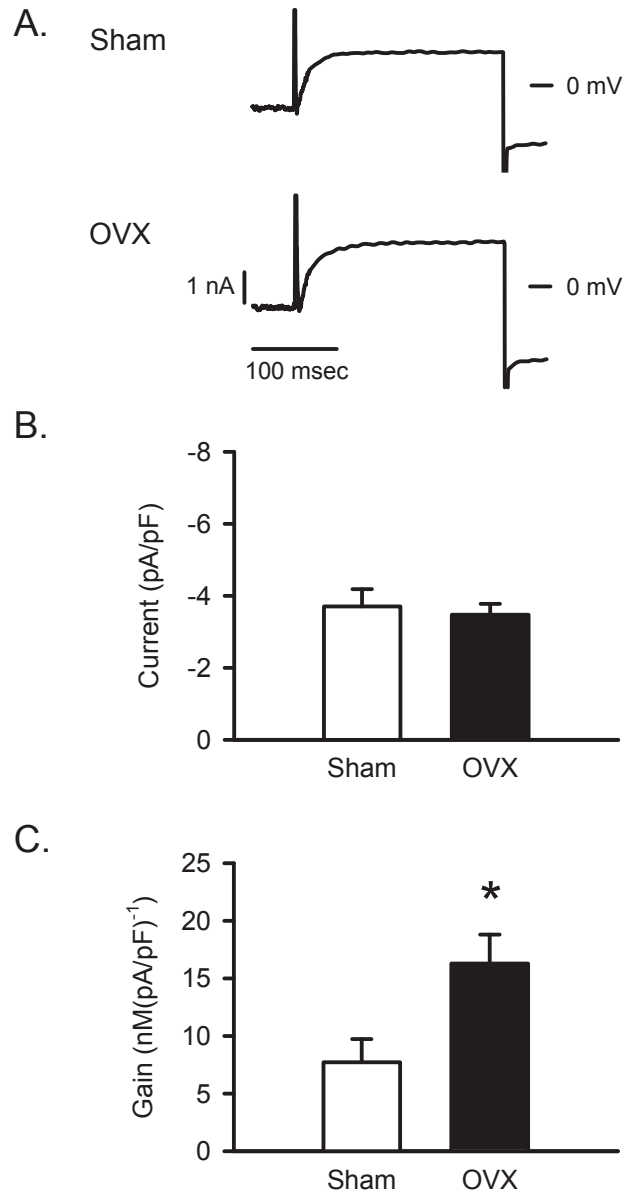


Figure 14. EC-coupling gain was enhanced in OVX myocytes when compared to sham controls. **A.** Representative Ca^{2+} currents from a sham (top) and OVX (bottom) myocyte activated by a test step to 0 mV. **B.** Peak Ca^{2+} currents were similar between sham and OVX myocytes. **C.** OVX significantly increased EC-coupling gain in comparison to sham. (n=8 sham and n=10 OVX myocytes; * denotes p<0.05).

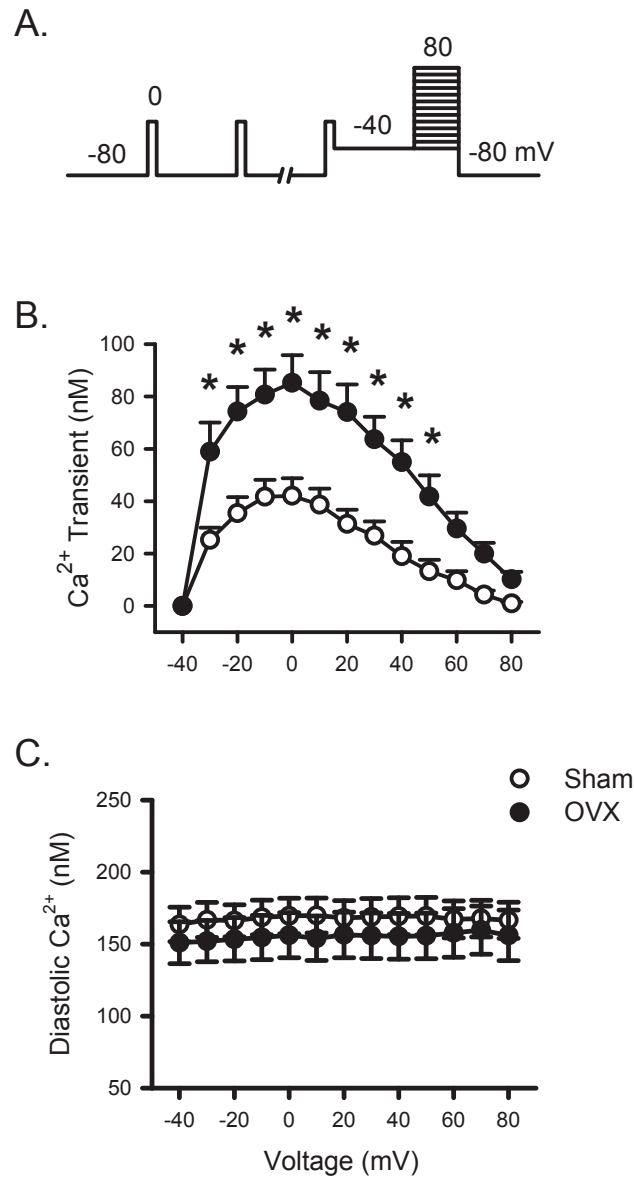


Figure 15. OVX enhanced Ca^{2+} transients across a range of membrane potentials.
A. The voltage clamp protocol used to investigate the current-voltage (IV) relationship is shown. Myocytes were stimulated with conditioning pulses at 2 Hz prior to various test steps from -40 mV. **B.** Peak Ca^{2+} transients were larger in OVX myocytes in comparison to sham controls at test potentials between -30 and +50 mV. **C.** Diastolic Ca^{2+} levels were similar between the two groups. (n=12 sham and n=16 OVX myocytes; * denotes $p < 0.05$).

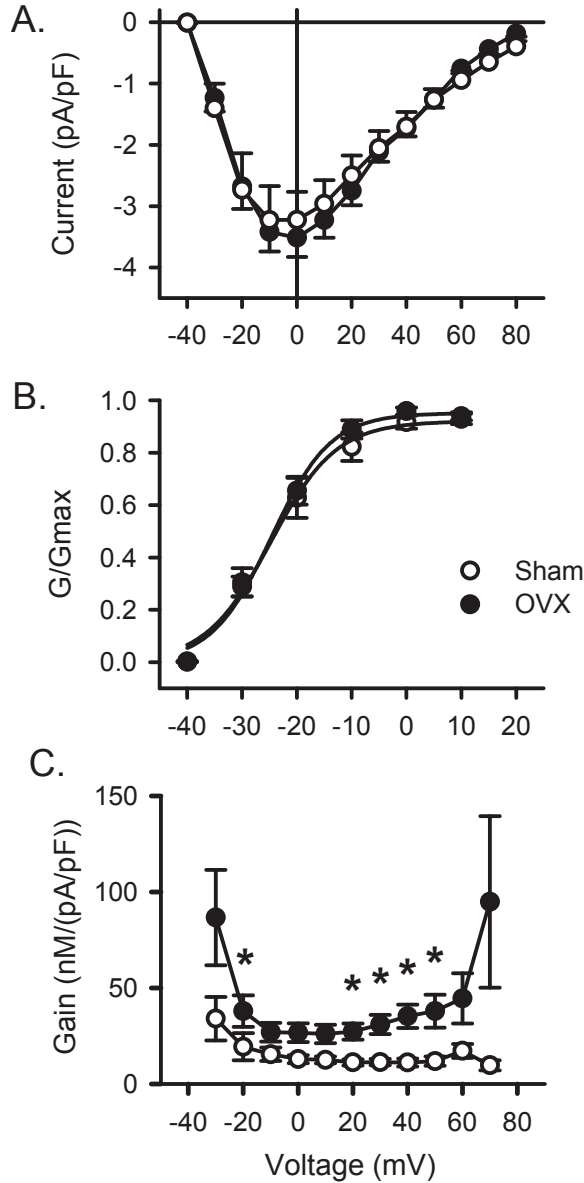


Figure 16. OVX increased EC-coupling gain at several membrane potentials.

A. Average Ca^{2+} currents were identical between OVX and sham myocytes at all membrane potentials tested. **B.** Activation of the Ca^{2+} current was similar in the two groups. **C.** EC-coupling gain values were significantly greater in OVX myocytes when compared to sham controls at -30 mV as well as between +20 and +50 mV. (n = 12 sham and n=16 OVX myocytes; * denotes $p < 0.05$).

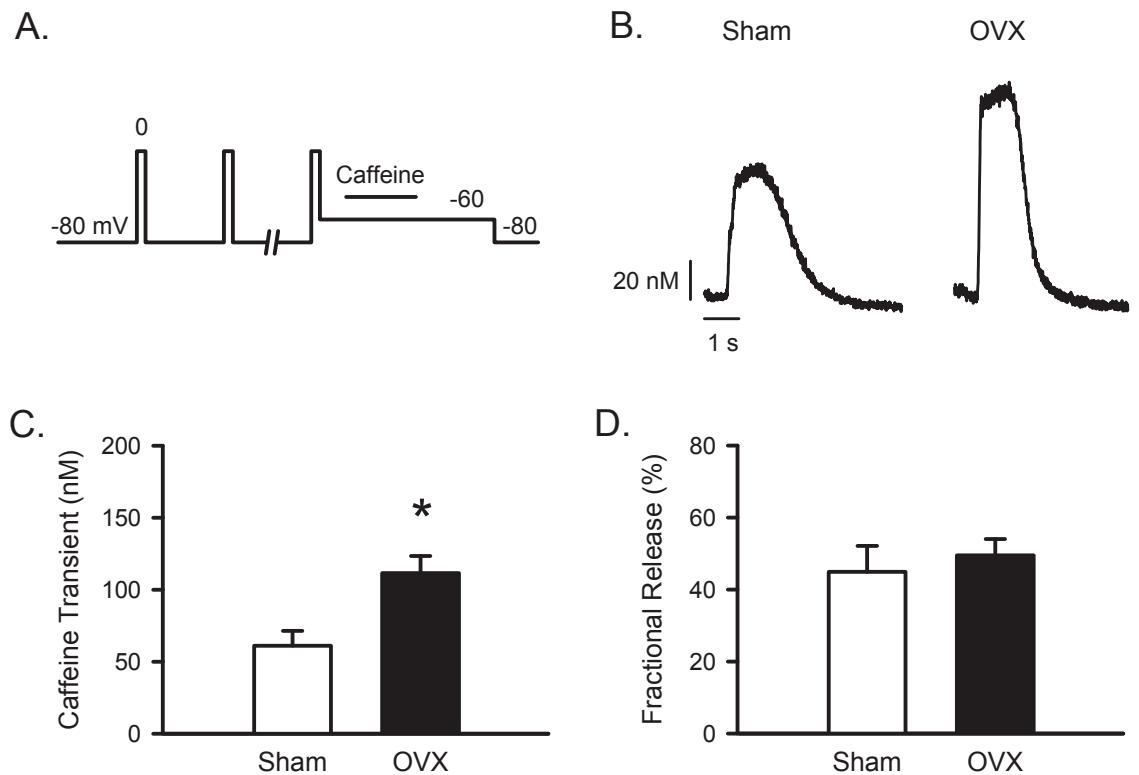


Figure 17. OVX significantly increased SR Ca^{2+} content. **A.** The voltage clamp protocol used to assess SR Ca^{2+} content is shown. Myocytes were stimulated with conditioning pulses at 2 Hz prior to application of 10 mM caffeine. **B.** Representative recordings of caffeine-induced Ca^{2+} transients from a sham (left) and OVX (right) myocyte. **C.** OVX increased the size of caffeine-induced transients in comparison to sham controls. **D.** Fractional release of SR Ca^{2+} (calculated as the ratio of Ca^{2+} transient/caffeine-induced transient) was similar between the experimental groups. (n=6 sham and n=9 OVX myocytes; * denote p<0.05).

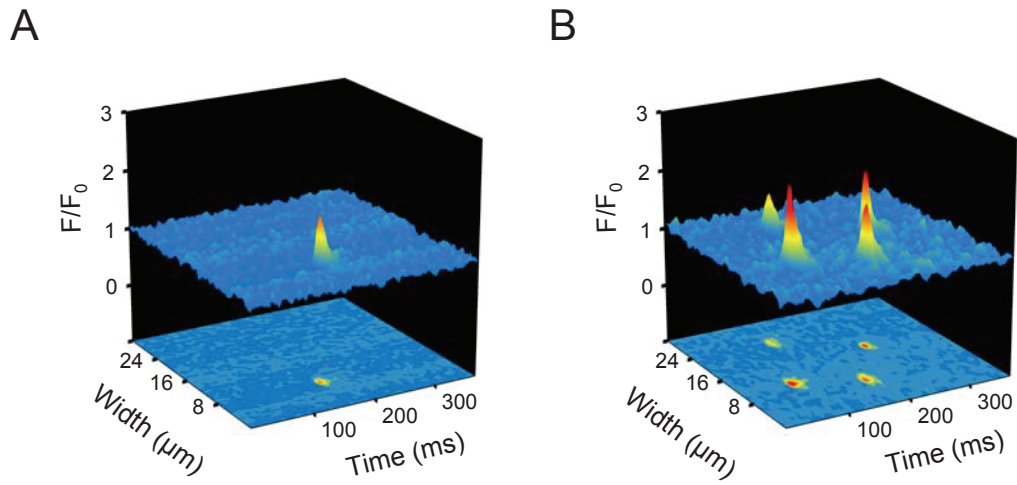


Figure 18. Three dimensional representative plots of unitary Ca^{2+} release events from sham and OVX myocytes. Representative recordings of Ca^{2+} sparks from a sham (A) and an OVX (B) myocyte. Ca^{2+} sparks were larger and more frequent in OVX when compared to sham.

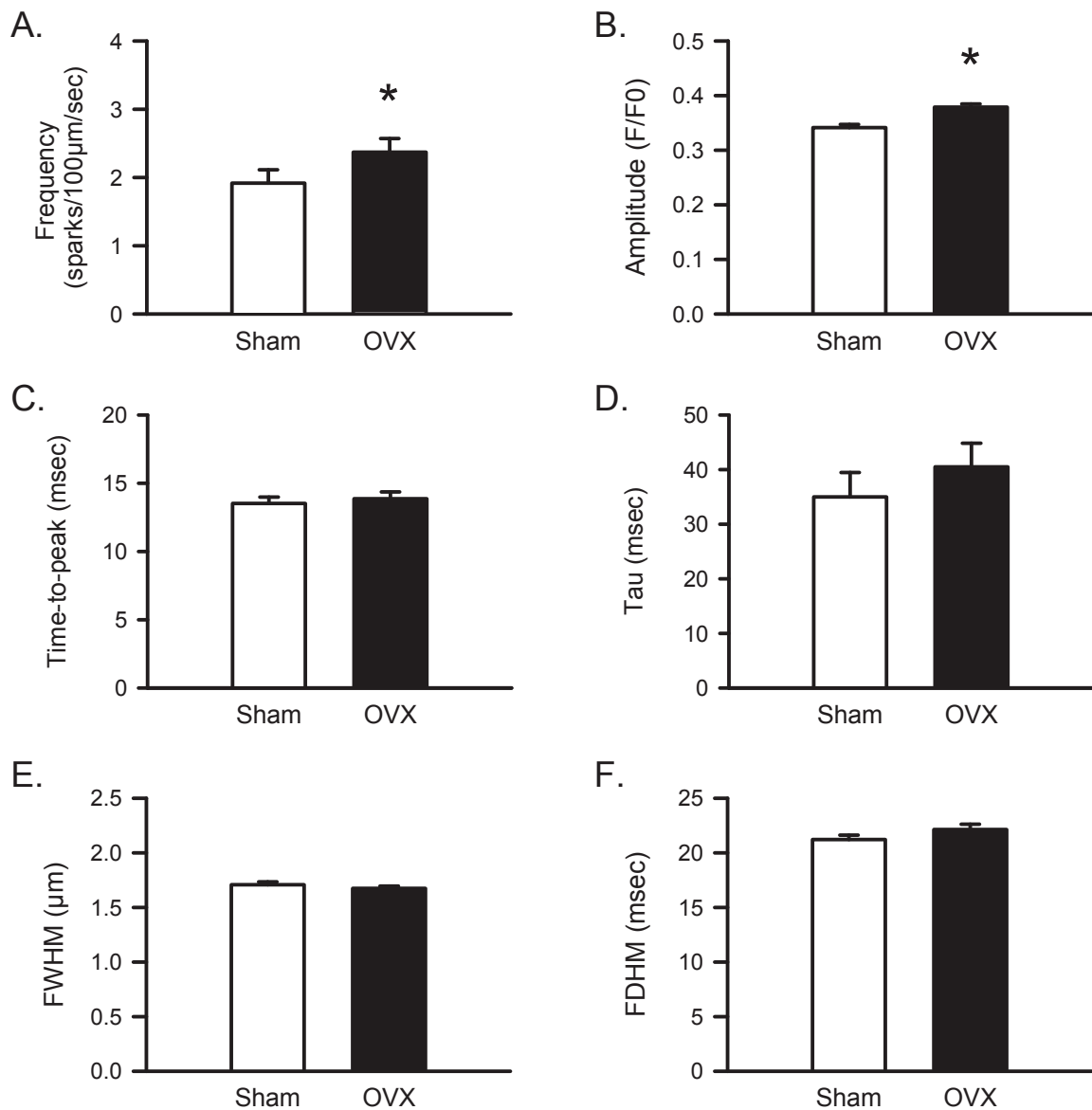


Figure 19. OVX enhanced Ca^{2+} spark frequency and amplitudes.

A,B. OVX increased mean Ca^{2+} spark frequency and amplitude when compared to sham controls. **C,D.** Mean values for Ca^{2+} spark time-to-peak and the time constant of Ca^{2+} spark decay (tau) were similar between sham and OVX myocytes. **E,F.** Full-width at half maximum (FWHM) and full-duration at half maximum (FDHM) values were similar between the two groups. The value of $n=894$ sham and $n=1255$ OVX sparks; for frequency, $n=130$ sham and $n=142$ OVX myocytes. In these experiments, cells from 6 sham animals and 7 OVX animals were used (* denotes $p<0.05$)

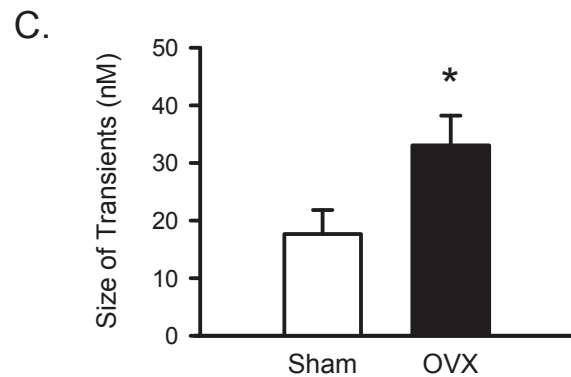
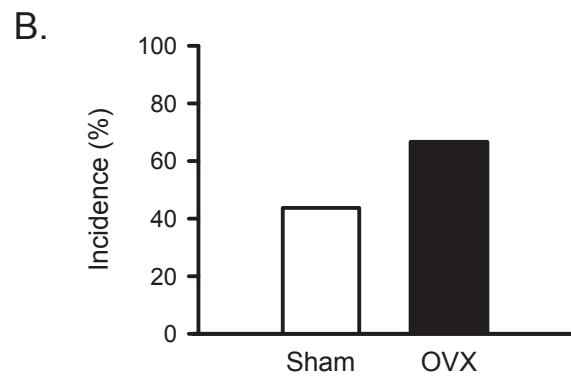
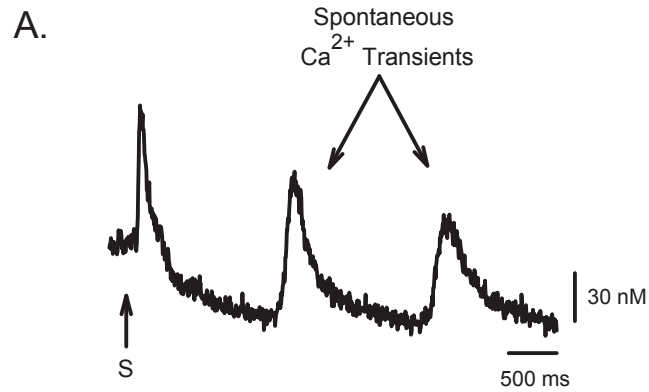


Figure 20. Spontaneous Ca²⁺ transients were larger in OVX myocytes.

A. Representative example of spontaneous Ca²⁺ transients recorded from an OVX myocyte. A stimulated Ca²⁺ transient (S, arrow) is followed by two spontaneous Ca²⁺ releases during repolarization. **B.** Incidence of spontaneous releases was higher, although this was not statistically significant, between sham and OVX myocytes. **C.** Spontaneous transients were markedly larger in cells from OVX when compared to sham myocytes. (n=37 sham and n=38 OVX myocytes; * denotes p<0.05).

3.3 THE IMPACT OF OVX AND AGING ON CARDIAC CONTRACTILE FUNCTION IN FEMALE MICE

3.3.1 Physical characteristics of aged sham and OVX mice

Animal characteristics were compared between aged OVX and sham animals. These results are summarized in Table 11. Results showed that OVX and sham animals were similar ages (23.2 ± 0.5 mos for OVX and 24.5 ± 0.5 mos for sham). Additionally, body weights were not significantly different between OVX mice and sham mice (36.7 ± 2.4 g for OVX and 32.2 ± 1.7 g for sham). However, OVX did result in significant uterine atrophy when comparing dry uterine weights to sham (6.2 ± 0.9 μ g for OVX and 19.6 ± 2 μ g for sham, $p < 0.05$). Cell capacitance was measured to compare cell membrane area in sham and OVX cells. Results showed that cell capacitance was significantly reduced in myocytes from OVX mice in comparison to myocytes from sham animals (230.7 ± 16.3 for OVX myocytes and 302.6 ± 20.6 for sham myocytes). These results indicate that long term OVX decreases cardiomyocyte membrane area in comparison to sham controls.

3.3.2 Cardiac contractile function and Ca^{2+} handling in field stimulated myocytes from aged sham and OVX mice

To determine whether long term OVX disrupts Ca^{2+} homeostasis and contractile function, myocytes from sham and OVX mice were compared in field stimulation experiments. Bipolar pulses (3 ms) were delivered at a rate of 2 Hz and Ca^{2+} transients and contractions were recorded simultaneously (described in Chapter 2). Figure 21A depicts examples of Ca^{2+} transients from sham (left) and OVX (right) myocytes stimulated at 2 Hz. As seen in these traces, the Ca^{2+} transient from OVX myocyte was significantly larger, and faster when compared to the sham control. Mean peak Ca^{2+}

transient amplitudes were 41% larger in myocytes from OVX mice when compared to myocytes from sham mice (Figure 21B). However, diastolic Ca^{2+} levels were similar between cells from sham and OVX mice (Figure 21C). The rates of rise (Figure 21D) and decay to 50% (Figure 21E) of the Ca^{2+} transient were determined by calculating the changes in intracellular Ca^{2+} concentration as a function of time. The results show that both the mean rate of rise of the Ca^{2+} transient and the average decay rate were 43% and 71% faster in myocytes from OVX mice when compared to myocytes from sham controls.

Representative cellular contractions from ventricular myocytes paced at 2 Hz from sham (left) and OVX (right) are shown in Figure 22A. These traces show that contractions were similar in size between cells from sham and OVX mice. Indeed, mean fractional shortening did not differ between cells from OVX and sham mice under field stimulation conditions (Figure 22B). Average diastolic cell length was also similar between sham and OVX mice (Figure 22C). However, the time-to-peak contraction (Figure 22D) and the time-to-50% decay (Figure 22E) of responses were significantly faster with OVX in comparison to sham. Thus, the size and speed of Ca^{2+} transients were significantly increased by OVX. While the speed of contractile responses was also enhanced by OVX, the degree of cellular contraction was unchanged when compared to sham-controls. Table 12 summarizes these findings from field stimulation experiments.

3.3.3 *In vivo* ventricular function in aged sham and OVX mice

To relate cellular contraction to *in vivo* ventricular function, two-dimensional guided M-Mode echocardiography was performed. Using a high-resolution linear

transducer (i13L, GE ultrasound, Horten, Norway) connected to a Vivid 7 imaging system (GE Medical Systems, Horten, Norway), echocardiography images were obtained from anesthetized mice (described in Chapter 2). Figure 23A illustrates representative M-mode recordings from OVX and sham mice. In assessing *in vivo* function, sham and OVX mice showed a similar degree of LV fractional shortening (Figure 23B). In addition, no differences in ejection fraction were observed between the two groups (Figure 23C). Electrocardiogram measurements were used to compare heart rate. Figure 23D shows that sham and OVX mice had similar heart rates. These findings demonstrate that *in vivo* contractile function was not affected by long term OVX.

3.3.4 Action potential properties in aged sham and OVX mice

Differences in the functional responses between sham and OVX myocytes could be due to alterations in the action potential configuration; hence action potential responses were compared in myocytes from sham and OVX mice. Myocytes were impaled using high resistance microelectrodes. Under current clamp conditions, action potentials were generated at a rate of 2 Hz (described in Chapter 2). Action potentials and cellular contractions were recorded simultaneously using pClamp software (version 8.2; Molecular Devices, Sunnyvale, CA). Figure 24A illustrates representative action potentials measured from sham (left) and OVX (right) myocytes. Action potentials recorded from OVX and sham mice had similar configurations. Mean resting membrane potential was similar between sham and OVX groups (Figure 24B). Further, action potential durations at 50% repolarization (Figure 24C) and 90% repolarization (Figure 24D) were similar in cells from OVX and sham mice. In addition, the amplitudes of

contractions measured with action potentials did not differ in cells from sham and OVX mice (Figure 24E). Table 13 summarizes mean data from action potential recordings. These results indicate that differences in action potential configuration did not account for differences in Ca^{2+} transients between sham and OVX mice.

3.3.5 Voltage clamp assessment of EC-coupling mechanisms in aged sham and OVX mice

To determine the impact of long term OVX on cardiac EC-coupling mechanisms, myocytes were examined under voltage clamp conditions. A uniform voltage protocol was used to assess the current-voltage (IV) relationship between older sham and OVX mice (Figure 25A). Myocytes were stimulated with five conditioning pulses administered at a frequency of 2 Hz before test steps. Cells were repolarized to -40 mV after the last conditioning pulse, and test steps were made in 10 mV increments to potentials between -40 to +80 mV to activate Ca^{2+} transients and Ca^{2+} currents. Representative Ca^{2+} transients recorded during steps to 0 mV are shown in Figure 25B for sham (left) and OVX (right) myocytes. These examples show that Ca^{2+} transients were larger and faster in myocytes from OVX than from sham mice in voltage clamped cells. Ca^{2+} transients were significantly larger at voltages between -20 and +40 mV as seen in Figure 25C, with OVX causing a 91% increase in Ca^{2+} transient size at the peak of the IV curve. Diastolic Ca^{2+} levels, as measured at the base of the last conditioning pulse prior to the test step, were similar between OVX and sham at all test potentials (Figure 25D).

To determine whether long term OVX affected Ca^{2+} current density, currents

were activated by test steps from -40 to 80 mV in myocytes from sham and OVX animals. Figure 26A shows representative current recordings for test steps to 0 mV for sham (left) and OVX (right) myocytes. As shown in these examples, peak Ca^{2+} current was larger in cells from OVX when compared to sham mice. Mean values indicated that OVX significantly increased Ca^{2+} current density at voltages between -30 and +30 mV (Figure 26B), and OVX resulted in a 48% increase in current density at the peak value of the IV curve. Ca^{2+} current activation curves were similar in myocytes from sham and OVX mice (Figure 26C). The gain of EC-coupling was calculated (Ca^{2+} transient amplitude/ Ca^{2+} current density) at each voltage used to generate the IV plots. EC-coupling gain was similar in sham and OVX myocytes across all membrane potentials (Figure 26D). These findings show that OVX increased Ca^{2+} current density, which in turn, led to greater Ca^{2+} release from the SR. This occurred without alterations in Ca^{2+} channel activation, resting Ca^{2+} levels, or EC-coupling gain. These findings are summarized in table 14.

3.3.6 Myofilament Ca^{2+} sensitivity in aged sham and OVX hearts

Since OVX enhanced SR Ca^{2+} release but did not alter *in vivo* or *in vitro* cardiac contractile function, the Ca^{2+} sensitivity of the contractile filaments was investigated. To evaluate myofilament Ca^{2+} sensitivity, phase-loop plots of cellular shortening- $[\text{Ca}^{2+}]_i$ relationships were compared between sham and OVX cells. These plots were constructed using paired contraction and Ca^{2+} transient data from field stimulated myocytes (Figures 21 and 22). Representative plots are depicted in Figure 27A. As shown, OVX shifted the descending portion of the loop to the right in comparison to

sham. The descending portion of the loop provides an estimation of myofilament Ca^{2+} sensitivity (Mellor et al., 2011; Spurgeon et al., 1992), and thus shows that greater $[\text{Ca}^{2+}]_i$ is required to generate a similar degree of cellular shortening in OVX when compared to sham. This shift was quantified by measuring the Ca^{2+} concentration at 50% relaxation, as in previous studies (Mellor et al., 2011). The Ca^{2+} concentration at 50% relaxation was significantly increased in OVX myocytes in comparison to sham (Figure 27B).

Next, myofilament Ca^{2+} sensitivity was assayed directly. This was examined in collaboration with Dr. W. Glen Pyle at the University of Guelph. Ventricular tissue from older sham and OVX mice was homogenized and subjected to differential centrifugation to isolate the myofilaments. Myofilament function then was assessed using a Carter assay to measure actomyosin MgATPase activity (described in detail in Chapter 2). Normalized data show a distinct rightward shift of the actomyosin MgATPase activity- Ca^{2+} curve of myofilaments from OVX mice when compared to sham (Figure 28A). This shows that a greater amount of Ca^{2+} was required to generate specific actomyosin MgATPase activity, indicating a decrease in myofilament Ca^{2+} sensitivity. Actomyosin MgATPase activity at saturating levels of free calcium (~10 mM) were similar between sham and OVX mice (Figure 28B), suggesting that OVX did not impact maximal actomyosin MgATPase activity. However, EC_{50} values for myofilaments isolated from OVX mice were 26% higher in comparison to samples from sham mice (Figure 28C), further indicating decreased myofilament Ca^{2+} sensitivity. Cooperativity, as measured by the Hill coefficient, was not different between sham and OVX (Figure 28D). These results show that long term OVX reduced myofilament Ca^{2+} sensitivity in the aging female heart.

To investigate whether changes in myofilament Ca^{2+} sensitivity were due to differential phosphorylation, the phosphorylation status of several key contractile proteins was assessed. Figure 29A shows a resulting SDS-PAGE gel stained with ProQ Diamond (left) to detect protein phosphorylation and Coomassie (right) to assess protein loading. Myosin binding protein-C (MyBP-C), troponin I (TnI), and troponin T (TnT) are labeled next to the respective bands. This representative blot shows that phosphorylation of myofilament proteins appeared similar between sham and OVX hearts. Indeed, mean values showed that phosphorylation of MyBP-C, TnI, and TnT were not significantly different between sham and OVX mice (Figure 29B). These results show that differences in phosphorylation of MyBP-C, TnI, and TnT did not account for decreased myofilament Ca^{2+} sensitivity in the older OVX heart.

3.3.7 Assessment of SR Ca^{2+} stores in aged sham and OVX mice

To establish whether enhanced SR Ca^{2+} release was due to increased SR Ca^{2+} loading, SR Ca^{2+} stores were compared in sham and OVX myocytes. The voltage protocol used in these experiments is shown in Figure 30A. Cells were stimulated with ten conditioning pulses at a pacing rate of 2 Hz and then repolarized to -60 mV. Caffeine (10 mM) was acutely applied with a rapid solution switcher for 1 s, 500 ms after the last conditioning pulse. Figure 30B shows representative recordings of caffeine-induced Ca^{2+} transients from sham (left) and OVX (right) myocytes. These examples show that cells from OVX mice had larger caffeine-induced transients than those from sham mice. Indeed, mean SR Ca^{2+} stores were 90% larger in myocytes from OVX mice when compared to myocytes from sham mice (Figure 30C). The fractional release of Ca^{2+}

from the SR, calculated by dividing the amplitude of the Ca^{2+} transient by the amplitude of the caffeine-induced transient, was also determined for myocytes from OVX and sham animals. Average fractional release values did not differ between cells from OVX and sham mice (Figure 30D). These results show that long-term OVX increased SR Ca^{2+} stores in older female mice, but did not alter the fractional release of Ca^{2+} from the SR.

3.3.8 Unitary Ca^{2+} release properties in aged sham and OVX mice

Changes in unitary SR Ca^{2+} release events could also contribute to the increase in size of the Ca^{2+} transient observed in cells from OVX mice. To examine this, properties of spontaneous Ca^{2+} sparks were examined and compared in myocytes from aged OVX and sham animals loaded with Fluo-4 as described in detail in Chapter 2. Examples of Ca^{2+} sparks recorded from aged sham and OVX myocytes are shown in Figure 31. In these examples, Ca^{2+} sparks appeared larger and occurred more frequently in OVX (right) than in sham myocytes (left). Mean data showed that the frequency of Ca^{2+} sparks was 71% greater in OVX than sham myocytes (Figure 32A). Ca^{2+} sparks from OVX cells were also 43% larger in amplitude when compared to those from sham (Figure 32B). The time courses of the Ca^{2+} spark responses were compared between sham and OVX cells. Figure 32C shows that the spark time-to-peak was shorter in OVX cells in comparison to sham myocytes. However, the time constant of spark decay (τ) was prolonged by OVX (Figure 32D). Spark widths were also examined for sham and OVX myocytes. The full width at half maximum (FWHM) was increased by 22% in Ca^{2+} sparks from OVX myocytes (Figure 32E). However, the full duration at half maximum (FDHM) values did not differ between Ca^{2+} sparks from OVX and sham myocytes

(Figure 32F). Therefore, these results show that long-term OVX promoted larger, wider Ca^{2+} sparks that occurred more frequently than in myocytes from sham. Mean Ca^{2+} spark data are summarized in table 15.

3.3.9 Spontaneous Ca^{2+} transients and triggered electrical activity in aged sham and OVX mice

Higher SR Ca^{2+} levels in OVX myocytes might promote spontaneous Ca^{2+} release from the SR. To determine whether spontaneous Ca^{2+} release occurred as a consequence of enhanced SR Ca^{2+} loading in OVX cells, spontaneous activity was compared in myocytes from sham and OVX mice. To quantify this, spontaneous Ca^{2+} transients were measured in voltage clamped myocytes during repolarization to -80 mV. Figure 33A depicts a spontaneous Ca^{2+} transient that follows a stimulated Ca^{2+} transient in a myocyte from an OVX mouse. Mean data showed that the incidence of spontaneous Ca^{2+} transients was greater in OVX than in sham cells, although this increase was not statistically significant (Figure 33B). However, the magnitude of spontaneous Ca^{2+} transients was 93% larger in myocytes from OVX when compared to sham (Figure 33C).

As spontaneous SR Ca^{2+} release can promote triggered activity (Clusin, 2003), sham and OVX myocytes were assessed for spontaneous electrical activity. Action potentials were generated in myocytes at a rate of 2 Hz (described in Chapter 2), and two types of triggered activity were observed. The first type of triggered activity observed was early afterdepolarizations (EADs). EADs were quantified as spontaneous electrical disruptions that occurred prior to full repolarization. Figure 34A shows a train of normal action potentials followed by an EAD, which occurred in an OVX myocyte. The incidence of EADs was significantly greater in OVX cells than in sham cells (Figure

34B). In addition, EADs were preceded by gradual prolongation of the APD₉₀ in OVX cells (from 119.7 ± 18.8 ms during steady state pacing to 255.8 ± 27.3 ms). The second type of triggered activity observed was delayed afterdepolarizations (DADs). DADs were observed as spontaneous electrical activity that occurred after a stimulated beat had returned to baseline. Figure 34C shows a train of normal action potentials followed by a DAD, which occurred in a sham myocyte. The incidence of DADs was significantly higher in sham than in OVX myocytes (Figure 34D). Thus, long term estrogen deprivation increased spontaneous SR Ca²⁺ release and promoted action potential prolongation leading to EADs in the aging female heart.

3.3.10 Summary of Section 3.3

In summary, long term OVX altered Ca²⁺ homeostasis and contractile function in the aging heart. OVX increased I_{CaL} and peak Ca²⁺ transients. While the rates of the contractile responses were significantly faster, OVX had no effect on contraction size in comparison to sham. This was due to decreased myofilament Ca²⁺ sensitivity in the OVX heart. Elevated intracellular Ca²⁺ in OVX cells led to higher SR Ca²⁺ stores, and increased Ca²⁺ spark size and frequency. OVX also promoted spontaneous Ca²⁺ release and triggered activity, especially EADs. Thus, long term estrogen deprivation may increase the susceptibility to cardiovascular disease in the aging female heart.

TABLE 11**Physical Characteristics of Animals and Cells Used in this Study**

Parameter	Sham	OVX	p value
Age (months)	24.5 ± 0.5 (22)	23.2 ± 0.5 (22)	p=0.215
Body weight (g)	32.2 ± 1.7 (18)	36.7 ± 2.4 (15)	P=0.130
Uterine dry wt. (µg)	19.6 ± 2 (13)	5.3 ± 0.7* (16)	p<0.001
Cell capacitance (pF)	302.6 ± 20.6 (15)	230.7 ± 16.3* (16)	p=0.010

Numbers represent mean ± SEM; values in brackets represent the number of cells. The * denotes significantly different from sham values as determined by unpaired Student's *t*-tests, p<0.05.

TABLE 12**Summary of Responses from Field Stimulation Experiments**

Parameter	Sham	OVX	p value
Fractional shortening (%)	1.54 ± 0.3 (25)	1.66 ± 0.5 (26)	p=0.826
Time-to-peak contraction (msec)	33.7 ± 2.1 (25)	27.5 ± 1.7* (26)	p=0.016
Time-to-50% relaxation (msec)	33.7 ± 3.1 (25)	25.2 ± 1.6* (26)	p=0.022
Ca ²⁺ transient (nM)	61.8 ± 3.5 (25)	87.2 ± 7.0* (26)	p=0.002
Diastolic Ca ²⁺ (nM)	186.0 ± 7.6 (25)	205.9 ± 7.8 (26)	p=0.073
Rate of Ca ²⁺ transient rise (nM/msec)	3.09 ± 0.30 (25)	4.42 ± 0.39* (26)	p=0.009
Velocity to 50% transient decay (nM/msec)	0.65 ± 0.05 (25)	1.11 ± 0.10* (26)	p<0.001

Numbers represent mean ± SEM; values in brackets represent the number of cells. The * denotes significantly different from sham values as determined by unpaired Student's *t*-tests, p<0.05.

TABLE 13**Summary of Responses from Current Clamp Experiments**

Parameter	Sham	OVX	p value
Resting Membrane Potential (RMP, mV)	-68.4 ± 3.9 (18)	-69.5 ± 3.9 (19)	p=0.843
APD ₅₀ (msec)	30.0 ± 7.3 (18)	33.2 ± 6.8 (19)	p=0.750
APD ₉₀ (msec)	128.4 ± 26.6 (18)	119.7 ± 18.8 (19)	p=0.789
Contraction (μm)	3.37 ± 0.5 (17)	3.18 ± 0.5 (17)	p=0.808

Numbers represent mean ± SEM; values in brackets represent the number of cells. The * denotes significantly different from sham values as determined by unpaired Student's *t*-tests, $p < 0.05$.

TABLE 14**Ca²⁺ Handling Parameters in Voltage Clamp Experiments**

Parameter	Sham	OVX	p value
Ca ²⁺ transient (nM)	37.9 ± 4.8 (14)	72.5 ± 8.9* (16)	p=0.002
Ca ²⁺ current (pA/pF)	-2.9 ± 0.2 (14)	-4.3 ± 0.5* (16)	p=0.014
Gain (nM pA/pF ⁻¹)	12.6 ± 1.4 (14)	20.6 ± 3.8 (16)	p=0.060
Diastolic Ca ²⁺ (nM)	162.0 ± 13.6 (14)	156.1 ± 15.7 (16)	p=0.785
SR Ca ²⁺ stores (nM)	64.0 ± 6.7 (9)	121.3 ± 15.3* (11)	p=0.030
Fractional release (%)	43.3 ± 3.8 (9)	46.7 ± 4.9 (11)	p=0.594

Numbers represent mean ± SEM; values in brackets represent the number of cells. Mean Ca²⁺ transients, Ca²⁺ current, and Gain were calculated for responses activated by a test step to 0 mV. The * denotes significantly different from sham values as determined by unpaired Student's *t*-tests, p<0.05.

TABLE 15**Characteristics of Spontaneous Ca²⁺ Sparks**

Parameter	Sham	OVX	p value
Spark Frequency (sparks/100 μ m/sec)	1.56 \pm 0.23 (56)	2.75 \pm 0.34* (74)	p=0.008
Spark Amplitude (Δ F/F ₀)	0.303 \pm 0.005 (323)	0.434 \pm 0.006* (780)	p<0.001
Spark time-to-peak (TTP, msec)	14.4 \pm 0.8 (323)	10.9 \pm 0.4* (780)	p<0.001
Tau for spark decay (msec)	21.0 \pm 1.5 (323)	25.4 \pm 2.6* (780)	p=0.039
Full duration at half maximum (FDHM, msec)	19.42 \pm 0.67 (323)	19.43 \pm 0.47 (780)	p=0.983
Full width at half maximum (FWHM, μ m)	1.62 \pm 0.04 (323)	1.97 \pm 0.03* (780)	p<0.001

Numbers represent mean \pm SEM. The numbers in brackets denote the value of n. For spark frequency, n= number of cells; for all other spark parameters, n= the total number of sparks analyzed. In these experiments, cells from 3 sham animals and 6 OVX animals were used. The * denotes significantly different from sham values as determined by unpaired Student's *t*-tests, p<0.05.

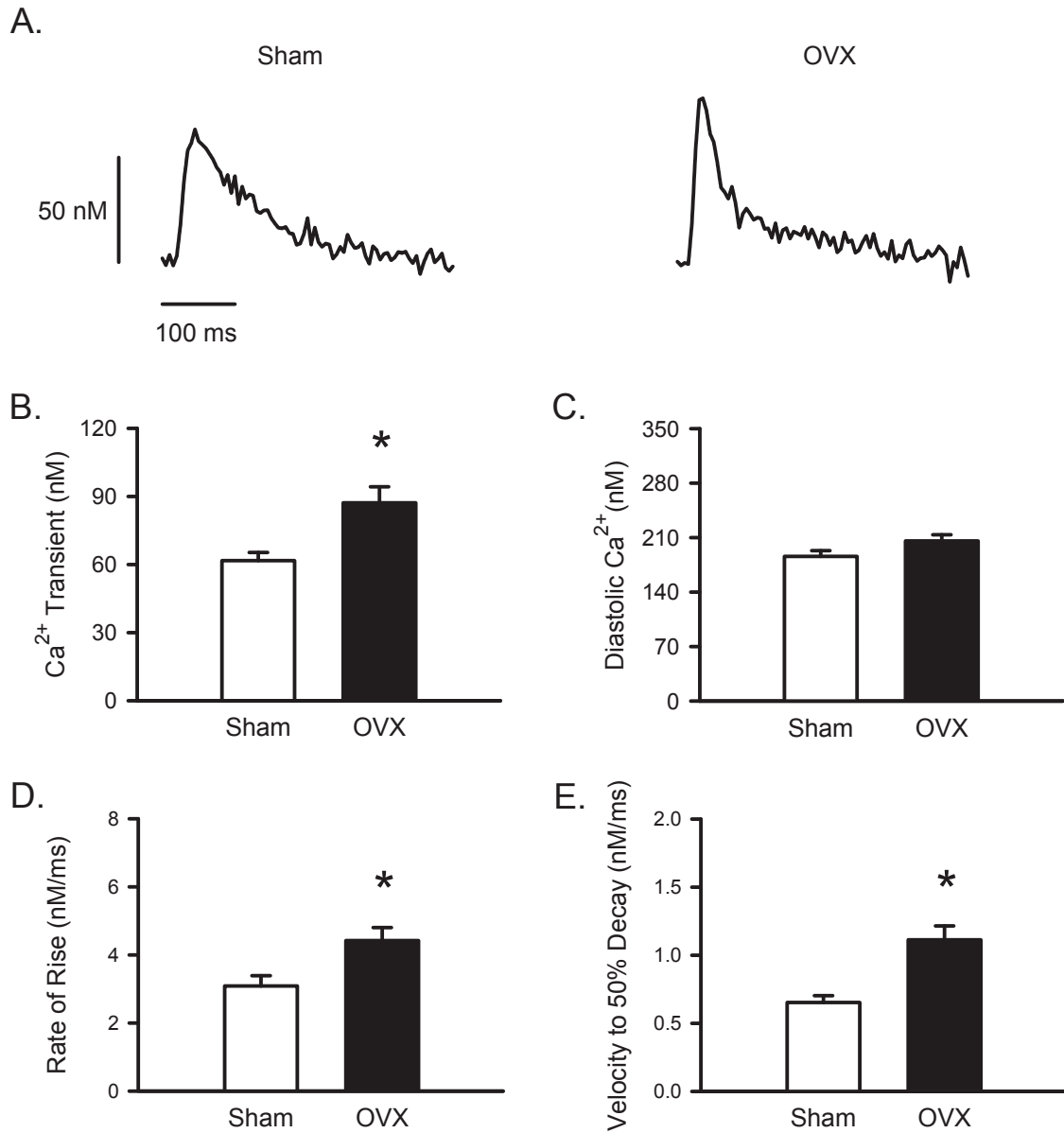


Figure 21. Ca²⁺ transients were larger and faster in myocytes from OVX mice in comparison to sham controls. **A.** Representative Ca²⁺ transients from sham (left) and OVX (right) myocytes field stimulated at 2 Hz. **B.** Peak Ca²⁺ transients were significantly larger in myocytes from OVX when compared to sham. **C.** Diastolic Ca²⁺ levels were similar between sham and OVX mice. **D,E.** OVX increased the rate-of-rise and the velocity to 50% decay of the Ca²⁺ transient in comparison to sham controls. (n=25 sham and n=26 OVX myocytes; * denotes p<0.05)

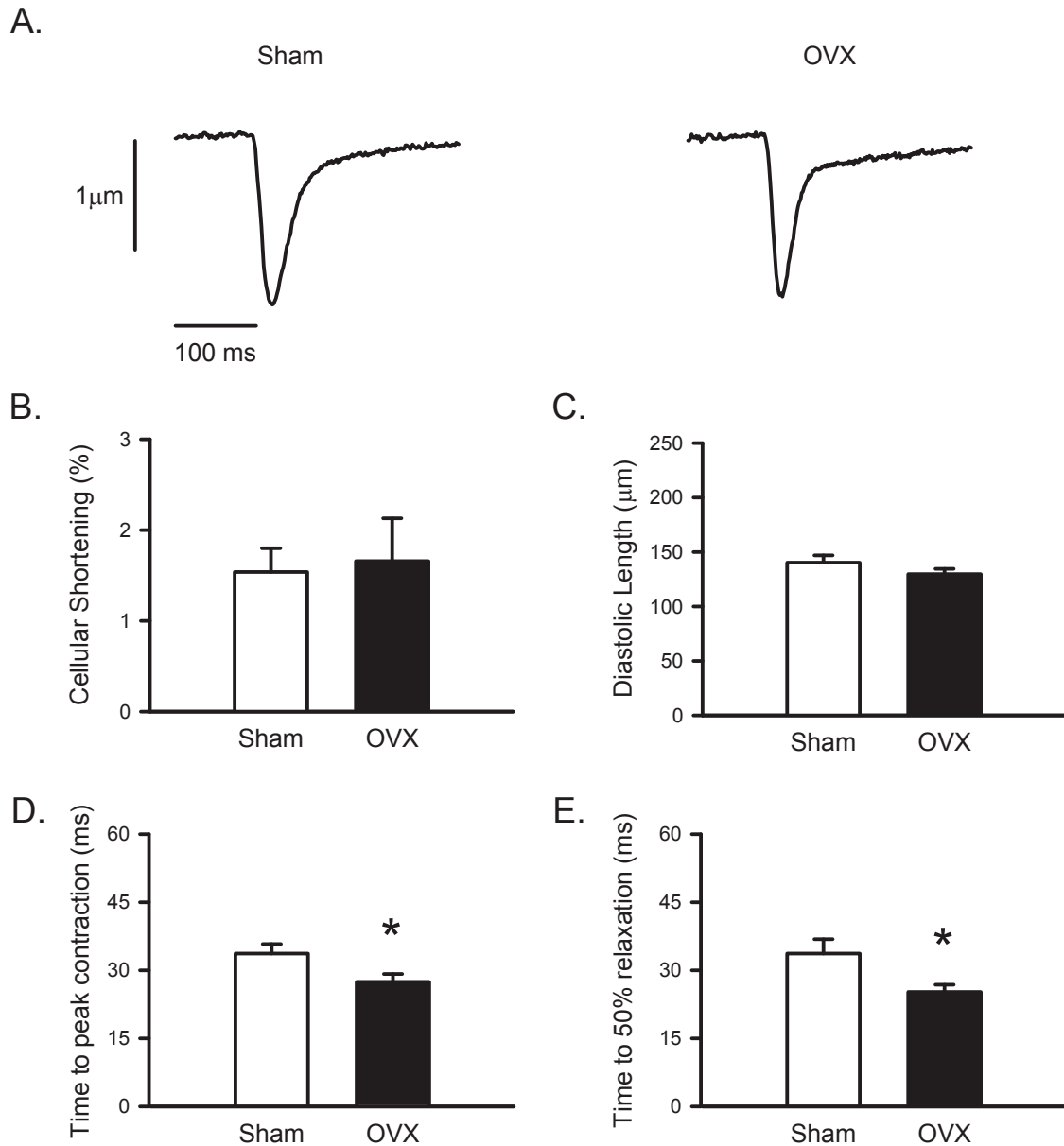


Figure 22. Cellular shortening was similar between myocytes from sham and OVX mice. **A.** Representative contractions from sham (left) and OVX (right) myocytes that were field stimulated at 2 Hz. **B.** Peak contractions did not differ between myocytes from sham and OVX mice. **C.** Diastolic cell length was similar between sham and OVX mice. **D,E.** OVX reduced the time-to-peak and time to 50% relaxation in comparison to sham controls. (n=25 for sham and n=26 for OVX myocytes; * denotes $p < 0.05$).

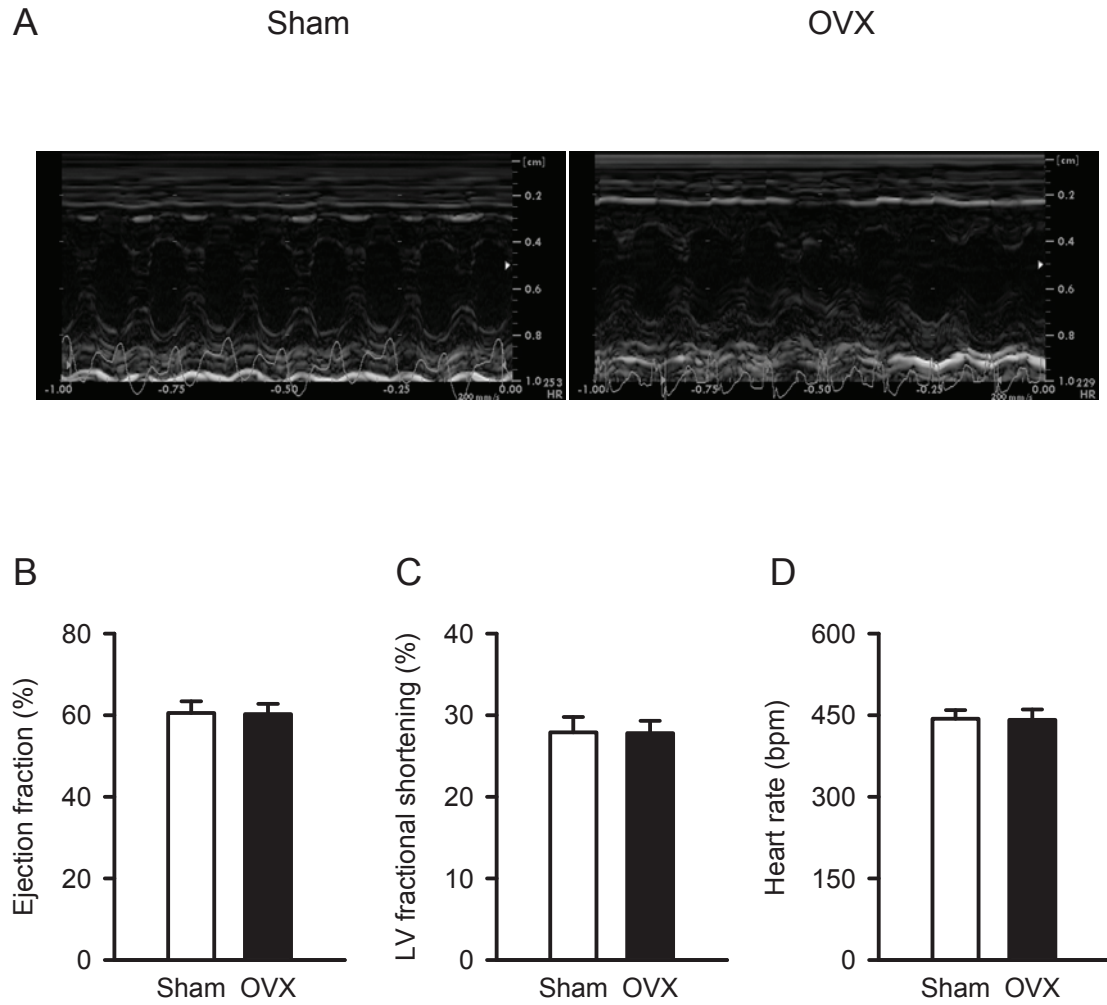


Figure 23. *In vivo* ventricular function and heart rate were similar in sham and OVX mice. A. Representative M-mode images of cardiac function from sham (left) and OVX (right) mice. B,C,D. Mean values for *in vivo* ejection fraction, left ventricular fractional shortening, and heart rate were identical in sham and OVX mice. (n=6 sham and 6 OVX mice; * denotes $p < 0.05$).

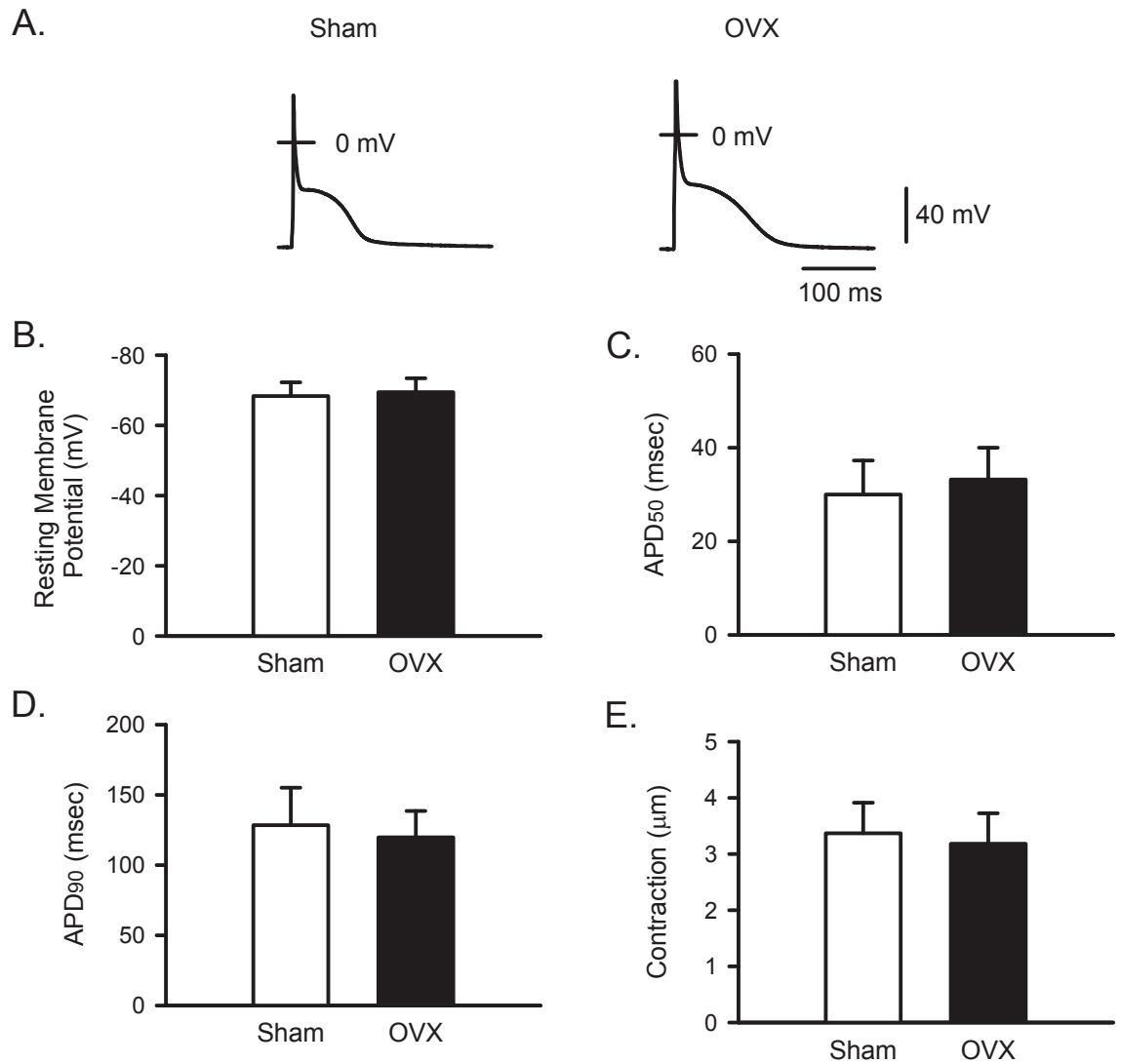


Figure 24. Action potentials and contractions were unaffected by OVX.

A. Representative examples of action potentials recorded from sham (left) and OVX (right) myocytes. **B.** Resting membrane potential was identical between sham and OVX myocytes. **C,D.** APD₅₀ and APD₉₀ values were similar between both groups. **E.** Cellular contractions were unaffected by OVX. (n=18 sham and n=19 OVX myocytes; * denotes p<0.05).

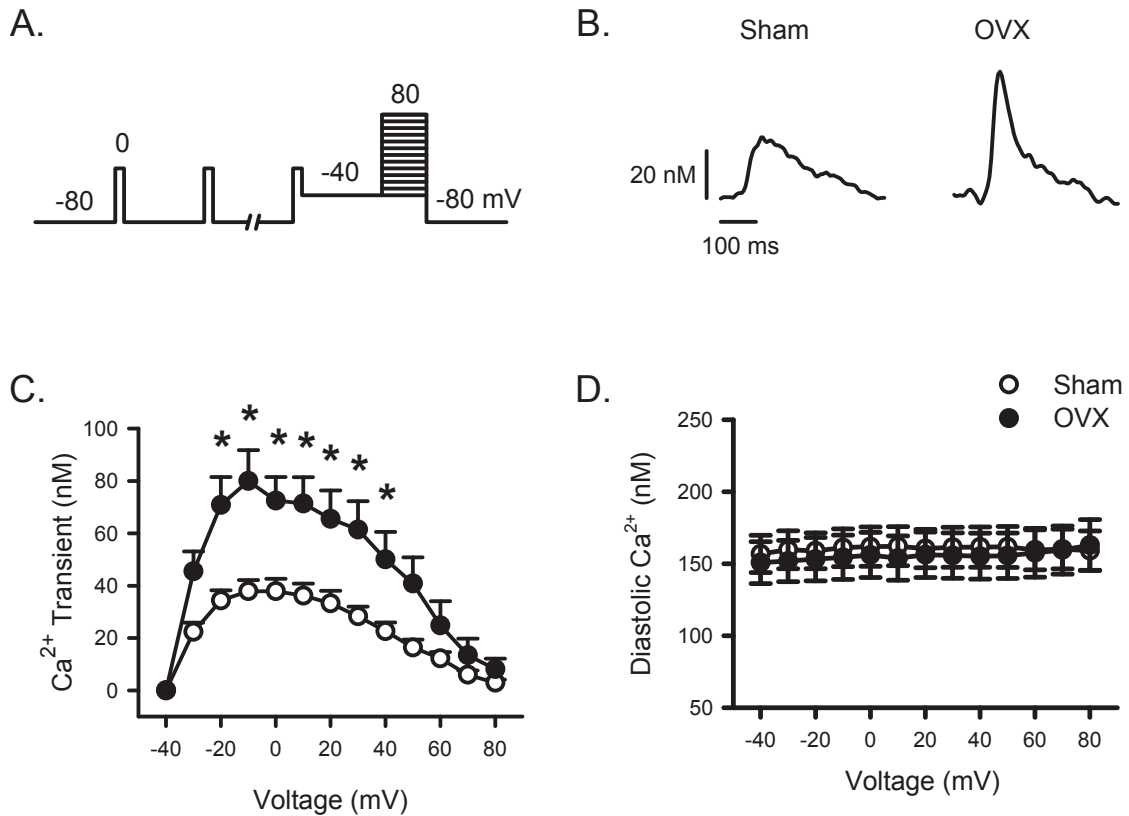


Figure 25. OVX increased Ca^{2+} transients across several membrane potentials. **A.** The voltage clamp protocol used to investigate the current-voltage (IV) relationship is shown. Myocytes were stimulated with conditioning pulses at 2 Hz prior to test steps from -40 mV to potentials up to +80 mV. **B.** Representative Ca^{2+} transients activated by a test step to 0 mV are shown for sham (left) and OVX (right) myocytes. **C.** Mean Ca^{2+} transients were significantly larger in myocytes from OVX mice when compared to sham at potentials between -20 and +40 mV. **D.** Diastolic Ca^{2+} levels were similar between sham and OVX cells across all test potentials. (n=17 sham and n=16 OVX myocytes; * denotes $p < 0.05$).

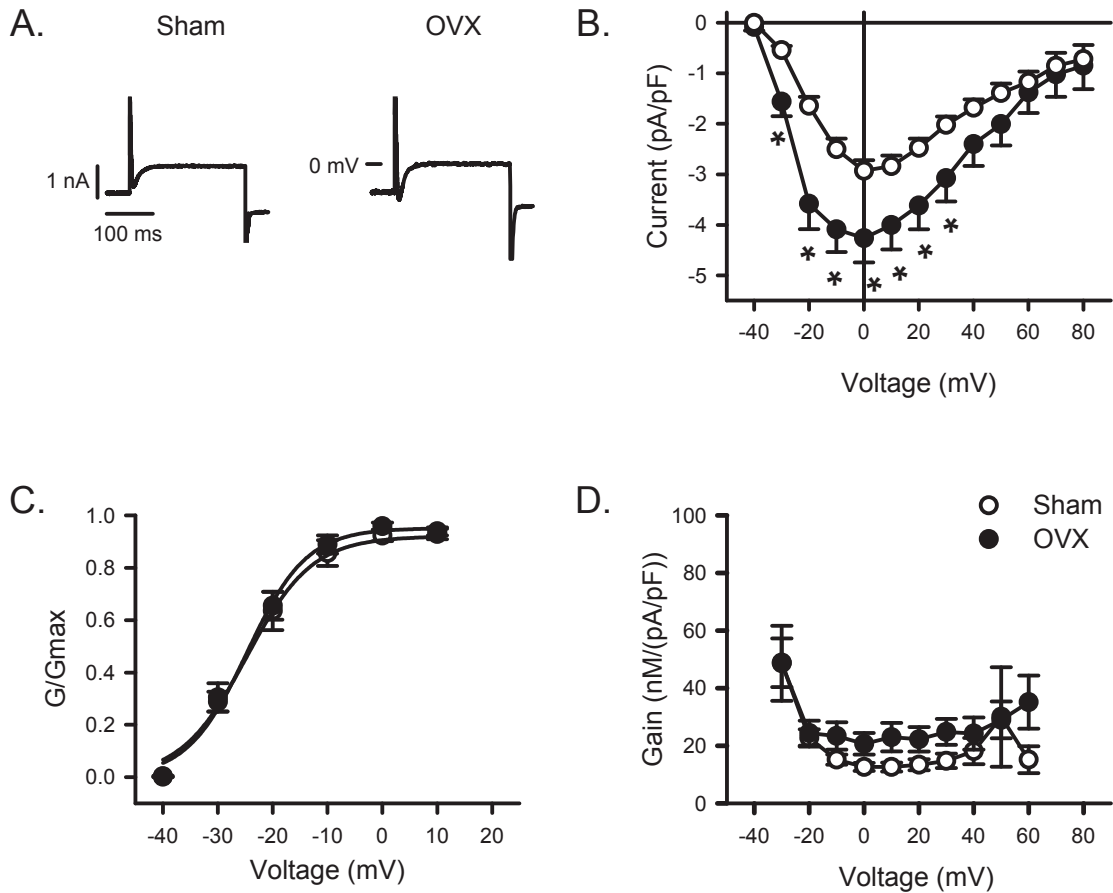


Figure 26. Ca^{2+} current density was enhanced by OVX at membrane potentials near the peak of the IV curve. **A.** Representative Ca^{2+} currents recorded during a test step to 0 mV from sham (left) and OVX (right) myocytes. **B.** Mean Ca^{2+} current density was significantly increased between -30 and +30 mV in OVX myocytes when compared to sham. **C,D.** Ca^{2+} current activation and EC-coupling gain values were similar in sham and OVX myocytes. (n = 17 sham and n=16 OVX myocytes; * denotes $p < 0.05$).

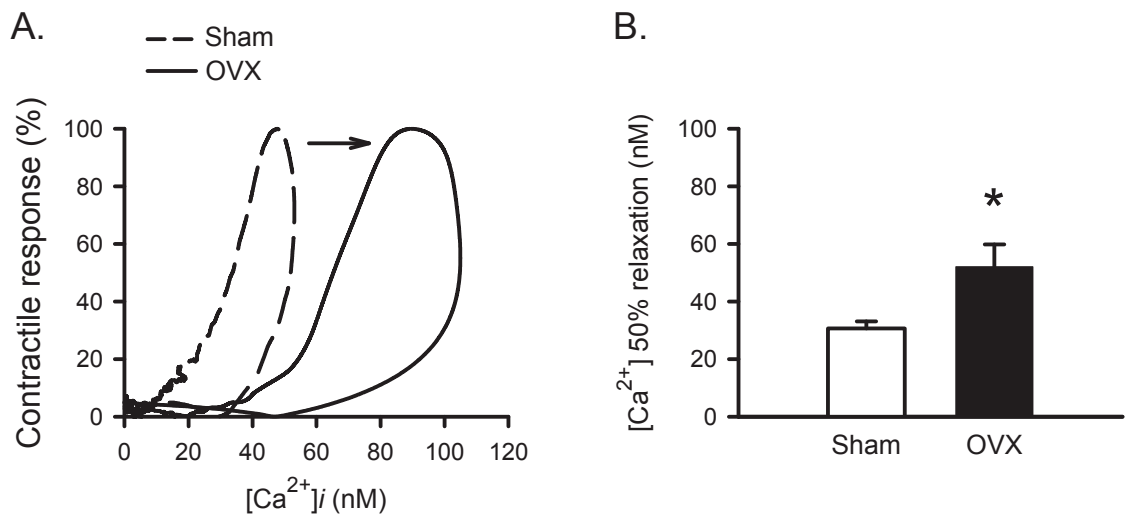
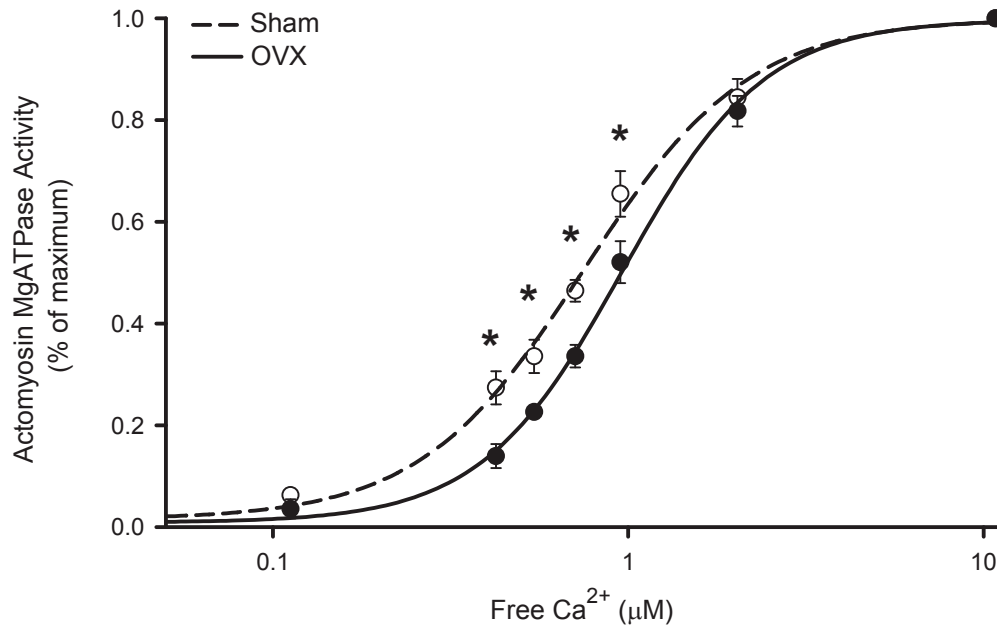
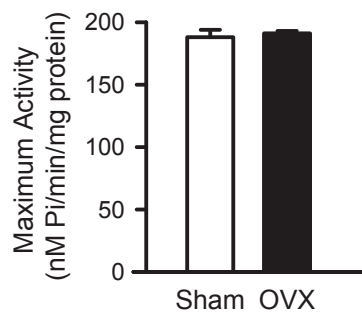


Figure 27. OVX reduced myofilament Ca^{2+} sensitivity. **A.** Contractions were plotted as a function of Ca^{2+} concentration for representative sham and OVX myocytes to generate shortening- $[Ca^{2+}]$ phase loop plots. OVX caused a distinct rightward shift of this plot (shown by the arrow) in comparison to sham, indicating a decrease in myofilament Ca^{2+} sensitivity. **B.** Intracellular Ca^{2+} levels at 50% relaxation in field-stimulated myocytes were measured to quantify this shift. OVX myocytes had higher intracellular Ca^{2+} levels at 50% relaxation when compared to sham controls. (n=25 sham and n=26 OVX myocytes; * denotes $p < 0.05$)

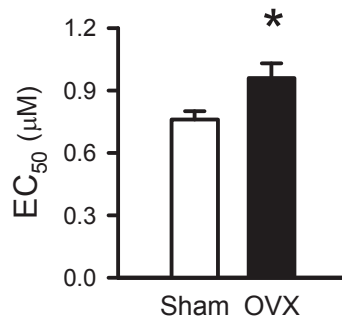
A.



B.



C.



D.

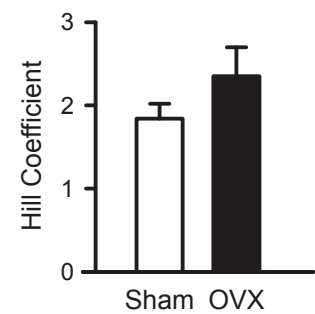


Figure 28. OVX reduced myofilament Ca²⁺ sensitivity as assessed by actomyosin MgATPase activity. **A.** Normalized actomyosin MgATPase activity-[Ca²⁺] curves show a significant rightward shift in the ventricular myofilament samples from OVX mice in comparison to sham controls, indicating that myofilament Ca²⁺ sensitivity was decreased in OVX hearts. **B.** Maximum actomyosin MgATPase activity was similar between sham and OVX samples. **C.** EC₅₀ was markedly increased in OVX hearts when compared to sham. **D.** Values of the hill coefficient were similar in both experimental groups. (n=5 sham and n=4 OVX hearts; * denotes p<0.05).

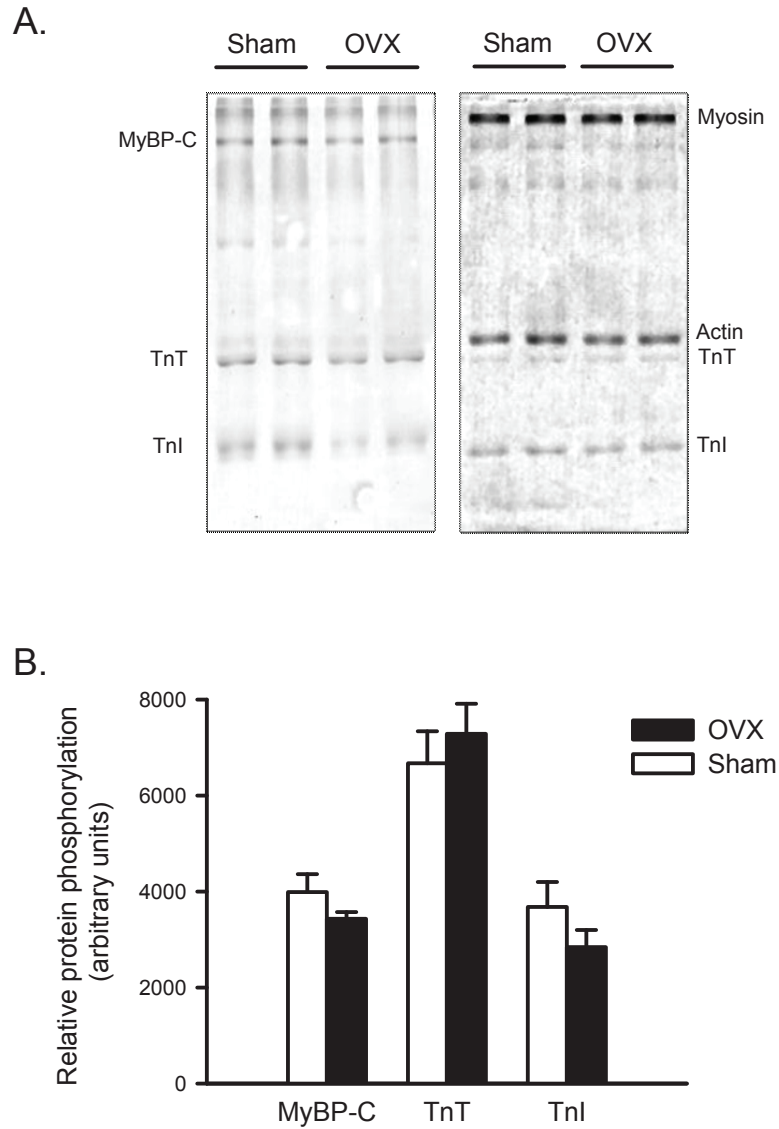


Figure 29. Decreased myofilament Ca^{2+} sensitivity in OVX mice was not due to changes in phosphorylation of myofilament proteins. **A.** Representative blots of Pro-Q Diamond stain (left) to assess phosphorylation and Coomassie (right) to confirm protein loading. Myosin binding protein-C (MyBP-C), troponin I (TnI) and troponin T (TnT) are labeled and show similar levels between sham and OVX samples. **B.** Mean values show no difference in the phosphorylation of key myofilament proteins between sham and OVX hearts. (n=5 sham and n=4 OVX hearts)

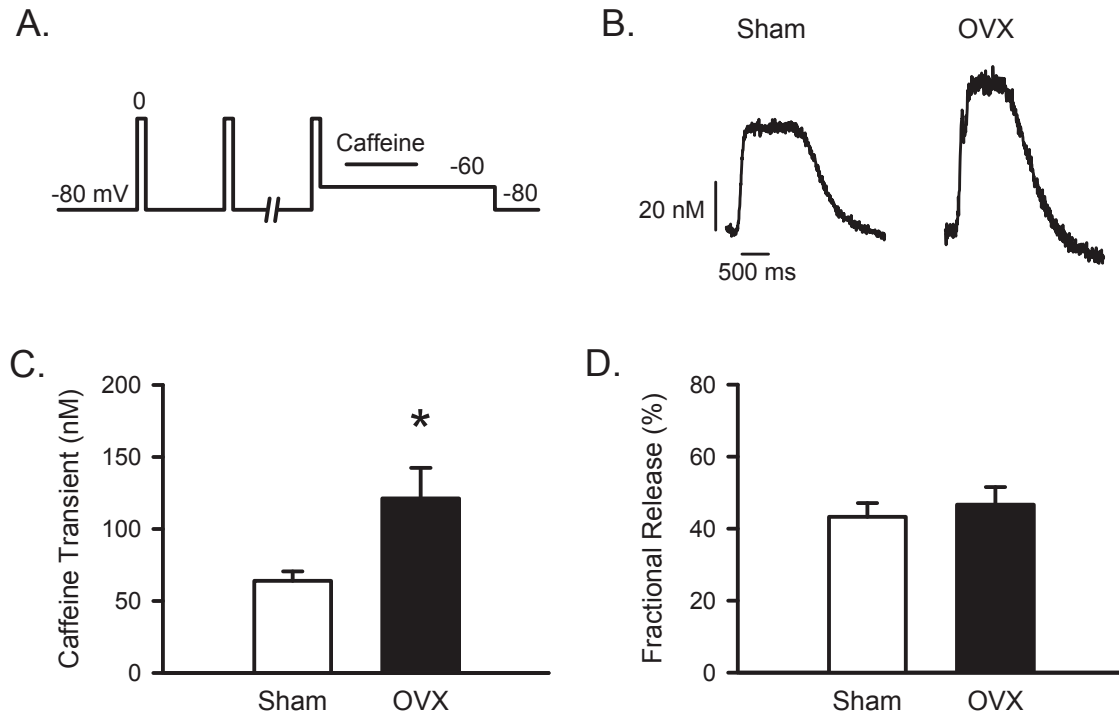


Figure 30. OVX greatly increased intracellular Ca^{2+} loads. **A.** The voltage clamp protocol used to assess SR Ca^{2+} content is shown. Myocytes were stimulated with conditioning pulses at 2 Hz prior to application of 10 mM caffeine. **B.** Representative recordings of caffeine-induced Ca^{2+} transients in myocytes from sham (left) and OVX (right) mice. **C.** Average peak caffeine transients were significantly larger in cells from OVX in comparison to those from sham. **D.** Fractional release of Ca^{2+} from the SR (calculated as the ratio of Ca^{2+} transient/caffeine-induced transient) was similar between sham and OVX. (n=9 sham and n=11 OVX myocytes; * denote $p < 0.05$).

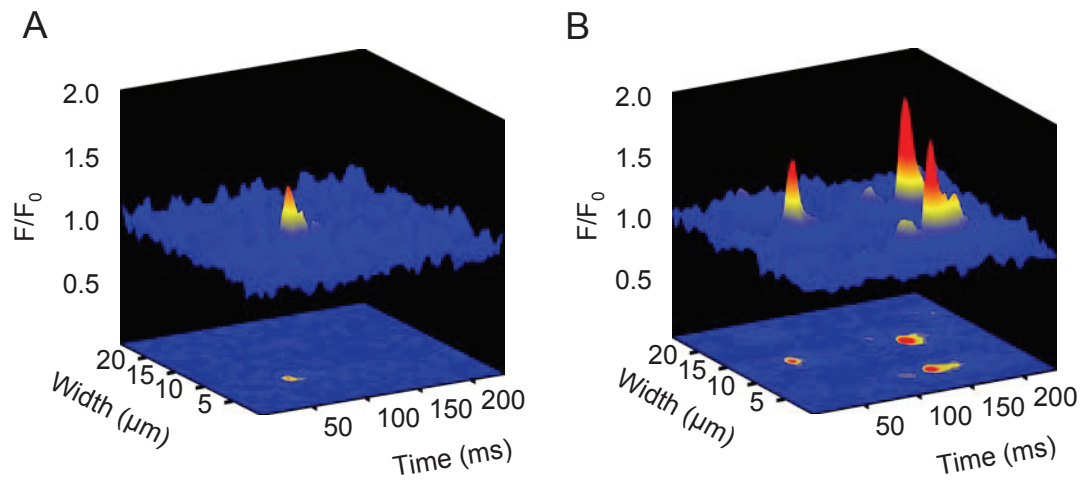


Figure 31. Three dimensional representative plots of Ca^{2+} sparks from aged sham and OVX myocytes. Representative plots of unitary Ca^{2+} release events from an aged sham (A) and OVX (B) myocyte. Ca^{2+} sparks were larger, wider, and more frequent in OVX in comparison to sham.

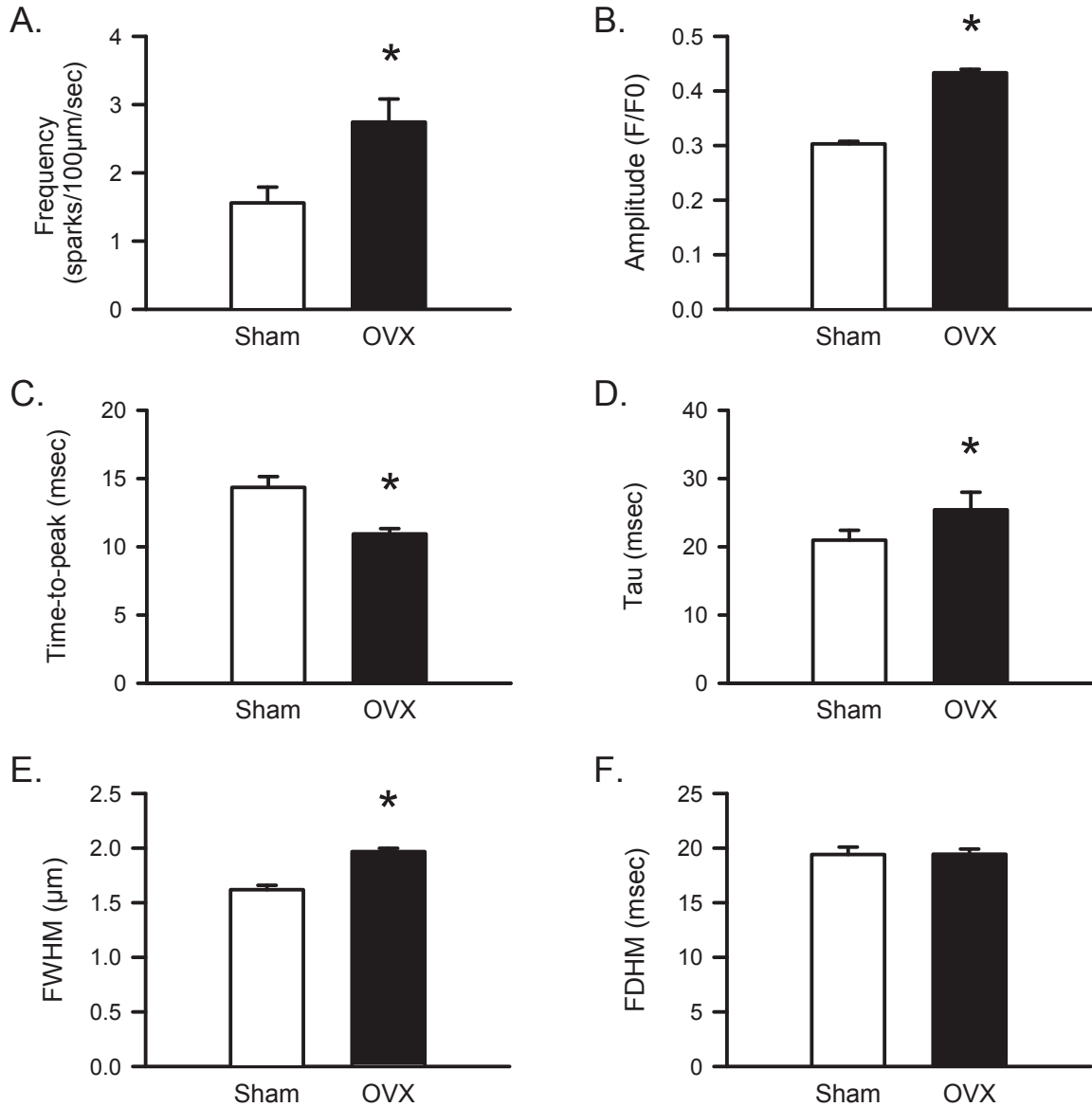


Figure 32. Ca^{2+} spark frequency, amplitudes, and widths were significantly increased in myocytes from OVX mice when compared to sham controls.

A,B. OVX increased mean Ca^{2+} spark frequency and amplitude when compared to those from sham. **C.** Average values for spark time-to-peak were significantly reduced in myocytes from OVX mice when compared to sham. **D.** Mean values for the time constant of Ca^{2+} spark decay (tau) were prolonged in cells from OVX when compared to sham controls. **E.** OVX significantly increased full-width at half maximum (FWHM) compared to sham. **F.** Full-duration at half maximum (FDHM) was similar between the two groups. The value of $n=323$ sham and $n=780$ OVX sparks; for frequency, $n=56$ sham and $n=74$ OVX myocytes. In these experiments, cells from 3 sham animals and 6 OVX animals were used (* denotes $p<0.05$)

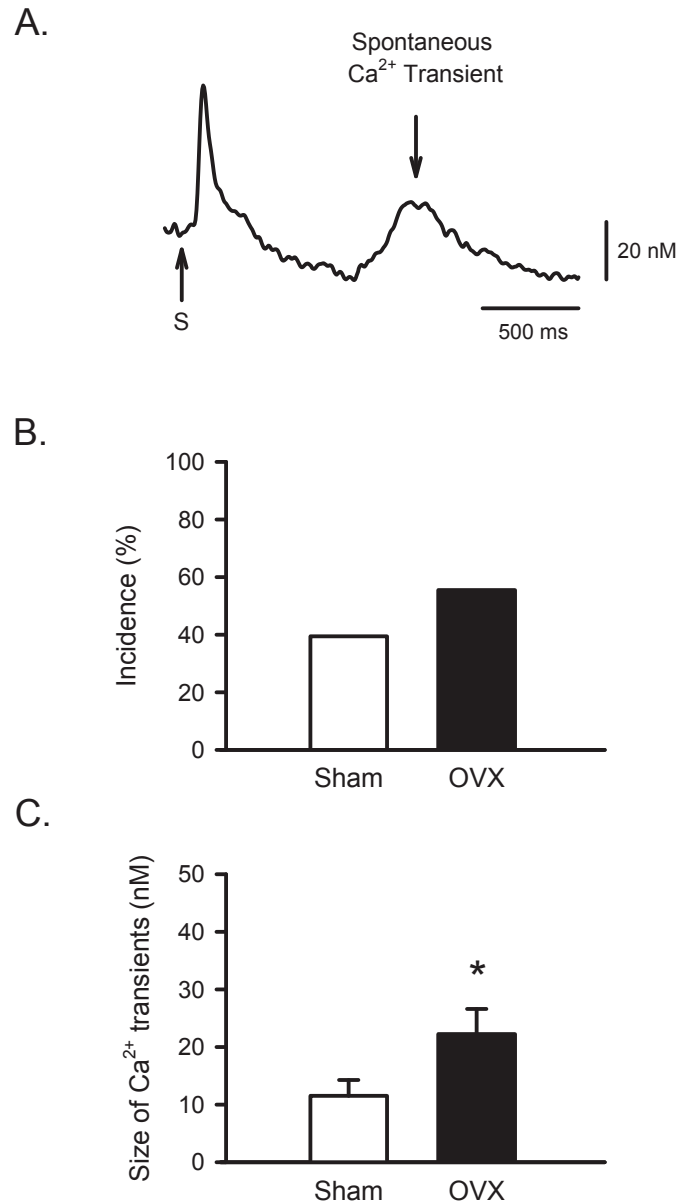


Figure 33. OVX increased the size of spontaneous Ca^{2+} transients.

A. Representative example of a spontaneous Ca^{2+} transient recorded from an OVX myocyte. A stimulated Ca^{2+} transient (S, arrow) is followed by a spontaneous Ca^{2+} release during repolarization. **B.** Incidence of spontaneous transients did not differ significantly between sham and OVX myocytes. **C.** Spontaneous transients were significantly larger in OVX when compared to sham myocytes. (n=37 sham and 38 OVX myocytes; * denotes $p < 0.05$).

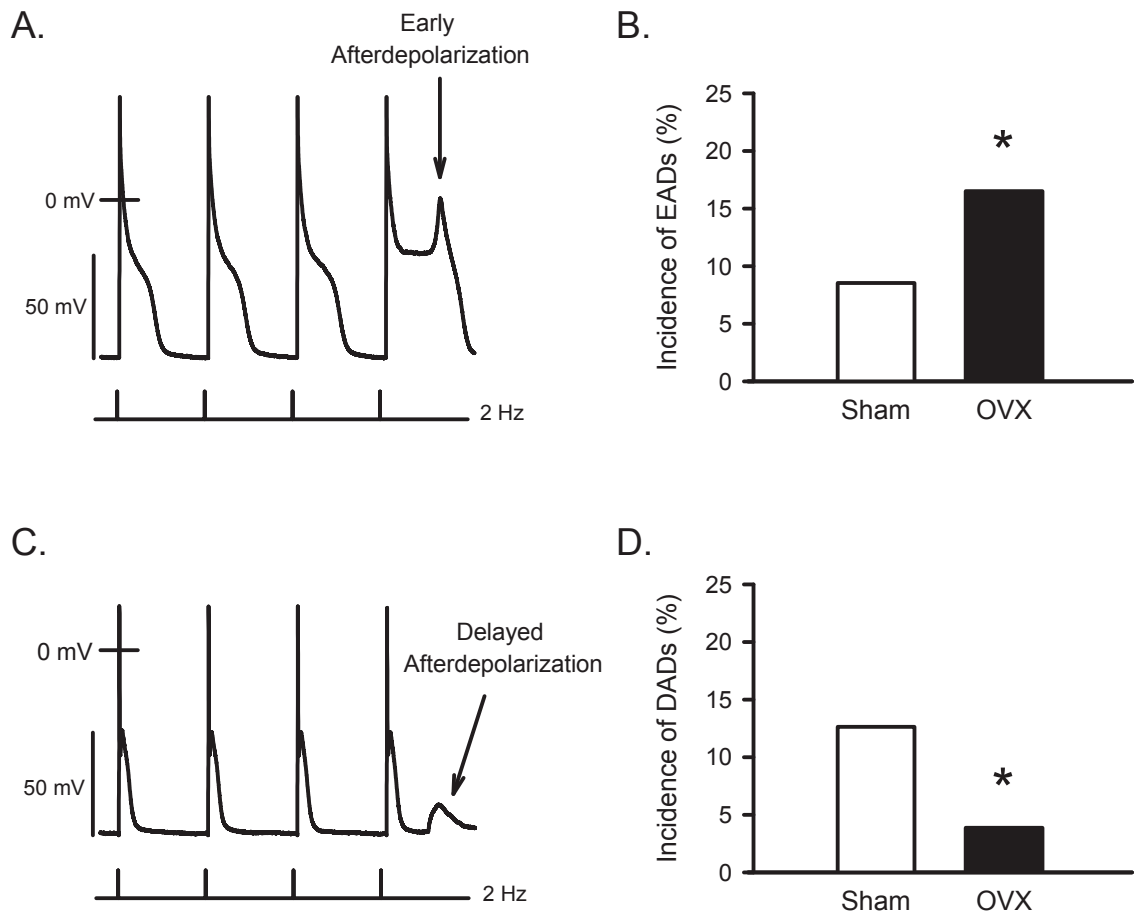


Figure 34. OVX promoted early afterdepolarizations.

A. Representative example of a DAD recorded from a sham myocyte. **B.** The incidence of DADs was higher in sham than OVX myocytes. **C.** Representative example of an EAD recorded from an OVX myocyte. **D.** The incidence of EADs was significantly higher in OVX myocytes in comparison to sham controls. (n=18 sham and n=19 OVX myocytes; * denotes p<0.05).

CHAPTER 4 DISCUSSION

The overall goal of this thesis was to examine the impact of natural aging on the male and female heart, and to investigate the effects of estrogen reduction on cardiac contractile function in females. Previous laboratory studies have shown that the age-associated decline in cardiac contractile function occurs predominantly in the hearts of males, but not females in 24 month old animals (Grandy and Howlett, 2006; Howlett, 2010). Thus, one goal of the present studies was to investigate whether cardiac contractile function would deteriorate in 32 month old female mice, where estrogen levels have declined naturally with age. Results showed that peak contractions were preserved in extremely old female mice, but declined with age in male mice. However, both sexes exhibited a marked disruption in Ca^{2+} homeostasis in aging. This suggests that the aging process disrupts heart function in both males and females. However, while extremely old males and females exhibit Ca^{2+} dysregulation, some form of compensation may occur in the female heart to maintain cardiac contractile function.

A second objective of this thesis was to examine the effect of short term OVX on specific components of the EC-coupling pathway and Ca^{2+} handling mechanisms in isolated myocytes. The results showed that short term OVX promoted SR Ca^{2+} loading and enhanced SR Ca^{2+} release mechanisms in the female heart. This resulted in larger Ca^{2+} transients, an increase in Ca^{2+} sparks, and spontaneous Ca^{2+} release. Taken together, these findings suggest that estrogen may play a role in limiting Ca^{2+} transients, SR Ca^{2+} load and spontaneous Ca^{2+} release in the female heart.

The final goal of this thesis was to examine whether long term OVX impaired

cardiac contractile function and Ca^{2+} homeostasis in the aging female heart. The results showed that long term OVX enhanced Ca^{2+} influx as well as SR Ca^{2+} storage and release, but did not affect cardiac contractile function. This was due to a decrease in myofilament Ca^{2+} sensitivity with long term OVX. However, enhanced Ca^{2+} levels did lead to larger spontaneous Ca^{2+} release and greater abnormal electrical activity in the form of EADs in myocytes from the OVX heart. Together, the results suggest that long term estrogen deprivation leads to Ca^{2+} dysregulation, reduced myofilament Ca^{2+} sensitivity, spontaneous SR Ca^{2+} release and triggered activity in the aging heart. This may increase the susceptibility to cardiovascular disease and dysfunction in hearts of older females.

4.1 THE EFFECT OF EXTREME AGING ON SEX DIFFERENCES IN THE HEART

4.1.1 Summary of key findings

The present study examined whether myocytes from the hearts of extremely old male and female mice exhibit similar deficits in contractile function, or whether females continue to maintain cardiac function later in life. The results showed aging caused cellular hypertrophy in the hearts of male but not female mice. In terms of function, fractional shortening significantly declined in cells from males but not females with extreme old age. Interestingly, peak Ca^{2+} transient amplitude was significantly reduced in both older male and female mice. Investigation of the underlying EC-coupling mechanisms showed that Ca^{2+} current density was markedly decreased in older males, but not females when compared to young adults. Although SR Ca^{2+} content was similar in both sexes and age groups, EC-coupling gain and the fraction of Ca^{2+} released from the SR were markedly reduced in 32 month old male and female mice when compared to

younger adults. These results suggest that cardiomyocyte contractile function does not deteriorate in myocytes from females, even in extreme old age. However, cells from males exhibit profound contractile dysfunction. While senescent male and female myocytes both exhibit reduced SR Ca^{2+} release and smaller Ca^{2+} transients, compensation in the female heart, possibly to myofilament Ca^{2+} sensitivity, may occur to preserve cellular shortening and maintain cardiac function.

4.1.2 The effect of extreme old age on myocyte size and function

This thesis found that body weights were significantly greater in senescent male and female mice in comparison to young adults. An increase in body weight could lead to an increase systemic volume load, which could stimulate myocyte hypertrophy. However, results of the present study showed that cellular hypertrophy only occurred in ventricular myocytes from the hearts of extremely old male, but not female mice. Similar findings have been reported in other animal models. Studies have shown that age-associated cellular hypertrophy is more prominent in myocytes from males than females in mice, rats and monkeys (Forman et al., 1997; Grandy and Howlett, 2006; Howlett, 2010; Zhang et al., 2007). Previous studies have suggested that estrogen may activate anti-apoptotic signaling pathways (Bhuiyan et al., 2007; Patten et al., 2004) and inhibit hypertrophic response signals (Donaldson et al., 2009; Pedram et al., 2008). Together, these may prevent cardiac hypertrophy even in the presence of an increase in body weight. Indeed, an age-associated increase in necrotic and apoptotic cell death has been attributed for greater hypertrophy in cells from male, but not female rats (Kajstura et al., 1996). This causes a compensatory increase in the size of surviving myocytes in

response to cell death (Olivetti et al., 1995). This also agrees with findings from humans. As men age, they exhibit a greater degree of ventricular myocyte hypertrophy in comparison to women (Olivetti et al., 1995). In contrast, both the number and size of ventricular myocytes are not affected by age in women (Olivetti et al., 1995). Data from the present study further support these findings and show that myocytes do not hypertrophy in the female heart, even with extreme old age and an increase in body weight.

A key finding of the present study is that contractile function declined in male, but not female mice with extreme old age. While contractile responses are larger in cells from younger males than females, the results of this study show that the age-related decline in cellular shortening only occurred in myocytes from male mice and not female mice. Previous studies have also shown that the size of contractile responses declines with age in cells from male animals (Grandy and Howlett, 2006; Howlett, 2010; Lim et al., 2000; Xiao et al., 1994). In addition, the literature shows that while contractile responses in myocytes from younger female animals are smaller than those from males, females do not show an age-associated decline in cardiac contractile function (Dibb et al., 2004; Farrell et al., 2010; Grandy and Howlett, 2006; Howlett, 2010). However, previous studies in rats and mice have only assessed 24 month old animals. The present study provides first evidence that an age-associated decline in cardiac contractile function does not occur in female mice with prolonged aging. It is possible that this is due to the age-related decline in estrogen levels (Czubryt et al., 2006; Luczak and Leinwand, 2009). Previous studies have shown that removal of the ovaries in female rats increases fractional shortening both in the intact heart (Stice et al., 2011) and at the level of the

myocyte (Curl et al., 2003; Wu et al., 2008). This suggests that estrogen may suppress contractile function. As hormone levels decline with aging, this may increase cellular shortening and help maintain contractile function in the female heart.

Previous studies have also provided evidence that there are age-associated changes in the underlying Ca^{2+} transients. Peak Ca^{2+} transients are reported to be larger in young adult males than in females, but Ca^{2+} transient amplitudes decline in older males (Grandy and Howlett, 2006; Howlett, 2010; Isenberg et al., 2003; Lim et al., 2000). By contrast, Ca^{2+} transient size is maintained in myocytes from older female animals (Dibb et al., 2004; Grandy and Howlett, 2006; Howlett, 2010). Interestingly, findings from the present study indicate that, while peak Ca^{2+} transients are larger in myocytes from young adult males than females, Ca^{2+} transient amplitudes decline in cells from both males and females with extreme old age. In senescent males, peak Ca^{2+} transient amplitudes decreased by 65%, whereas in senescent females Ca^{2+} transients were only 35% smaller when compared to responses from younger animals. This suggests that with extreme old age both male and female myocytes exhibit Ca^{2+} dysregulation. However, these effects are more profound in the extremely old male heart. The underlying basis for the decline in peak Ca^{2+} transients was further examined in this study.

4.1.3 The effect of extreme old age on components of the EC-coupling pathway in male mice

The present study investigated the underlying EC-coupling mechanisms that regulate Ca^{2+} entry, storage and release to determine whether age-dependent modifications in these mechanisms accounted for differences in Ca^{2+} handling between

males and females. The results of the present study showed that in young adults, Ca^{2+} current density was similar between males and females. This agrees with results of previous studies that have shown I_{CaL} is similar between young adults of both sexes (Brouillette et al., 2007; Farrell et al., 2010; Grandy and Howlett, 2006; Howlett, 2010; LeBlanc et al., 1998; Trepanier-Boulay et al., 2001). However, I_{CaL} significantly declined with age in cells from senescent males. Previous studies have shown that both I_{CaL} and contractile function decline with age in male mice at 24 months of age (Grandy and Howlett, 2006). Findings from the present study further support previous results and suggest that the decrease in I_{CaL} density underlies the impaired contractile function in cells from older male mice.

Ca^{2+} transient amplitude also declined in cells from senescent male mice. To investigate this age-associated reduction in Ca^{2+} transient size, SR Ca^{2+} stores were assessed. SR Ca^{2+} stores were similar in cells from young adult and senescent male mice. This suggests that extreme old age does not affect SR Ca^{2+} content in male C57BL/6 mice. This contrasts with previous findings that SR Ca^{2+} stores are reduced in 24 month old B6SJLF1/J male mice when compared to young adults (Grandy and Howlett, 2006). However, SR Ca^{2+} content has been reported to be similar between young adult and 24 month old male Fischer 344 rats (Howlett, 2010). This suggests that the effect of age on SR Ca^{2+} content may vary in different animal models of aging. However, the present study shows that SR Ca^{2+} content does not decline with age in C57BL/6 male mice.

As SR Ca^{2+} content is similar in cells from younger and older male mice, but Ca^{2+} transient amplitude declines with extreme old age, SR Ca^{2+} release mechanisms were assessed. The findings show that, in individual myocytes, the gain of SR Ca^{2+} release

was significantly lower in senescent males when compared to young adults. This means that the amount of Ca^{2+} released per unit Ca^{2+} current was reduced in cells from male mice with extreme old age. In addition, fractional release declined in cells from senescent male mice. This finding suggests that, while SR Ca^{2+} content is preserved, the fraction of Ca^{2+} that is released from the SR to form the Ca^{2+} transient decreases in extremely old males. Taken together, these results suggest that SR Ca^{2+} release mechanisms are impaired in cells from 32 month old male mice. The findings of the present study agree with results from a previous study that has shown both EC-coupling gain and fractional release decline with age in myocytes from 24 month old male rats (Howlett, 2010).

Overall, the findings of the present study show that I_{CaL} density significantly declines in 32 month old male mice. This results in impaired SR Ca^{2+} release giving rise to smaller Ca^{2+} transients and contractions. As the amount of Ca^{2+} released from the SR is proportional to the amount that enters via L-type Ca^{2+} channels (Bers, 2008), reduced I_{CaL} density in senescent male mice may be the underlying mechanism for impaired Ca^{2+} -induced Ca^{2+} release (CICR) and cardiac contractile function in older males. One possibility is that age-associated decreases in the phosphorylation of EC-coupling pathway targets may account for the decline in contractile function in older males. Previous studies have shown that the amount of cAMP produced in response to β -adrenergic stimulation declines in older male rats when compared to young adults (Farrell and Howlett, 2008). This would decrease the activation of PKA in the hearts of older males (Farrell and Howlett, 2008). Phosphorylation of L-type Ca^{2+} channels by PKA has been shown to increase I_{CaL} density within ventricular myocytes (McDonald et al., 1994;

Tsien et al., 1986). A decrease in phosphorylation at these channels by PKA may result in a decline in I_{CaL} density in older males. Previous studies have also shown that phosphorylation of RyR2 by CaMKII is reduced in the aging heart (Xu and Narayanan, 1998). As phosphorylation of RyR2 is thought to increase Ca^{2+} release channel activity (Marx et al., 2000), an age-associated decrease in RyR2 phosphorylation might reduce SR Ca^{2+} release in older hearts. Together, changes in phosphorylation could account for decreased I_{CaL} density and impaired SR Ca^{2+} release in cells from older males, which would compromise overall cardiac contractile function in the aging heart. Figure 35 summarizes the effects of extreme old age on cardiac contractile function in male mice.

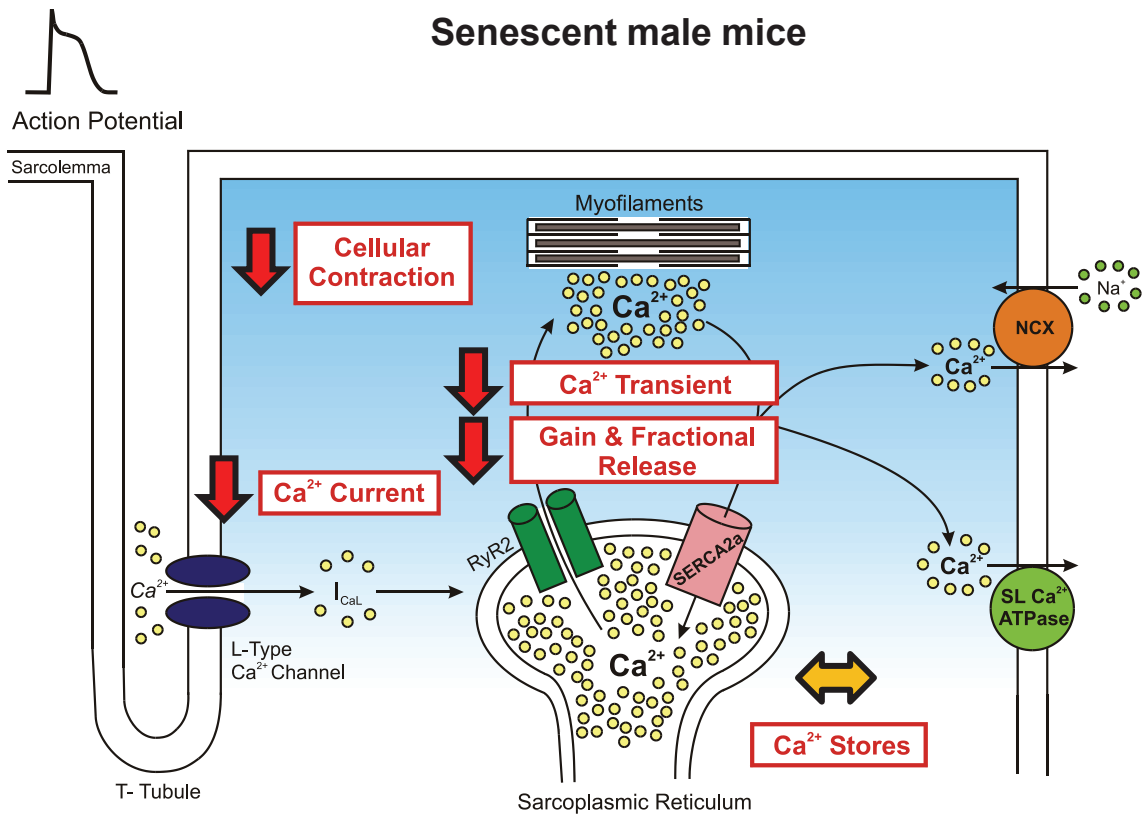


Figure 35. Summary of the effects of extreme old age on components of the EC-coupling pathway in male mice. Ca²⁺ current density significantly declined in cells from senescent male mice. This resulted in impaired Ca²⁺-induced Ca²⁺-release (CICR) due to a decrease in EC-coupling gain and SR fractional release. This led to smaller Ca²⁺ transients in cells from senescent males. Overall, this Ca²⁺ dysregulation caused a decline in contractile function in older males. This shows that age-associated changes to the EC-coupling pathway compromise cardiac function in the heart of older males.

4.1.4 The effect of extreme old age on components of the EC-coupling pathway in female mice

Although I_{CaL} declined with extreme old age in cells from male mice, I_{CaL} density was preserved in young adult and senescent female mice. This finding agrees with results from previous studies that have shown I_{CaL} density is preserved with age in cells from mice and sheep (Dibb et al., 2004; Grandy and Howlett, 2006). Together these results suggest that Ca^{2+} current does not decrease in older females, unlike older males.

While contractile function is maintained in the female heart, Ca^{2+} transient amplitude declined in cells from senescent female mice. One possibility is that SR Ca^{2+} content decreased in female mice with extreme old age, thus, underlying SR Ca^{2+} stores were examined. The findings of the present study showed that SR Ca^{2+} content was similar in young adult and senescent female mice. Therefore, a decline in intracellular Ca^{2+} storage did not account for the decline in Ca^{2+} transient size in older females. Interestingly, SR Ca^{2+} stores have been reported to increase in size in female mice and rats at 24 months of age (Grandy and Howlett, 2006; Howlett, 2010). However, findings from the present study suggest that SR Ca^{2+} stores may return to levels similar to those in younger adults by the time animals are 32 months of age.

As Ca^{2+} stores were preserved, SR Ca^{2+} release mechanisms were examined. The results of the present study showed that EC-coupling gain significantly decreased with extreme old age in cells from female mice. This indicates that less Ca^{2+} was released per unit Ca^{2+} current in cells from 32 month old female mice. In addition, fractional release was significantly lower in cells from senescent female mice, meaning that a smaller fraction of available Ca^{2+} was released from the SR to generate the Ca^{2+} transient. Thus, even though SR Ca^{2+} content is maintained in 32 month old females, SR Ca^{2+} release

mechanisms decline resulting in smaller Ca^{2+} transients. Interestingly, these results contrast with findings from previous studies that have shown that EC-coupling gain is maintained in older female mice, rats and sheep (Dibb et al., 2004; Grandy and Howlett, 2006; Howlett, 2010). The results of the present study suggest that with continued aging, SR Ca^{2+} release becomes impaired in myocytes from the female heart.

Taken together, these findings suggest that in myocytes from 32 month old females I_{CaL} density and SR Ca^{2+} content are preserved, but a decline in SR Ca^{2+} release mechanisms leads to smaller Ca^{2+} transients. One possibility is that the activity or density of RyR2 is decreased in the female heart with extreme old age. However, changes in protein expression in the aging female heart have not been examined. Another possibility is that changes in SR Ca^{2+} load altered SR Ca^{2+} release. SR Ca^{2+} content has been shown to modulate EC-coupling gain (Ginsburg and Bers, 2004). Previous studies have reported that the size of SR Ca^{2+} stores increases in female mice and rats at 24 months of age (Grandy and Howlett, 2006; Howlett, 2010). An increase in SR stores in the hearts of females may serve to maintain EC-coupling gain and preserve Ca^{2+} transients and cardiac contractile function at 24 months of age. This supports the notion that estrogen may suppress Ca^{2+} content and contractile function (Curl et al., 2003; Wu et al., 2008). As estrogen levels decline in the aging female heart this may promote SR Ca^{2+} loading, which would maintain SR Ca^{2+} release and preserve cardiac contractile function at 24 months of age. However, with extreme old age SR Ca^{2+} content appears to return to levels observed in younger females. This would impair both EC-coupling gain and the fraction of Ca^{2+} released from the SR, resulting in smaller Ca^{2+} transients.

However, cardiac contractile function is maintained in the female heart at extreme old ages despite the decrease in the Ca^{2+} transient. This suggests another form of compensation may be present in the aging female heart. One possibility may be changes in myofilament Ca^{2+} sensitivity. Previous studies have shown that myofilament Ca^{2+} sensitivity increases in the hearts of young adult OVX rats (Bupha-Intr and Wattanapermpool, 2004; Thawornkaiwong et al., 2007). This suggests that estrogen may decrease myofilament Ca^{2+} sensitivity in hearts of young adults. However, whether age modifies myofilament Ca^{2+} sensitivity in the female heart has not been investigated. Examination of the myofilaments may further provide a mechanism for sex-based differences in cardiac contractile function in the aging heart. Figure 36 summarizes the effects of extreme old age on cardiac contractile function in female mice.

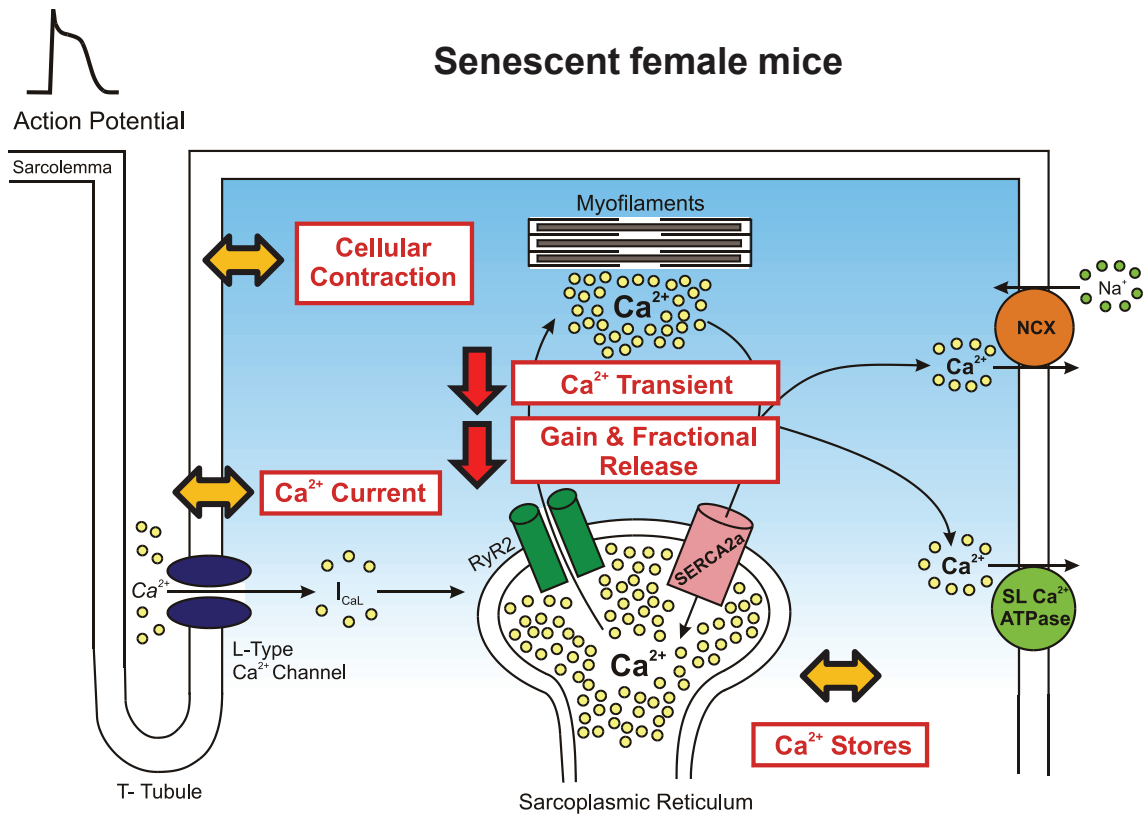


Figure 36. Summary of the effects of extreme old age on components of the EC-coupling pathway in female mice. Ca²⁺ current density and SR Ca²⁺ stores are preserved in cells from senescent female mice. However, EC-coupling gain and SR fractional release are impaired in extremely old females, resulting in smaller Ca²⁺ transients. Still, cardiac contractile function is maintained even in the presence of impaired SR Ca²⁺ release. This suggests senescent females exhibit intracellular Ca²⁺ dysregulation, yet undergo some form of compensation to preserve cardiac contractile function with extreme old age.

4.2 THE IMPACT OF SHORT TERM OVARIECTOMY ON CARDIAC CONTRACTILE FUNCTION

4.2.1 Summary of key findings

The present study provides evidence that short term OVX alters myocardial Ca^{2+} handling mechanisms in ventricular myocytes from female mice. The results showed that while Ca^{2+} currents were similar in the two groups, Ca^{2+} transients were larger and faster in OVX myocytes when compared to sham controls. This was due to the fact that short term OVX increased the gain of SR Ca^{2+} release. To determine whether changes in unitary Ca^{2+} release might contribute to the increased gain in OVX cells, spontaneous Ca^{2+} sparks were compared in sham and OVX myocytes. Short term OVX increased the amplitude of Ca^{2+} sparks, although spark widths and time courses were similar in comparison to sham. As SR Ca^{2+} content can modulate SR Ca^{2+} release, intracellular Ca^{2+} stores were examined in cells from sham and OVX mice. The results also showed that short term OVX promoted intracellular Ca^{2+} loading, as SR Ca^{2+} content was substantially higher in cells from OVX than sham controls. This increase in SR Ca^{2+} content led to an increase in the frequency of Ca^{2+} sparks as well as larger spontaneous Ca^{2+} transients in OVX myocytes. These observations show that short term OVX modifies Ca^{2+} handling mechanisms in individual ventricular myocytes to promote SR Ca^{2+} loading, enhance unitary Ca^{2+} release, and increase the size of spontaneous Ca^{2+} transients. A schematic of the effects of short term OVX on components of the EC-coupling pathway is shown in figure 37.

4.2.2 The effect of short term ovariectomy of Ca²⁺ transients

A key finding in this study was that short term OVX caused a significant increase in peak Ca²⁺ transient amplitudes in both field-stimulated and voltage-clamped myocytes. Previous studies have shown that Ca²⁺ transients in field-stimulated myocytes are larger in males than females (Curl et al., 2001; Farrell et al., 2010; Leblanc et al., 1998) and that OVX increases peak Ca²⁺ transients in field-stimulated cells (Curl et al., 2003; Kravtsov et al., 2007; Ma et al., 2009; Wu et al., 2008). However, in field stimulation experiments responses are activated by action potentials and it has been suggested that action potential duration can vary with the level of circulating estrogen (James et al., 2004; Saito et al., 2009). Using voltage clamp, the duration of depolarization can be controlled to give cells an identical waveform and hence a comparable activation history. The results of the present study showed that short term OVX increased the size of Ca²⁺ transients, even when the time of depolarization was identical in sham and OVX cells. Thus, short term OVX increases SR Ca²⁺ release through a mechanism that is not related to a change in the duration of membrane depolarization.

This study also showed that short term OVX enhanced the decay rate of the Ca²⁺ transient when compared to sham controls. Previous studies have also reported faster rates of Ca²⁺ transient decay with OVX (Kravtsov et al., 2007; Curl et al., 2003). Together, these findings suggest that the rate of Ca²⁺ removal from the cytosol by SERCA2a and/or the NCX is higher in OVX myocytes. There is evidence that the activity of the NCX is higher in OVX hearts (Kravtsov et al., 2007) and this may explain faster decay rates of the Ca²⁺ transient in OVX cells. However, SERCA2a expression is either unchanged or reduced in OVX hearts and levels of the endogenous SERCA2a

inhibitor PLB are unchanged after OVX (Bupha-Intr et al., 2009; Bupha-Intr and Wattanapermpool, 2006; Chu et al., 2006; Kravtsov et al., 2007; Ren et al., 2003). This suggests that faster Ca^{2+} transient decay is not due to upregulation of the Ca^{2+} reuptake protein, SERCA2a. However, OVX has been shown to increase in PKA activity (Kam et al., 2005; Kravtsov et al., 2007) and expression of CaMKII (Ma et al., 2009). An increase in the phosphorylation of PLB by PKA and CaMKII would alleviate inhibition of SERCA2a, resulting in enhanced Ca^{2+} decay rates. Overall, the results of the present study show that short term OVX results in larger, faster Ca^{2+} transients. This suggests that estrogen may suppress SR Ca^{2+} release and slow Ca^{2+} removal in the female heart.

4.2.3 The effect of short term ovariectomy on components of the EC-coupling pathway

The present study investigated the mechanisms underlying enhanced Ca^{2+} release in OVX myocytes. Under voltage clamp conditions, Ca^{2+} current densities were compared between sham and OVX myocytes. As the magnitude of SR Ca^{2+} release is proportional to the magnitude of the Ca^{2+} current (Bers, 2008), greater Ca^{2+} entry in OVX cells could explain enhanced SR Ca^{2+} release. The results of this study showed that short term OVX had no effect on peak Ca^{2+} current density in comparison to sham. Other studies have shown that there is no sex difference in Ca^{2+} current densities in myocytes from rats and mice (Farrell et al., 2010; Grandy & Howlett, 2006; Howlett, 2010; Leblanc et al., 1998; Trépanier-Boulay et al., 2001). There is evidence that acute application of high concentrations of estradiol reduces the magnitude of Ca^{2+} current in ventricular myocytes (Jiang et al., 1992). Still, these experiments have used supraphysiological

concentrations of estradiol, so whether lower, physiological levels of estradiol affects I_{CaL} has not been determined (Jiang et al., 1992). Interestingly, an increase in the expression of the Cav1.2 protein has been reported in OVX animals (Chu et al., 2006). Despite this increase in Cav1.2 protein, the findings of the present study show that short term OVX does not increase Ca^{2+} current density to augment SR Ca^{2+} release and Ca^{2+} transients.

This study showed that short term OVX significantly increased the gain of SR Ca^{2+} release. Gain is defined as the amount of SR Ca^{2+} release divided by the amount of Ca^{2+} influx (Ca^{2+} transient/ I_{CaL} ; Bers, 2008). While Ca^{2+} currents were not different between the two groups, short term OVX increased gain to amplify SR Ca^{2+} release resulting in larger Ca^{2+} transients. This increase in gain by short term OVX was greatest at voltages between +20 and +50 mV, corresponding to the peak of the cardiac action potential. This suggests that an action potential will trigger more SR Ca^{2+} release per unit current in OVX cells than in sham myocytes. A sex difference has been reported where the gain of Ca^{2+} release is higher in myocytes from males than females over a similar voltage range (Farrell et al., 2010). Together with the results of the present study, these findings suggest that estrogen may suppress SR Ca^{2+} release.

The present study also showed that short term OVX increased the amplitude of individual Ca^{2+} sparks. Since the Ca^{2+} transient represents the sum of individual Ca^{2+} sparks, these data suggest that larger Ca^{2+} sparks account for larger Ca^{2+} transients and increased gain in OVX myocytes. Interestingly, a previous study showed that Ca^{2+} spark amplitudes were larger in myocytes from male rats when compared to female rats (Farrell et al., 2010). Together with the results of the present study, these findings suggest that estrogen may suppress Ca^{2+} spark amplitude. However, the pathway by which estrogen

modifies Ca^{2+} sparks is not known. One thought is that phosphorylation of ryanodine receptors increases the amplitude of SR Ca^{2+} sparks (Bers, 2008; Guo et al., 2006). As OVX has been shown to increase in PKA activity (Kam et al., 2005; Kravtsov et al., 2007) and CaMKII expression (Ma et al., 2009), it is possible that OVX increases Ca^{2+} spark size by increasing RyR phosphorylation. Additional experiments designed to investigate whether greater phosphorylation of RyR by these kinases modulates the size of Ca^{2+} sparks in OVX hearts would be interesting.

4.2.4 The effect of short term ovariectomy on SR Ca^{2+} content and spontaneous Ca^{2+} release

The present study showed that short term OVX enhanced the gain of SR Ca^{2+} release, resulting in larger Ca^{2+} transients in isolated ventricular myocytes. One factor that regulates SR Ca^{2+} release is SR Ca^{2+} content (Kettlewell et al., 2005). The results of this study showed that short term OVX caused a marked increase in SR Ca^{2+} content in voltage clamped myocytes. This finding supports previous observations that OVX resulted in higher SR Ca^{2+} content when compared to sham controls (Kratsov et al., 2007). The results of the present study also showed that short term OVX increased the frequency of spontaneous Ca^{2+} sparks. Previous studies have shown that the frequency of Ca^{2+} sparks increases as SR Ca^{2+} content increases, suggesting that spontaneous release of SR Ca^{2+} in the form of sparks may function to limit SR Ca^{2+} load (Satoh et al., 1997). As SR Ca^{2+} content was higher in OVX cells than in sham cells, the increase in spark frequency in OVX myocytes is likely linked to the increase in SR Ca^{2+} load. Overall, greater SR Ca^{2+} content leads to increased gain of SR Ca^{2+} release (Kettlewell et al.,

2005). Thus, higher SR Ca^{2+} loads in OVX myocytes would contribute to enhanced EC-coupling gain characteristic of OVX myocytes. Taken together, these findings suggest that estrogen may serve to limit SR Ca^{2+} loading in the female heart.

An increase in SR Ca^{2+} content and enhanced EC-coupling gain could promote spontaneous SR Ca^{2+} release in OVX cells. Spontaneous Ca^{2+} release can lead to triggered electrical activity and arrhythmias (Sipido, 2006). As spontaneously released Ca^{2+} from the SR is removed from the cytosol by the NCX, a transient inward current (I_{Ti}) is produced (Bers et al., 2002; Clusin, 2003). If this inward current is large enough to reach threshold, a delayed afterdepolarization (DAD) can occur resulting in a spontaneous action potential and contractile activity (Clusin, 2003; Ferrier and Moe, 1973). Indeed, the results of this study show that spontaneous Ca^{2+} transients were larger in myocytes from OVX mice than sham mice, which would be expected to induce larger DADs in OVX cells. The findings of this study help explain previous observations that OVX promotes ventricular arrhythmias under conditions of Ca^{2+} overload such as myocardial ischemia and adrenergic stimulation (Chung et al., 2010; Huggins et al., 2009; Teplitz et al., 2005). However, additional experiments to record electrical activity along with Ca^{2+} concentrations would be required to demonstrate this experimentally. This study also helps explain findings that post-menopausal women have an increased incidence of arrhythmias (Peters and Gold, 2004). The results of this study suggest that estrogen deprivation promotes SR Ca^{2+} loading and spontaneous Ca^{2+} release in the female heart. When estrogen levels decline, such as in postmenopausal women, SR Ca^{2+} loading and spontaneous Ca^{2+} release may be one mechanism that underlies the increased incidence of arrhythmias in the aging female heart.

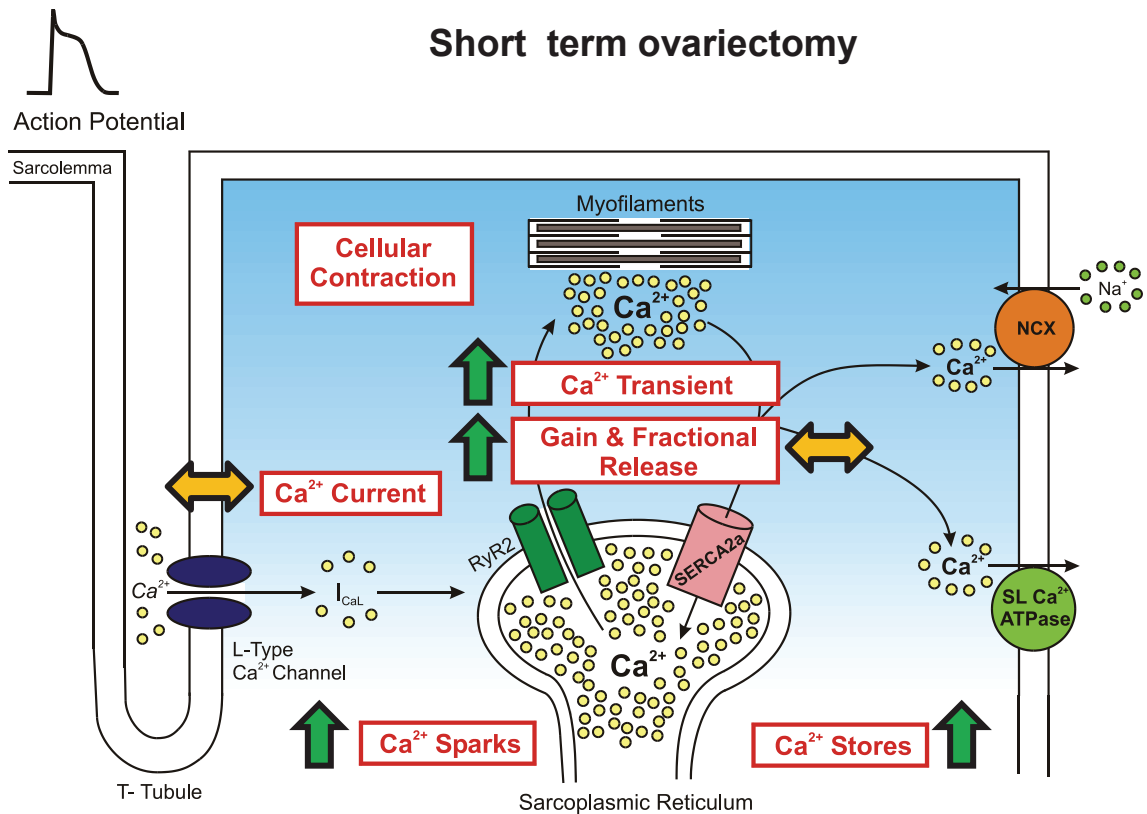


Figure 37. Summary of the effects of short term OVX on components of the EC-coupling pathway. Short term OVX increased the size of Ca²⁺ transients and enhanced EC-coupling gain. This was due to larger Ca²⁺ sparks and greater SR Ca²⁺ stores. Short term OVX did not effect Ca²⁺ current density. However, SR Ca²⁺ loading did lead to larger spontaneous Ca²⁺ transients. This suggests that estrogen deprivation may promote SR Ca²⁺ loading and spontaneous Ca²⁺ release, which would be detrimental to the female heart.

4.3 THE EFFECT OF LONG TERM OVARIECTOMY ON THE AGING FEMALE HEART

4.3.1 Summary of key findings

The results of this study provide evidence that long term OVX alters cardiomyocyte Ca^{2+} homeostasis and contractile function in the aging mouse heart. Myocytes from aging OVX mice exhibited a significant increase in the size of Ca^{2+} transients in comparison to sham controls. Interestingly, enhanced Ca^{2+} levels did not cause larger contractions in ventricular myocytes, and ventricular function measured *in vivo* was similar in hearts from sham and OVX mice. It appears that OVX disrupted the relationship between intracellular Ca^{2+} and cardiac contraction. The underlying mechanisms involved were examined and results showed that long term OVX reduced myofilament Ca^{2+} sensitivity in the aging heart. EC-coupling mechanisms implicated in the disruption of Ca^{2+} handling in OVX myocytes were also compared in cells from both groups. These studies showed that long term OVX increased Ca^{2+} current density and resulted in larger, wider Ca^{2+} sparks which amplified Ca^{2+} transients in cells from OVX mice. This elevated intracellular Ca^{2+} also led to higher SR Ca^{2+} loads, increased spark frequency, spontaneous SR Ca^{2+} release in OVX myocytes. OVX also promoted triggered activity, particularly EADs. Thus, myocytes subjected to long term estrogen reduction exhibited Ca^{2+} dysregulation, reduced myofilament Ca^{2+} responsiveness, spontaneous SR Ca^{2+} release and triggered activity. This may increase susceptibility to cardiovascular disease in hearts from aging females. Figure 38 summarizes the effects of long term OVX on components of the EC-coupling pathway.

4.3.2 Changes in Ca²⁺ transients and contractile function with long term ovariectomy

Studies in myocytes from young adult females have shown that removal of ovarian-derived estrogen increases the magnitude of Ca²⁺ transients (Curl et al., 2003; Fares et al., 2011; Kravtsov et al., 2007; Ma et al., 2009; Wu et al., 2008). Results of experiments on the effects of short term OVX (Section 4.2) further supported these findings. The present study demonstrates that Ca²⁺ transients remained larger in OVX myocytes than in sham controls, even with aging. Previous studies have shown that aging is associated with a decrease in the size of Ca²⁺ transients in myocytes from older males, but not females (Grandy and Howlett, 2006; Howlett, 2010). The data presented in this study suggests that long term reduction of ovarian-derived estrogen does not result in impaired SR Ca²⁺ release consistent with conversion to an aged male phenotype. It is possible that lower testosterone levels in older male rodents (Castilla-Cortazar et al., 2011) may suppress Ca²⁺ release, as seen in myocytes from younger males after gonadectomy (Curl et al., 2009). However, the results of the present study show that removal of ovarian-derived estrogen is not sufficient to reduce Ca²⁺ transient size with aging.

A key finding in this study was the observation that long term OVX altered the relationship between intracellular Ca²⁺ levels and contraction in the aging heart. Both *in vivo* and *in vitro* studies showed that increased intracellular Ca²⁺ levels did not result in larger contractions in hearts from aged OVX mice. Previous studies have shown that both Ca²⁺ transients and cardiac contractile function decline in cells from the hearts of male, but not female rodents (Grandy and Howlett, 2006; Howlett, 2010). Findings from the present study show that, with long term OVX, intracellular Ca²⁺ levels rise to

preserve contractile function in ventricular myocytes. This suggests that long-term removal of ovarian-derived estrogen is not sufficient to cause a deterioration in cardiac contractile function in the aging female heart. Rather, it appears that long term estrogen deprivation results in compensation through intracellular Ca^{2+} loading to maintain cellular shortening.

The underlying mechanism in the altered Ca^{2+} -contraction relationship was found to be a decrease in myofilament Ca^{2+} sensitivity in the hearts of older OVX mice. However, previous studies have shown that myofilament Ca^{2+} sensitivity actually increases with short term OVX (10 weeks) in hearts from young adult female rats (Bupha-Intr et al., 2011; Thawornkaiwong et al., 2007). The results of the present study suggest that this early increase in myofilament Ca^{2+} sensitivity by OVX does not continue in hearts subjected to a long term reduction in ovarian estrogen. Instead, myocardial contractile function was maintained in the aging OVX heart by a substantial increase in the amount of intracellular Ca^{2+} available to the myofilaments. The phosphorylation status of several key myofilament proteins also was examined in this study. Interestingly, the results showed that phosphorylation of the myofilament proteins MyBP-C, TnT, and TnI were similar between aged OVX and sham mice. Phosphorylation of TnI and MyBP-C by PKA or phosphorylation of TnT by PKC has been shown to decrease myofilament Ca^{2+} sensitivity and speed cardiomyocyte relaxation (Barefield and Sadayappan, 2010; Kobayashi and Solaro, 2005). However, the findings of the present study suggest that the decrease in myofilament Ca^{2+} sensitivity by long term OVX occurs through a mechanism independent of MyBP-C, TnT, and TnI phosphorylation. This is surprising, as OVX has been shown to increase the activity of PKA (Kam et al., 2005; Kravtsov et al., 2007).

However, whether long term OVX has a specific effect at the myofilaments, such as an increase in phosphatase localization and activity, has yet to be determined.

One possibility is that long term OVX promotes a change in myosin heavy chain expression. Studies in OVX rats have shown that there is a reduced expression of the fast α -myosin heavy chain isoform and increased expression of the slower β -myosin heavy chain isoform in comparison to sham controls (Bupha-Intr and Wattanapermpool, 2004; Thawornkaiwong et al., 2007). A change from α - to β -myosin heavy chain expression has been shown to reduce myofilament Ca^{2+} sensitivity (Mellor et al., 2011; Metzger et al., 1999). It is possible that a reduction in female sex steroids by OVX may cause a shift in myosin heavy chain expression towards the β -myosin heavy chain, which would promote a decrease in myofilament Ca^{2+} sensitivity.

The results of this study showed that the rates of contraction and relaxation were faster in cells from aged OVX mice when compared to sham controls. The rates of rise and decay of the Ca^{2+} transient were also significantly faster with long term OVX. Previous studies have reported that contractile response rates and the rates of rise and decay of the Ca^{2+} transient are significantly faster in myocytes from younger OVX animals in comparison to shams (Curl et al., 2003; Kravtsov et al., 2007). This is reinforced by the results of this thesis, as discussed in section 4.2. Studies in younger animals have shown that the expression of SERCA2a, PLB, and NCX are unchanged or reduced with OVX, but the activity of the NCX is elevated, which could account for enhanced decay rates (Bupha-Intr et al., 2009; Bupha-Intr and Wattanapermpool, 2006; Chu et al., 2006; Kravtsov et al., 2007). In addition, an increase in PKA-dependent phosphorylation (Kam et al., 2005; Kravtsov et al., 2007) and expression of CaMKII (Ma

et al., 2009) in younger OVX animals has been reported. An increase in the phosphorylation of PLB by PKA and CaMKII in the aged OVX heart may increase inhibition of SERCA2a resulting in an enhanced rate of Ca^{2+} decay. Thus, the increased speed of responses with OVX could be due to enhanced NCX activity or alleviation of SERCA2a inhibition by PLB caused by phosphorylation. This would serve to rapidly remove or re-sequester cytosolic Ca^{2+} , resulting in enhanced relaxation.

4.3.3 Changes in components of the EC-coupling pathway with long term ovariectomy

This study investigated the mechanisms underlying the disruption of Ca^{2+} homeostasis in OVX myocytes. The results showed that the increase in peak Ca^{2+} transient amplitude in OVX myocytes was accompanied by an increase in Ca^{2+} current density. This occurred without a change in the gain of SR Ca^{2+} release. As the magnitude of the Ca^{2+} transient is proportional to the underlying Ca^{2+} current density (Bers, 2008), the results suggest that this increase in Ca^{2+} current is responsible for amplifying SR Ca^{2+} release in myocytes from aged OVX mice. This contrasts with findings in myocytes from mice subjected to short term OVX, where SR Ca^{2+} release was increased without an effect on Ca^{2+} current (discussed in section 4.2). This increase in Ca^{2+} current density in aged OVX myocytes was not due to prolongation of the action potential, as this study found that mean action potential durations were similar in aged sham and OVX myocytes. An increase in the expression of the Cav1.2 protein (Chu et al., 2006) and greater PKA activity (Kam et al., 2005; Kravtsov et al., 2007) have been reported in OVX animals. These mechanisms could increase Ca^{2+} current density in aged

OVX myocytes. However, further investigation is warranted to determine the cellular mechanisms underlying the increase in Ca^{2+} current in aged OVX cells.

The present study showed that long term OVX increased Ca^{2+} spark amplitude and width resulting in larger, wider unitary Ca^{2+} release events. Long term OVX also modified the time course of Ca^{2+} sparks, by abbreviating the time-to-peak and lengthening the time course of spark decay, although these changes did not result in an overall effect on spark duration. However, the shorter time-to-peak may underlie the increase in the rate of rise of the Ca^{2+} transient and shorter time-to-peak contraction observed in OVX myocytes in this study. Together, these observations suggest that long-term estrogen deprivation amplifies SR Ca^{2+} release, which, in part, is due to a marked increase in the magnitude of the underlying SR Ca^{2+} release units.

The present study demonstrated that long term OVX increased SR Ca^{2+} load by almost 90% in the aging female heart. Aging has been shown to increase SR Ca^{2+} content in myocytes from female rodents (Grandy and Howlett, 2006; Howlett, 2010). Findings from the present study showed that this age-related increase in SR Ca^{2+} load is exacerbated by long term OVX. Additionally, higher SR Ca^{2+} loads are thought to promote Ca^{2+} release as spontaneous Ca^{2+} sparks, and thereby limit SR content (Bassani and Bers, 1995; Satoh et al., 1997). The present study also showed that Ca^{2+} spark frequency was greater in OVX cells when compared to sham cells. Taken together, these results suggest that an increase in SR Ca^{2+} load is mediated by a decline in estrogen levels in aged female animals (Wu et al., 2005).

The mechanism behind this elevation in SR Ca^{2+} content could be the increase in Ca^{2+} current and greater SERCA2a activity in OVX cells. While increased SERCA2a

expression has not been examined after OVX in younger animals (Bupha-Intr et al., 2009; Bupha-Intr and Wattanapermpool, 2006), the rapid decay of Ca^{2+} transients and contractions observed here and in previous studies (Curl et al., 2003; Kravtsov et al., 2007) suggests that the rate of SR Ca^{2+} reuptake is increased in OVX myocytes. An increase in PKA activity (Kam et al., 2005; Kravtsov et al., 2007) and CaMKII expression (Ma et al., 2009) in OVX may increase SERCA2a activity by alleviating inhibition by PLB. Thus, greater Ca^{2+} influx and enhanced Ca^{2+} reuptake in long term OVX would promote SR Ca^{2+} loading in ventricular myocytes.

4.3.4 Spontaneous Ca^{2+} release and triggered activity with long term ovariectomy

High levels of SR Ca^{2+} lead to Ca^{2+} overload and induce spontaneous Ca^{2+} release from the SR (Sipido, 2006). The present study showed that spontaneous SR Ca^{2+} release occurred in myocytes from both sham and OVX mice, although the magnitude of this effect was larger in the OVX animals. Ca^{2+} overload and spontaneous SR Ca^{2+} release lead to the appearance of triggered electrical activity and arrhythmias in the form of DADs (Clusin, 2003). Indeed, DADs occurred in myocytes from both groups, but they were more common in sham controls. As DADs are implicated in the initiation of triggered arrhythmias (Clusin, 2003), the results suggest that DADs are an important mechanism in the generation of arrhythmias in the aging female heart.

Triggered activity in the form of early afterdepolarizations (EADs) also occurred in sham and OVX myocytes. The results of this study showed that EADs occurred much more frequently in myocytes from OVX mice than in sham controls. Two mechanisms

that promote EADs are spontaneous SR Ca^{2+} release and increased L-type Ca^{2+} current (Choi et al., 2002; Clusin, 2003). The mechanism involving spontaneous SR Ca^{2+} release requires Ca^{2+} removal via NCX, similar to that of DADs (Volders et al., 2000). Conversely, a prolonged action potential allowing Ca^{2+} channels to recover from inactivation increases Ca^{2+} entry via L-type Ca^{2+} channels. This can result in additional Ca^{2+} release from the SR and lead to an EAD (Clusin, 2003; Volders et al., 2000). Interestingly, both spontaneous SR Ca^{2+} release and Ca^{2+} currents were increased by long term OVX, which may account for the high incidence of EADs observed in OVX myocytes. Moreover, APD_{90} was significantly prolonged prior to the occurrence of EADs in OVX myocytes. Whether additional mechanisms, such as changes in K^+ currents, contribute to an increase in the incidence of EADs with long term OVX has yet to be established.

However, even though there were larger spontaneous SR Ca^{2+} releases with long term OVX the incidence of DADs was lower when compared to sham myocytes. As spontaneous SR Ca^{2+} releases are thought to be a mechanism that underlies EADs and DADs, both an EAD and DAD cannot occur simultaneously. Given that an EAD would precede a DAD, this suggests that greater incidence of EADs would decrease the total number of DADs in myocytes from females subjected to long term OVX. Nonetheless, these results indicate that long term ovarian estrogen deprivation leads to significant Ca^{2+} dysregulation and the initiation of triggered activity, which may promote cardiac arrhythmias in the aging female heart.

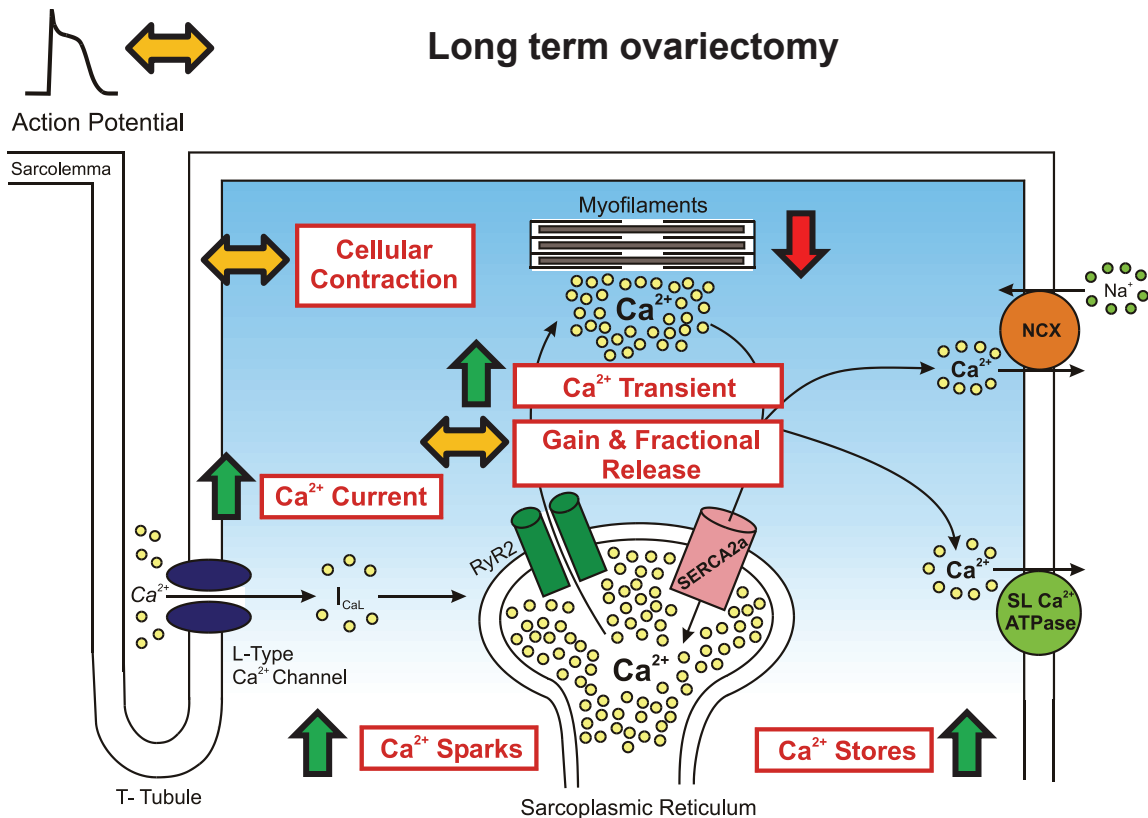


Figure 38. Summary of the effects of long term OVX on the EC-coupling pathway. Long term OVX significantly increased Ca^{2+} current density in cells from the aging female heart. This caused greater Ca^{2+} -induced Ca^{2+} -release (CICR) resulting in larger Ca^{2+} transients. Long term OVX also increased the size of SR Ca^{2+} stores and Ca^{2+} sparks. This suggests that long term OVX promotes Ca^{2+} loading and Ca^{2+} release. However, contractile function was unaffected by long term OVX even though Ca^{2+} transients were larger. This was due to a decline in myofilament Ca^{2+} sensitivity with long term OVX. Although Ca^{2+} loading may occur to maintain contractile function, long term OVX caused larger spontaneous Ca^{2+} releases from the SR. Long term OVX also led to greater triggered activity in the form of EADs. Overall, this suggests that long term OVX promotes SR Ca^{2+} loading and greater SR Ca^{2+} release to maintain cardiac function, but results in abnormal spontaneous and electrical activity. In turn, this could lead to cardiac dysfunction in the hearts of older females.

4.4 LIMITATIONS

There are some limitations to the work presented in this thesis. Overall, these studies have examined cardiac contractile function and Ca^{2+} handling in unloaded isolated ventricular myocytes, although unloaded cell shortening was related to intact ventricular function in some experiments. Findings from this experiment showed that contractile function in individual cells mimicked results from intact hearts. However, caution must be used when extrapolating findings from unloaded cells to intact heart, isolated tissues, or stretched myocytes. Additional experiments investigating Ca^{2+} homeostasis and contractile function in tissue preparations, whole hearts and *in vivo* may be useful to reinforce data collected from unloaded cardiomyocytes.

In some studies the ovaries of young female mice were removed approximately one month after birth. Mice were then aged for approximately seven or 24 months before experiments were conducted. This resulted in an OVX model characterized by both a short term and long term deficiency of ovarian-derived estrogen. These models however, lacked exposure of the heart to the normal pubertal systemic estrogen modelling. This model has been used previously in other studies (Lizotte et al., 2009), but it contrasts with a commonly approach, which is to investigate the effects of OVX in adult animals where tissues have already been exposed to estrogen. In addition, this model differs from the more gradual reduction in ovarian steroids that would be observed during reproductive senescence in animals or during menopause in women. Estrogen can also be produced at various extragonadal sites within the body, such as bone, adipose and vascular tissue (Simpson, 2003). Peripheral tissue aromatase activity can also become a significant source of estrogen in postmenopausal women, through the local conversion of

testosterone to estrogen (Purohit and Reed, 2002). Thus, the contribution of estrogen produced from sources other than the ovaries in our models could also influence the results. Additional experiments with other time frames for estrogen deprivation and quantification of plasma estradiol levels could be explored in the future to further clarify the effects of sex hormones on the female heart.

4.5 SIGNIFICANCE OF FINDINGS

This risk of cardiovascular disease in women increases markedly after the onset of menopause (Bhupathy et al., 2010; Murphy and Steenbergen, 2007), or after bilateral ovariectomy, especially in women who have not taken hormone replacement therapy (Parker et al., 2009). Thus, ovarian hormones, in particular estrogen, may reduce the risk of cardiovascular disease (Bhupathy et al., 2010). The results of these studies suggest that removal of ovarian estrogen promotes intracellular Ca^{2+} loading in individual cardiac myocytes. OVX increases SR Ca^{2+} release by both augmenting SR Ca^{2+} content and increasing the size of Ca^{2+} sparks. These studies also show that even as estrogen levels decline naturally, cardiac contractile function is preserved. If estrogen suppresses Ca^{2+} release and contractile function, declining hormone levels may actually help maintain cardiac function in the aging female heart.

Yet intracellular Ca^{2+} dysregulation is implicated in many cardiovascular diseases (Ferdinandy et al., 2007; Sipido, 2006), and Ca^{2+} loading can be detrimental to the aging female heart. Higher SR Ca^{2+} loads within myocytes can lead to increased SR Ca^{2+} leak and spontaneous and triggered activity (Venetucci et al., 2008). In the intact heart, this can generate ectopic foci and lead to cardiac arrhythmias (Venetucci et al., 2008).

Indeed, findings from this study suggest that both short and long term deprivation of ovarian estrogen leads to spontaneous Ca^{2+} release. Further, long term OVX was shown to promote triggered activity, particularly EADs. EADs are the mechanism underlying life-threatening long QT syndrome-related arrhythmias such as torsade des pointes (Clusin, 2003). Women tend to have longer corrected QT intervals at baseline than men (Yarnoz and Curtis, 2008), and QT prolongation leading to torsade des pointes more commonly occurs in older women than older men (Regitz-Zagrosek, 2006). Thus, the findings from these studies show that long term estrogen reduction promotes EADs, suggesting that a decline in estrogen levels may be a mechanism by which postmenopausal women have an increased susceptibility to long QT syndrome-related arrhythmias such as torsade des pointes.

On the other hand, the benefits of hormone replacement therapy remain controversial. Findings from observational studies regarding the benefit of HRT are contradicted by results from randomized controlled trials (Harman, 2006). This may in part be due to the “timing” of HRT, as treating patients early in menopause provided more beneficial cardiovascular results (Anderson et al., 2004). However estrogen supplementation itself may be unfavourable. While results from this study show that estrogen deprivation promotes SR Ca^{2+} loading and detrimental electrical activity, SR Ca^{2+} release is lower in the presence of estrogen. This suggests that HRT may suppress contractile function and compromise the ability to increase cardiac output. Overall, this could promote heart failure in the setting of cardiovascular disease. This finding may help explain why hormone replacement therapy is not always beneficial in postmenopausal women (Miller et al., 2009).

REFERENCES

- Abete, P., N. Ferrara, A. Cioppa, P. Ferrara, S. Bianco, C. Calabrese, C. Napoli, and F. Rengo. 1996. The role of aging on the control of contractile force by Na⁽⁺⁾-Ca²⁺ exchange in rat papillary muscle. *J Gerontol A Biol Sci Med Sci*. 51:M251-259.
- Altamirano, J., and D.M. Bers. 2007. Voltage dependence of cardiac excitation-contraction coupling: unitary Ca²⁺ current amplitude and open channel probability. *Circulation research*. 101:590-597.
- Anderson, G.L., M. Limacher, A.R. Assaf, T. Bassford, S.A. Beresford, H. Black, D. Bonds, R. Brunner, R. Brzyski, B. Caan, R. Chlebowski, D. Curb, M. Gass, J. Hays, G. Heiss, S. Hendrix, B.V. Howard, J. Hsia, A. Hubbell, R. Jackson, K.C. Johnson, H. Judd, J.M. Kotchen, L. Kuller, A.Z. LaCroix, D. Lane, R.D. Langer, N. Lasser, C.E. Lewis, J. Manson, K. Margolis, J. Ockene, M.J. O'Sullivan, L. Phillips, R.L. Prentice, C. Ritenbaugh, J. Robbins, J.E. Rossouw, G. Sarto, M.L. Stefanick, L. Van Horn, J. Wactawski-Wende, R. Wallace, and S. Wassertheil-Smoller. 2004. Effects of conjugated equine estrogen in postmenopausal women with hysterectomy: the Women's Health Initiative randomized controlled trial. *JAMA*. 291:1701-1712.
- Anversa, P., T. Palackal, E.H. Sonnenblick, G. Olivetti, L.G. Meggs, and J.M. Capasso. 1990. Myocyte cell loss and myocyte cellular hyperplasia in the hypertrophied aging rat heart. *Circulation research*. 67:871-885.
- Assayag, P., C.H. D, I. Marty, J. de Leiris, A.M. Lompre, F. Boucher, P.E. Valere, S. Lortet, B. Swynghedauw, and S. Besse. 1998. Effects of sustained low-flow ischemia on myocardial function and calcium-regulating proteins in adult and senescent rat hearts. *Cardiovasc Res*. 38:169-180.
- Babiker, F.A., D. Lips, R. Meyer, E. Delvaux, P. Zandberg, B. Janssen, G. van Eys, C. Grohe, and P.A. Doevendans. 2006. Estrogen receptor beta protects the murine heart against left ventricular hypertrophy. *Arterioscler Thromb Vasc Biol*. 26:1524-1530.
- Barajas-Martinez, H., V. Haufe, C. Chamberland, M.J. Roy, M.H. Fecteau, J.M. Cordeiro, and R. Dumaine. 2009. Larger dispersion of INa in female dog ventricle as a mechanism for gender-specific incidence of cardiac arrhythmias. *Cardiovascular research*. 81:82-89.
- Barefield, D., and S. Sadayappan. 2010. Phosphorylation and function of cardiac myosin binding protein-C in health and disease. *Journal of molecular and cellular cardiology*. 48:866-875.
- Bassani, R.A., and D.M. Bers. 1995. Rate of diastolic Ca release from the sarcoplasmic reticulum of intact rabbit and rat ventricular myocytes. *Biophys J*. 68:2015-2022.

- Bers, D.M. 2001. *Excitation-Contraction Coupling and Cardiac Contractile Force*. Kluwer Academic Press, Dordrecht, the Netherlands.
- Bers, D.M. 2002. Cardiac excitation-contraction coupling. *Nature*. 415:198-205.
- Bers, D.M. 2008. Calcium cycling and signaling in cardiac myocytes. *Annu Rev Physiol*. 70:23-49.
- Bers, D.M., S.M. Pogwizd, and K. Schlotthauer. 2002. Upregulated Na/Ca exchange is involved in both contractile dysfunction and arrhythmogenesis in heart failure. *Basic Res Cardiol*. 97 Suppl 1:136-42.
- Bhuiyan, M.S., N. Shioda, and K. Fukunaga. 2007. Ovariectomy augments pressure overload-induced hypertrophy associated with changes in Akt and nitric oxide synthase signaling pathways in female rats. *Am J Physiol Endocrinol Metab*. 293:E1606-1614.
- Bhupathy, P., C.D. Haines, and L.A. Leinwand. 2010. Influence of sex hormones and phytoestrogens on heart disease in men and women. *Womens Health (Lond Engl)*. 6:77-95.
- Bidoggia, H., J.P. Maciel, N. Capalozza, S. Mosca, E.J. Blaksley, E. Valverde, G. Bertran, P. Arini, M.O. Biagetti, and R.A. Quintero. 2000. Sex differences on the electrocardiographic pattern of cardiac repolarization: possible role of testosterone. *Am Heart J*. 140:678-683.
- Birkeland, J.A., O.M. Sejersted, T. Taraldsen, and I. Sjaastad. 2005. EC-coupling in normal and failing hearts. *Scand Cardiovasc J*. 39:13-23.
- Booth, E.A., M. Marchesi, E.J. Kilbourne, and B.R. Lucchesi. 2003. 17Beta-estradiol as a receptor-mediated cardioprotective agent. *J Pharmacol Exp Ther*. 307:395-401.
- Bootman, M.D., D.R. Higazi, S. Coombes, and H.L. Roderick. 2006. Calcium signalling during excitation-contraction coupling in mammalian atrial myocytes. *J Cell Sci*. 119:3915-3925.
- Brillantes, A.B., K. Ondrias, A. Scott, E. Kobrinsky, E. Ondriasova, M.C. Moschella, T. Jayaraman, M. Landers, B.E. Ehrlich, and A.R. Marks. 1994. Stabilization of calcium release channel (ryanodine receptor) function by FK506-binding protein. *Cell*. 77:513-523.
- Brinckmann, M., E. Kaschina, W. Altarache-Xifro, C. Curato, M. Timm, A. Grzesiak, J. Dong, K. Kappert, U. Kintscher, T. Unger, and J. Li. 2009. Estrogen receptor alpha supports cardiomyocytes indirectly through post-infarct cardiac c-kit+ cells. *Journal of molecular and cellular cardiology*. 47:66-75.

- Brouillette, J., M.A. Lupien, C. St-Michel, and C. Fiset. 2007. Characterization of ventricular repolarization in male and female guinea pigs. *J Mol Cell Cardiol.* 42:357-366.
- Brouillette, J., K. Rivard, E. Lizotte, and C. Fiset. 2005. Sex and strain differences in adult mouse cardiac repolarization: importance of androgens. *Cardiovascular research.* 65:148-157.
- Brouillette, J., V. Trepanier-Boulay, and C. Fiset. 2003. Effect of androgen deficiency on mouse ventricular repolarization. *The Journal of physiology.* 546:403-413.
- Bupha-Intr, T., J. Laosiripisan, and J. Wattanapermpool. 2009. Moderate intensity of regular exercise improves cardiac SR Ca²⁺ uptake activity in ovariectomized rats. *J Appl Physiol.* 107:1105-1112.
- Bupha-Intr, T., Y.W. Oo, and J. Wattanapermpool. 2011. Increased myocardial stiffness with maintenance of length-dependent calcium activation by female sex hormones in diabetic rats. *American journal of physiology. Heart and circulatory physiology.* 300:H1661-1668.
- Bupha-Intr, T., and J. Wattanapermpool. 2004. Cardioprotective effects of exercise training on myofilament calcium activation in ovariectomized rats. *Journal of applied physiology.* 96:1755-1760.
- Bupha-Intr, T., and J. Wattanapermpool. 2006. Regulatory role of ovarian sex hormones in calcium uptake activity of cardiac sarcoplasmic reticulum. *Am J Physiol Heart Circ Physiol.* 291:H1101-1108.
- Buttrick, P., A. Malhotra, S. Factor, D. Greenen, L. Leinwand, and J. Scheuer. 1991. Effect of aging and hypertension on myosin biochemistry and gene expression in the rat heart. *Circulation research.* 68:645-652.
- Cachelin, A.B., J.E. de Peyer, S. Kokubun, and H. Reuter. 1983. Ca²⁺ channel modulation by 8-bromocyclic AMP in cultured heart cells. *Nature.* 304:462-464.
- Camper-Kirby, D., S. Welch, A. Walker, I. Shiraishi, K.D. Setchell, E. Schaefer, J. Kajstura, P. Anversa, and M.A. Sussman. 2001. Myocardial Akt activation and gender: increased nuclear activity in females versus males. *Circulation research.* 88:1020-1027.
- Capasso, J.M., D. Fitzpatrick, and P. Anversa. 1992. Cellular mechanisms of ventricular failure: myocyte kinetics and geometry with age. *Am J Physiol.* 262:H1770-1781.
- Castilla-Cortazar, I., M. Garcia-Fernandez, G. Delgado, J.E. Puche, I. Sierra, R. Barhoum, and S. Gonzalez-Baron. 2011. Hepatoprotection and neuroprotection induced by low doses of IGF-II in aging rats. *J Transl Med.* 9:103.

- Chen, J., J. Petranka, K. Yamamura, R.E. London, C. Steenbergen, and E. Murphy. 2003. Gender differences in sarcoplasmic reticulum calcium loading after isoproterenol. *American journal of physiology. Heart and circulatory physiology*. 285:H2657-2662.
- Cheng, H., W.J. Lederer, and M.B. Cannell. 1993. Calcium sparks: elementary events underlying excitation-contraction coupling in heart muscle. *Science*. 262:740-744.
- Choi, B.R., F. Burton, and G. Salama. 2002. Cytosolic Ca²⁺ triggers early afterdepolarizations and Torsade de Pointes in rabbit hearts with type 2 long QT syndrome. *The Journal of physiology*. 543:615-631.
- Chu, S.H., P. Goldspink, J. Kowalski, J. Beck, and D.W. Schwertz. 2006. Effect of estrogen on calcium-handling proteins, beta-adrenergic receptors, and function in rat heart. *Life Sci*. 79:1257-1267.
- Chung, M.T., P.Y. Cheng, K.K. Lam, S.Y. Chen, Y.F. Ting, M.H. Yen, and Y.M. Lee. 2010. Cardioprotective effects of long-term treatment with raloxifene, a selective estrogen receptor modulator, on myocardial ischemia/reperfusion injury in ovariectomized rats. *Menopause*. 17:127-134.
- Claessens, T.E., E.R. Rietzschel, M.L. De Buyzere, D. De Bacquer, G. De Backer, T.C. Gillebert, P.R. Verdonck, and P. Segers. 2007. Noninvasive assessment of left ventricular and myocardial contractility in middle-aged men and women: disparate evolution above the age of 50? *American journal of physiology. Heart and circulatory physiology*. 292:H856-865.
- Clusin, W.T. 2003. Calcium and cardiac arrhythmias: DADs, EADs, and alternans. *Crit Rev Clin Lab Sci*. 40:337-375.
- Colditz, G.A., S.E. Hankinson, D.J. Hunter, W.C. Willett, J.E. Manson, M.J. Stampfer, C. Hennekens, B. Rosner, and F.E. Speizer. 1995. The use of estrogens and progestins and the risk of breast cancer in postmenopausal women. *N Engl J Med*. 332:1589-1593.
- Conference Board of Canada. 2010. The Canadian Heart Health Strategy: Risk Factors and Future Cost Implications.
- Curl, C.L., L.M. Delbridge, B.J. Canny, and I.R. Wendt. 2009. Testosterone modulates cardiomyocyte Ca²⁺ handling and contractile function. *Physiol Res*. 58:293-297.
- Curl, C.L., L.M. Delbridge, and I.R. Wendt. 2008. Sex differences in cardiac muscle responsiveness to Ca²⁺ and L-type Ca²⁺ channel modulation. *Eur J Pharmacol*. 586:288-292.

- Curl, C.L., I.R. Wendt, B.J. Canny, and G. Kotsanas. 2003. Effects of ovariectomy and 17 beta-oestradiol replacement on $[Ca^{2+}]_i$ in female rat cardiac myocytes. *Clin Exp Pharmacol Physiol*. 30:489-494.
- Curl, C.L., I.R. Wendt, and G. Kotsanas. 2001. Effects of gender on intracellular. *Pflugers Arch*. 441:709-716.
- Czubryt, M.P., L. Espira, L. Lamoureux, and B. Abrenica. 2006. The role of sex in cardiac function and disease. *Can J Physiol Pharmacol*. 84:93-109.
- Delbridge, L.M., J.W. Bassani, and D.M. Bers. 1996. Steady-state twitch Ca^{2+} fluxes and cytosolic Ca^{2+} buffering in rabbit ventricular myocytes. *The American journal of physiology*. 270:C192-199.
- Deschamps, A.M., and E. Murphy. 2009. Activation of a novel estrogen receptor, GPER, is cardioprotective in male and female rats. *American journal of physiology. Heart and circulatory physiology*. 297:H1806-1813.
- Dibb, K.M., U. Rueckschloss, D.A. Eisner, G. Isenberg, and A.W. Trafford. 2004. Mechanisms underlying enhanced cardiac excitation contraction coupling observed in the senescent sheep myocardium. *J Mol Cell Cardiol*. 37:1171-1181.
- Donaldson, C., S. Eder, C. Baker, M.J. Aronovitz, A.D. Weiss, M. Hall-Porter, F. Wang, A. Ackerman, R.H. Karas, J.D. Molkenin, and R.D. Patten. 2009. Estrogen attenuates left ventricular and cardiomyocyte hypertrophy by an estrogen receptor-dependent pathway that increases calcineurin degradation. *Circulation research*. 104:265-275, 211p following 275.
- Endoh, H., H. Sasaki, K. Maruyama, K. Takeyama, I. Waga, T. Shimizu, S. Kato, and H. Kawashima. 1997. Rapid activation of MAP kinase by estrogen in the bone cell line. *Biochem Biophys Res Commun*. 235:99-102.
- Fabiato, A. 1985a. Rapid ionic modifications during the aequorin-detected calcium transient in a skinned canine cardiac Purkinje cell. *J Gen Physiol*. 85:189-246.
- Fabiato, A. 1985b. Simulated calcium current can both cause calcium loading in and trigger calcium release from the sarcoplasmic reticulum of a skinned canine cardiac Purkinje cell. *J Gen Physiol*. 85:291-320.
- Fabiato, A. 1985c. Time and calcium dependence of activation and inactivation of calcium-induced release of calcium from the sarcoplasmic reticulum of a skinned canine cardiac Purkinje cell. *J Gen Physiol*. 85:247-289.
- Fares, E., R.J. Parks, J.K. Macdonald, J.M. Egar, and S.E. Howlett. 2011. Ovariectomy enhances SR Ca^{2+} release and increases Ca^{2+} spark amplitudes in isolated ventricular myocytes. *Journal of molecular and cellular cardiology*.

- Farrell, S.R., and S.E. Howlett. 2007. The effects of isoproterenol on abnormal electrical and contractile activity and diastolic calcium are attenuated in myocytes from aged Fischer 344 rats. *Mech Ageing Dev.* 128:566-573.
- Farrell, S.R., and S.E. Howlett. 2008. The age-related decrease in catecholamine sensitivity is mediated by beta(1)-adrenergic receptors linked to a decrease in adenylate cyclase activity in ventricular myocytes from male Fischer 344 rats. *Mechanisms of ageing and development.* 129:735-744.
- Farrell, S.R., J.L. Ross, and S.E. Howlett. 2010. Sex differences in mechanisms of cardiac excitation-contraction coupling in rat ventricular myocytes. *American journal of physiology. Heart and circulatory physiology.* 299:H36-45.
- Ferdinandy, P., R. Schulz, and G.F. Baxter. 2007. Interaction of cardiovascular risk factors with myocardial ischemia/reperfusion injury, preconditioning, and postconditioning. *Pharmacol Rev.* 59:418-458.
- Ferrier, G.R., and G.K. Moe. 1973. Effect of calcium on acetylcholine-induced transient depolarizations in canine Purkinje tissue. *Circulation research.* 33:508-515.
- Ferrier, G.R., R.H. Smith, and S.E. Howlett. 2003. Calcium sparks in mouse ventricular myocytes at physiological temperature. *American journal of physiology. Heart and circulatory physiology.* 285:H1495-1505.
- Fleg, J.L., F. O'Connor, G. Gerstenblith, L.C. Becker, J. Clulow, S.P. Schulman, and E.G. Lakatta. 1995. Impact of age on the cardiovascular response to dynamic upright exercise in healthy men and women. *J Appl Physiol.* 78:890-900.
- Fliegner, D., C. Schubert, A. Penkalla, H. Witt, G. Kararigas, E. Dworatzek, E. Staub, P. Martus, P. Ruiz Noppinger, U. Kintscher, J.A. Gustafsson, and V. Regitz-Zagrosek. 2010. Female sex and estrogen receptor-beta attenuate cardiac remodeling and apoptosis in pressure overload. *American journal of physiology. Regulatory, integrative and comparative physiology.* 298:R1597-1606.
- Folsom, A.R., P.J. Mink, T.A. Sellers, C.P. Hong, W. Zheng, and J.D. Potter. 1995. Hormonal replacement therapy and morbidity and mortality in a prospective study of postmenopausal women. *Am J Public Health.* 85:1128-1132.
- Forman, D.E., A. Cittadini, G. Azhar, P.S. Douglas, and J.Y. Wei. 1997. Cardiac morphology and function in senescent rats: gender-related differences. *Journal of the American College of Cardiology.* 30:1872-1877.
- Froehlich, J.P., E.G. Lakatta, E. Beard, H.A. Spurgeon, M.L. Weisfeldt, and G. Gerstenblith. 1978. Studies of sarcoplasmic reticulum function and contraction duration in young adult and aged rat myocardium. *J Mol Cell Cardiol.* 10:427-438.

- Furukawa, T., and J. Kurokawa. 2008. Non-genomic regulation of cardiac ion channels by sex hormones. *Cardiovasc Hematol Disord Drug Targets*. 8:245-251.
- Gavin, K.M., D.R. Seals, A.E. Silver, and K.L. Moreau. 2009. Vascular endothelial estrogen receptor alpha is modulated by estrogen status and related to endothelial function and endothelial nitric oxide synthase in healthy women. *J Clin Endocrinol Metab*. 94:3513-3520.
- Ginsburg, K.S., and D.M. Bers. 2004. Modulation of excitation-contraction coupling by isoproterenol in cardiomyocytes with controlled SR Ca²⁺ load and Ca²⁺ current trigger. *The Journal of physiology*. 556:463-480.
- Goldstein, J., C.K. Sites, and M.J. Toth. 2004. Progesterone stimulates cardiac muscle protein synthesis via receptor-dependent pathway. *Fertil Steril*. 82:430-436.
- Gottdiener, J.S., A.M. Arnold, G.P. Aurigemma, J.F. Polak, R.P. Tracy, D.W. Kitzman, J.M. Gardin, J.E. Rutledge, and R.C. Boineau. 2000. Predictors of congestive heart failure in the elderly: the Cardiovascular Health Study. *Journal of the American College of Cardiology*. 35:1628-1637.
- Grandi, A.M., A. Venco, F. Barzizza, F. Scalise, P. Pantaleo, and G. Finardi. 1992. Influence of age and sex on left ventricular anatomy and function in normals. *Cardiology*. 81:8-13.
- Grandy, S.A., and S.E. Howlett. 2006. Cardiac excitation-contraction coupling is altered in myocytes from aged male mice but not in cells from aged female mice. *Am J Physiol Heart Circ Physiol*. 291:H2362-2370.
- Grodstein, F., J.E. Manson, G.A. Colditz, W.C. Willett, F.E. Speizer, and M.J. Stampfer. 2000. A prospective, observational study of postmenopausal hormone therapy and primary prevention of cardiovascular disease. *Ann Intern Med*. 133:933-941.
- Grodstein, F., J.E. Manson, and M.J. Stampfer. 2001. Postmenopausal hormone use and secondary prevention of coronary events in the nurses' health study. a prospective, observational study. *Ann Intern Med*. 135:1-8.
- Grodstein, F., M.J. Stampfer, G.A. Colditz, W.C. Willett, J.E. Manson, M. Joffe, B. Rosner, C. Fuchs, S.E. Hankinson, D.J. Hunter, C.H. Hennekens, and F.E. Speizer. 1997. Postmenopausal hormone therapy and mortality. *N Engl J Med*. 336:1769-1775.
- Grodstein, F., M.J. Stampfer, J.E. Manson, G.A. Colditz, W.C. Willett, B. Rosner, F.E. Speizer, and C.H. Hennekens. 1996. Postmenopausal estrogen and progestin use and the risk of cardiovascular disease. *N Engl J Med*. 335:453-461.
- Grohe, C., S. Kahlert, K. Lobbert, M. Stimpel, R.H. Karas, H. Vetter, and L. Neyses. 1997. Cardiac myocytes and fibroblasts contain functional estrogen receptors. *FEBS Lett*. 416:107-112.

- Grohe, C., S. Kahlert, K. Lobbert, and H. Vetter. 1998. Expression of oestrogen receptor alpha and beta in rat heart: role of local oestrogen synthesis. *J Endocrinol.* 156:R1-7.
- Guatimosim, S., K. Dilly, L.F. Santana, M. Saleet Jafri, E.A. Sobie, and W.J. Lederer. 2002. Local Ca(2+) signaling and EC coupling in heart: Ca(2+) sparks and the regulation of the [Ca(2+)](i) transient. *Journal of molecular and cellular cardiology.* 34:941-950.
- Guo, T., T. Zhang, R. Mestril, and D.M. Bers. 2006. Ca2+/Calmodulin-dependent protein kinase II phosphorylation of ryanodine receptor does affect calcium sparks in mouse ventricular myocytes. *Circulation research.* 99:398-406.
- Hacker, T.A., S.H. McKiernan, P.S. Douglas, J. Wanagat, and J.M. Aiken. 2006. Age-related changes in cardiac structure and function in Fischer 344 x Brown Norway hybrid rats. *Am J Physiol Heart Circ Physiol.* 290:H304-311.
- Hanley, P.C., A.R. Zinsmeister, I.P. Clements, A.A. Bove, M.L. Brown, and R.J. Gibbons. 1989. Gender-related differences in cardiac response to supine exercise assessed by radionuclide angiography. *Journal of the American College of Cardiology.* 13:624-629.
- Harman, S.M. 2006. Estrogen replacement in menopausal women: recent and current prospective studies, the WHI and the KEEPS. *Gend Med.* 3:254-269.
- Harman, S.M., E.A. Brinton, M. Cedars, R. Lobo, J.E. Manson, G.R. Merriam, V.M. Miller, F. Naftolin, and N. Santoro. 2005. KEEPS: The Kronos Early Estrogen Prevention Study. *Climacteric.* 8:3-12.
- Hayward, C.S., W.V. Kalnins, and R.P. Kelly. 2001. Gender-related differences in left ventricular chamber function. *Cardiovascular research.* 49:340-350.
- Henderson, B.E., A. Paganini-Hill, and R.K. Ross. 1991. Decreased mortality in users of estrogen replacement therapy. *Arch Intern Med.* 151:75-78.
- Heyliger, C.E., A.R. Prakash, and J.H. McNeill. 1988. Alterations in membrane Na+–Ca2+ exchange in the aging myocardium. *Age.* 11:1-6.
- Hodis, H.N., W.J. Mack, and R. Lobo. 2002. Postmenopausal hormone replacement therapy as antiatherosclerotic therapy. *Curr Atheroscler Rep.* 4:52-58.
- Howlett, S.E. 2010. Age-associated changes in excitation-contraction coupling are more prominent in ventricular myocytes from male rats than in myocytes from female rats. *American journal of physiology. Heart and circulatory physiology.* 298:H659-670.

- Howlett, S.E., S.A. Grandy, and G.R. Ferrier. 2006. Calcium spark properties in ventricular myocytes are altered in aged mice. *American journal of physiology. Heart and circulatory physiology*. 290:H1566-1574.
- Howlett, S.E., and P.A. Nicholl. 1992. Density of 1,4-dihydropyridine receptors decreases in the hearts of aging hamsters. *J Mol Cell Cardiol*. 24:885-894.
- Huggins, C.E., C.L. Curl, R. Patel, P.L. McLennan, M.L. Theiss, T. Pedrazzini, S. Pepe, and L.M. Delbridge. 2009. Dietary fish oil is antihypertrophic but does not enhance postischemic myocardial function in female mice. *American journal of physiology. Heart and circulatory physiology*. 296:H957-966.
- Hulley, S., D. Grady, T. Bush, C. Furberg, D. Herrington, B. Riggs, and E. Vittinghoff. 1998. Randomized trial of estrogen plus progestin for secondary prevention of coronary heart disease in postmenopausal women. Heart and Estrogen/progestin Replacement Study (HERS) Research Group. *JAMA*. 280:605-613.
- Huxley, A.F. 1957. Muscle structure and theories of contraction. *Prog Biophys Biophys Chem*. 7:255-318.
- Huxley, V.H. 2007. Sex and the cardiovascular system: the intriguing tale of how women and men regulate cardiovascular function differently. *Adv Physiol Educ*. 31:17-22.
- Inoue, M., and J.H. Bridge. 2005. Variability in couplon size in rabbit ventricular myocytes. *Biophys J*. 89:3102-3110.
- Isenberg, G., B. Borschke, and U. Rueckschloss. 2003. Ca²⁺ transients of cardiomyocytes from senescent mice peak late and decay slowly. *Cell Calcium*. 34:271-280.
- James, A.F., L.A. Arberry, and J.C. Hancox. 2004. Gender-related differences in ventricular myocyte repolarization in the guinea pig. *Basic Res Cardiol*. 99:183-192.
- Janczewski, A.M., and E.G. Lakatta. 2010. Modulation of sarcoplasmic reticulum Ca(2+) cycling in systolic and diastolic heart failure associated with aging. *Heart Fail Rev*. 15:431-445.
- January, C.T., and J.M. Riddle. 1989. Early afterdepolarizations: mechanism of induction and block. A role for L-type Ca²⁺ current. *Circulation research*. 64:977-990.
- Jiang, C., P.A. Poole-Wilson, P.M. Sarrel, S. Mochizuki, P. Collins, and K.T. MacLeod. 1992. Effect of 17 beta-oestradiol on contraction, Ca²⁺ current and intracellular free Ca²⁺ in guinea-pig isolated cardiac myocytes. *British journal of pharmacology*. 106:739-745.

- Johnson, B.D., W. Zheng, K.S. Korach, T. Scheuer, W.A. Catterall, and G.M. Rubanyi. 1997. Increased expression of the cardiac L-type calcium channel in estrogen receptor-deficient mice. *The Journal of general physiology*. 110:135-140.
- Josephson, I.R., A. Guia, M.D. Stern, and E.G. Lakatta. 2002. Alterations in properties of L-type Ca channels in aging rat heart. *Journal of molecular and cellular cardiology*. 34:297-308.
- Kajstura, J., W. Cheng, R. Sarangarajan, P. Li, B. Li, J.A. Nitahara, S. Chapnick, K. Reiss, G. Olivetti, and P. Anversa. 1996. Necrotic and apoptotic myocyte cell death in the aging heart of Fischer 344 rats. *The American journal of physiology*. 271:H1215-1228.
- Kam, K.W., G.M. Kravtsov, J. Liu, and T.M. Wong. 2005. Increased PKA activity and its influence on isoprenaline-stimulated L-type Ca²⁺ channels in the heart from ovariectomized rats. *British journal of pharmacology*. 144:972-981.
- Katoh, H., K. Schlotthauer, and D.M. Bers. 2000. Transmission of information from cardiac dihydropyridine receptor to ryanodine receptor: evidence from BayK 8644 effects on resting Ca(2+) sparks. *Circulation research*. 87:106-111.
- Kentish, J.C., D.T. McCloskey, J. Layland, S. Palmer, J.M. Leiden, A.F. Martin, and R.J. Solaro. 2001. Phosphorylation of troponin I by protein kinase A accelerates relaxation and crossbridge cycle kinetics in mouse ventricular muscle. *Circulation research*. 88:1059-1065.
- Kerfant, B.G., D. Gidrewicz, H. Sun, G.Y. Oudit, J.M. Penninger, and P.H. Backx. 2005. Cardiac sarcoplasmic reticulum calcium release and load are enhanced by subcellular cAMP elevations in PI3Kgamma-deficient mice. *Circulation research*. 96:1079-1086.
- Kerfant, B.G., R.A. Rose, H. Sun, and P.H. Backx. 2006. Phosphoinositide 3-kinase gamma regulates cardiac contractility by locally controlling cyclic adenosine monophosphate levels. *Trends Cardiovasc Med*. 16:250-256.
- Kettlewell, S., P. Most, S. Currie, W.J. Koch, and G.L. Smith. 2005. S100A1 increases the gain of excitation-contraction coupling in isolated rabbit ventricular cardiomyocytes. *Journal of molecular and cellular cardiology*. 39:900-910.
- Kobayashi, T., and R.J. Solaro. 2005. Calcium, thin filaments, and the integrative biology of cardiac contractility. *Annu Rev Physiol*. 67:39-67.
- Kravtsov, G.M., K.W. Kam, J. Liu, S. Wu, and T.M. Wong. 2007. Altered Ca(2+) handling by ryanodine receptor and Na(+)-Ca(2+) exchange in the heart from ovariectomized rats: role of protein kinase A. *Am J Physiol Cell Physiol*. 292:C1625-1635.

- Lakatta, E.G., G. Gerstenblith, C.S. Angell, N.W. Shock, and M.L. Weisfeldt. 1975. Diminished inotropic response of aged myocardium to catecholamines. *Circ Res.* 36:262-269.
- Lakatta, E.G., and D. Levy. 2003. Arterial and cardiac aging: major shareholders in cardiovascular disease enterprises: Part II: the aging heart in health: links to heart disease. *Circulation.* 107:346-354.
- Lakatta, E.G., and S.J. Sollott. 2002. Perspectives on mammalian cardiovascular aging: humans to molecules. *Comp Biochem Physiol A Mol Integr Physiol.* 132:699-721.
- Leblanc, N., D. Chartier, H. Gosselin, and J.L. Rouleau. 1998. Age and gender differences in excitation-contraction coupling of the rat ventricle. *J Physiol.* 511 (Pt 2):533-548.
- Legato, M.J. 2000. Gender and the heart: sex-specific differences in normal anatomy and physiology. *J Gend Specif Med.* 3:15-18.
- Li, L., J. Desantiago, G. Chu, E.G. Kranias, and D.M. Bers. 2000. Phosphorylation of phospholamban and troponin I in beta-adrenergic-induced acceleration of cardiac relaxation. *American journal of physiology. Heart and circulatory physiology.* 278:H769-779.
- Lieber, S.C., H. Qiu, L. Chen, Y.T. Shen, C. Hong, W.C. Hunter, N. Aubry, S.F. Vatner, and D.E. Vatner. 2008. Cardiac dysfunction in aging conscious rats: altered cardiac cytoskeletal proteins as a potential mechanism. *American journal of physiology. Heart and circulatory physiology.* 295:H860-866.
- Liew, R., M.A. Stagg, J. Chan, P. Collins, and K.T. MacLeod. 2004. Gender determines the acute actions of genistein on intracellular calcium regulation in the guinea-pig heart. *Cardiovascular research.* 61:66-76.
- Lim, C.C., C.S. Apstein, W.S. Colucci, and R. Liao. 2000. Impaired cell shortening and relengthening with increased pacing frequency are intrinsic to the senescent mouse cardiomyocyte. *J Mol Cell Cardiol.* 32:2075-2082.
- Lim, C.C., R. Liao, N. Varma, and C.S. Apstein. 1999. Impaired lusitropy-frequency in the aging mouse: role of Ca(2+)-handling proteins and effects of isoproterenol. *The American journal of physiology.* 277:H2083-2090.
- Liu, S.J., R.P. Wyeth, R.B. Melchert, and R.H. Kennedy. 2000. Aging-associated changes in whole cell K(+) and L-type Ca(2+) currents in rat ventricular myocytes. *Am J Physiol Heart Circ Physiol.* 279:H889-900.
- Lizotte, E., S.A. Grandy, A. Tremblay, B.G. Allen, and C. Fiset. 2009. Expression, distribution and regulation of sex steroid hormone receptors in mouse heart. *Cell Physiol Biochem.* 23:75-86.

- Lloyd-Jones, D.M., M.G. Larson, A. Beiser, and D. Levy. 1999. Lifetime risk of developing coronary heart disease. *Lancet*. 353:89-92.
- Lompre, A.M., F. Lambert, E.G. Lakatta, and K. Schwartz. 1991. Expression of sarcoplasmic reticulum Ca(2+)-ATPase and calsequestrin genes in rat heart during ontogenic development and aging. *Circulation research*. 69:1380-1388.
- Lopez, A., G. Caselli, and T. Valkonen. 1995. Adult Mortality in Developed Countries: From Description to Explanation. Clarendon Press, Oxford, England.
- Lopez-Lopez, J.R., P.S. Shacklock, C.W. Balke, and W.G. Wier. 1994. Local, stochastic release of Ca²⁺ in voltage-clamped rat heart cells: visualization with confocal microscopy. *The Journal of physiology*. 480 (Pt 1):21-29.
- Luczak, E.D., and L.A. Leinwand. 2009. Sex-based cardiac physiology. *Annu Rev Physiol*. 71:1-18.
- Ma, Y., W.T. Cheng, S. Wu, and T.M. Wong. 2009. Oestrogen confers cardioprotection by suppressing Ca²⁺/calmodulin-dependent protein kinase II. *Br J Pharmacol*. 157:705-715.
- Mace, L.C., B.M. Palmer, D.A. Brown, K.N. Jew, J.M. Lynch, J.M. Glunt, T.A. Parsons, J.Y. Cheung, and R.L. Moore. 2003. Influence of age and run training on cardiac Na⁺/Ca²⁺ exchange. *Journal of applied physiology*. 95:1994-2003.
- Madigan, F.C. 1957. Are sex mortality differentials biologically caused? *Milbank Mem Fund Q*. 35:202-223.
- Maier, L.S., and D.M. Bers. 2007. Role of Ca²⁺/calmodulin-dependent protein kinase (CaMK) in excitation-contraction coupling in the heart. *Cardiovascular research*. 73:631-640.
- Marsh, J.D., M.H. Lehmann, R.H. Ritchie, J.K. Gwathmey, G.E. Green, and R.J. Schiebinger. 1998. Androgen receptors mediate hypertrophy in cardiac myocytes. *Circulation*. 98:256-261.
- Marx, S. 2003. Ion channel macromolecular complexes in the heart. *Journal of molecular and cellular cardiology*. 35:37-44.
- Marx, S.O., J. Gaburjakova, M. Gaburjakova, C. Henrikson, K. Ondrias, and A.R. Marks. 2001. Coupled gating between cardiac calcium release channels (ryanodine receptors). *Circulation research*. 88:1151-1158.
- Marx, S.O., S. Reiken, Y. Hisamatsu, T. Jayaraman, D. Burkhoff, N. Rosemlit, and A.R. Marks. 2000. PKA phosphorylation dissociates FKBP12.6 from the calcium release channel (ryanodine receptor): defective regulation in failing hearts. *Cell*. 101:365-376.

- McDonald, T.F., S. Pelzer, W. Trautwein, and D.J. Pelzer. 1994. Regulation and modulation of calcium channels in cardiac, skeletal, and smooth muscle cells. *Physiol Rev.* 74:365-507.
- Meissner, G. 2004. Molecular regulation of cardiac ryanodine receptor ion channel. *Cell Calcium.* 35:621-628.
- Mellor, K.M., I.R. Wendt, R.H. Ritchie, and L.M. Delbridge. 2011. Fructose diet treatment in mice induces fundamental disturbance of cardiomyocyte Ca²⁺ handling and myofilament responsiveness. *American journal of physiology. Heart and circulatory physiology.*
- Merz, C.N., M. Moriel, A. Rozanski, J. Klein, and D.S. Berman. 1996. Gender-related differences in exercise ventricular function among healthy subjects and patients. *Am Heart J.* 131:704-709.
- Messerli, F.H., G.E. Garavaglia, R.E. Schmieder, K. Sundgaard-Riise, B.D. Nunez, and C. Amodeo. 1987. Disparate cardiovascular findings in men and women with essential hypertension. *Ann Intern Med.* 107:158-161.
- Metzger, J.M., P.A. Wahr, D.E. Michele, F. Albayya, and M.V. Westfall. 1999. Effects of myosin heavy chain isoform switching on Ca²⁺-activated tension development in single adult cardiac myocytes. *Circulation research.* 84:1310-1317.
- Miller, V.M., D.M. Black, E.A. Brinton, M.J. Budoff, M.I. Cedars, H.N. Hodis, R.A. Lobo, J.E. Manson, G.R. Merriam, F. Naftolin, N. Santoro, H.S. Taylor, and S.M. Harman. 2009. Using basic science to design a clinical trial: baseline characteristics of women enrolled in the Kronos Early Estrogen Prevention Study (KEEPS). *J Cardiovasc Transl Res.* 2:228-239.
- Murphy, E. 2011. Estrogen signaling and cardiovascular disease. *Circulation research.* 109:687-696.
- Murphy, E., and C. Steenbergen. 2007. Gender-based differences in mechanisms of protection in myocardial ischemia-reperfusion injury. *Cardiovascular research.* 75:478-486.
- Najjar, S.S., S.P. Schulman, G. Gerstenblith, J.L. Fleg, D.A. Kass, F. O'Connor, L.C. Becker, and E.G. Lakatta. 2004. Age and gender affect ventricular-vascular coupling during aerobic exercise. *J Am Coll Cardiol.* 44:611-617.
- Nicholl, P.A., and S.E. Howlett. 2006. Sarcoplasmic reticulum calcium release channels in ventricles of older adult hamsters. *Can J Aging.* 25:107-113.
- Nikiforov, S.V., and V.B. Mamaev. 1998. The development of sex differences in cardiovascular disease mortality: a historical perspective. *Am J Public Health.* 88:1348-1353.

- Nordmeyer, J., S. Eder, S. Mahmoodzadeh, P. Martus, J. Fielitz, J. Bass, N. Bethke, H.R. Zurbrugg, R. Pregla, R. Hetzer, and V. Regitz-Zagrosek. 2004. Upregulation of myocardial estrogen receptors in human aortic stenosis. *Circulation*. 110:3270-3275.
- Okazaki, O., N. Suda, K. Hongo, M. Konishi, and S. Kurihara. 1990. Modulation of Ca²⁺ transients and contractile properties by beta-adrenoceptor stimulation in ferret ventricular muscles. *The Journal of physiology*. 423:221-240.
- Olivetti, G., G. Giordano, D. Corradi, M. Melissari, C. Lagrasta, S.R. Gambert, and P. Anversa. 1995. Gender differences and aging: effects on the human heart. *Journal of the American College of Cardiology*. 26:1068-1079.
- Olivetti, G., M. Melissari, J.M. Capasso, and P. Anversa. 1991. Cardiomyopathy of the aging human heart. Myocyte loss and reactive cellular hypertrophy. *Circulation research*. 68:1560-1568.
- Orchard, C.H., and E.G. Lakatta. 1985. Intracellular calcium transients and developed tension in rat heart muscle. A mechanism for the negative interval-strength relationship. *J Gen Physiol*. 86:637-651.
- Parker, W.H., V. Jacoby, D. Shoupe, and W. Rocca. 2009. Effect of bilateral oophorectomy on women's long-term health. *Womens Health (Lond Engl)*. 5:565-576.
- Patten, R.D., I. Pourati, M.J. Aronovitz, J. Baur, F. Celestin, X. Chen, A. Michael, S. Haq, S. Nuedling, C. Grohe, T. Force, M.E. Mendelsohn, and R.H. Karas. 2004. 17beta-estradiol reduces cardiomyocyte apoptosis in vivo and in vitro via activation of phospho-inositide-3 kinase/Akt signaling. *Circulation research*. 95:692-699.
- Patton, C., S. Thompson, and D. Epel. 2004. Some precautions in using chelators to buffer metals in biological solutions. *Cell Calcium*. 35:427-431.
- Pedram, A., M. Razandi, M. Aitkenhead, and E.R. Levin. 2005. Estrogen inhibits cardiomyocyte hypertrophy in vitro. Antagonism of calcineurin-related hypertrophy through induction of MCIP1. *J Biol Chem*. 280:26339-26348.
- Pedram, A., M. Razandi, D. Lubahn, J. Liu, M. Vannan, and E.R. Levin. 2008. Estrogen inhibits cardiac hypertrophy: role of estrogen receptor-beta to inhibit calcineurin. *Endocrinology*. 149:3361-3369.
- Peters, R.W., and M.R. Gold. 2004. The influence of gender on arrhythmias. *Cardiol Rev*. 12:97-105.

- Petre, R.E., M.P. Quaile, E.I. Rossman, S.J. Ratcliffe, B.A. Bailey, S.R. Houser, and K.B. Margulies. 2007. Sex-based differences in myocardial contractile reserve. *American journal of physiology. Regulatory, integrative and comparative physiology*. 292:R810-818.
- Pham, T.V., R.B. Robinson, P. Danilo, Jr., and M.R. Rosen. 2002. Effects of gonadal steroids on gender-related differences in transmural dispersion of L-type calcium current. *Cardiovascular research*. 53:752-762.
- Picht, E., A.V. Zima, L.A. Blatter, and D.M. Bers. 2007. SparkMaster: automated calcium spark analysis with ImageJ. *American journal of physiology. Cell physiology*. 293:C1073-1081.
- Pogwizd, S.M., R.H. Hoyt, J.E. Saffitz, P.B. Corr, J.L. Cox, and M.E. Cain. 1992. Reentrant and focal mechanisms underlying ventricular tachycardia in the human heart. *Circulation*. 86:1872-1887.
- Purohit, A., and M.J. Reed. 2002. Regulation of estrogen synthesis in postmenopausal women. *Steroids*. 67:979-983.
- Rautaharju, P.M., S.H. Zhou, S. Wong, H.P. Calhoun, G.S. Berenson, R. Prineas, and A. Davignon. 1992. Sex differences in the evolution of the electrocardiographic QT interval with age. *Can J Cardiol*. 8:690-695.
- Regitz-Zagrosek, V. 2006. Therapeutic implications of the gender-specific aspects of cardiovascular disease. *Nat Rev Drug Discov*. 5:425-438.
- Regitz-Zagrosek, V., S. Brokat, and C. Tschope. 2007. Role of gender in heart failure with normal left ventricular ejection fraction. *Prog Cardiovasc Dis*. 49:241-251.
- Ren, J., K.K. Hintz, Z.K. Routhead, J. Duan, P.B. Colligan, B.H. Ren, K.J. Lee, and H. Zeng. 2003. Impact of estrogen replacement on ventricular myocyte contractile function and protein kinase B/Akt activation. *American journal of physiology. Heart and circulatory physiology*. 284:H1800-1807.
- Revankar, C.M., D.F. Cimino, L.A. Sklar, J.B. Arterburn, and E.R. Prossnitz. 2005. A transmembrane intracellular estrogen receptor mediates rapid cell signaling. *Science*. 307:1625-1630.
- Rodriguez, P., and E.G. Kranias. 2005. Phospholamban: a key determinant of cardiac function and dysfunction. *Arch Mal Coeur Vaiss*. 98:1239-1243.
- Rossouw, J.E., G.L. Anderson, R.L. Prentice, A.Z. LaCroix, C. Kooperberg, M.L. Stefanick, R.D. Jackson, S.A. Beresford, B.V. Howard, K.C. Johnson, J.M. Kotchen, and J. Ockene. 2002. Risks and benefits of estrogen plus progestin in healthy postmenopausal women: principal results From the Women's Health Initiative randomized controlled trial. *JAMA*. 288:321-333.

- Rozenberg, S., B. Tavernier, B. Riou, B. Swynghedauw, C.L. Page, F. Boucher, J. Leiris, and S. Besse. 2006. Severe impairment of ventricular compliance accounts for advanced age-associated hemodynamic dysfunction in rats. *Exp Gerontol.* 41:289-295.
- Ruan, Q., and S.F. Nagueh. 2005. Effect of age on left ventricular systolic function in humans: a study of systolic isovolumic acceleration rate. *Exp Physiol.* 90:527-534.
- Saito, T., A. Ciobotaru, J.C. Bopassa, L. Toro, E. Stefani, and M. Eghbali. 2009. Estrogen contributes to gender differences in mouse ventricular repolarization. *Circulation research.* 105:343-352.
- Santana, L.F., H. Cheng, A.M. Gomez, M.B. Cannell, and W.J. Lederer. 1996. Relation between the sarcolemmal Ca²⁺ current and Ca²⁺ sparks and local control theories for cardiac excitation-contraction coupling. *Circulation research.* 78:166-171.
- Satoh, H., L.A. Blatter, and D.M. Bers. 1997. Effects of [Ca²⁺]_i, SR Ca²⁺ load, and rest on Ca²⁺ spark frequency in ventricular myocytes. *The American journal of physiology.* 272:H657-668.
- Schaible, T.F., and J. Scheuer. 1984. Comparison of heart function in male and female rats. *Basic Res Cardiol.* 79:402-412.
- Schairer, C., J. Lubin, R. Troisi, S. Sturgeon, L. Brinton, and R. Hoover. 2000. Menopausal estrogen and estrogen-progestin replacement therapy and breast cancer risk. *Jama.* 283:485-491.
- Schmidt, U., F. del Monte, M.I. Miyamoto, T. Matsui, J.K. Gwathmey, A. Rosenzweig, and R.J. Hajjar. 2000. Restoration of diastolic function in senescent rat hearts through adenoviral gene transfer of sarcoplasmic reticulum Ca(2+)-ATPase. *Circulation.* 101:790-796.
- Scriven, D.R., A. Klimek, K.L. Lee, and E.D. Moore. 2002. The molecular architecture of calcium microdomains in rat cardiomyocytes. *Ann N Y Acad Sci.* 976:488-499.
- Shlipak, M.G., B.G. Angeja, A.S. Go, P.D. Frederick, J.G. Canto, and D. Grady. 2001. Hormone therapy and in-hospital survival after myocardial infarction in postmenopausal women. *Circulation.* 104:2300-2304.
- Shutt, R.H., and S.E. Howlett. 2008. Hypothermia increases the gain of excitation-contraction coupling in guinea pig ventricular myocytes. *American journal of physiology. Cell physiology.* 295:C692-700.
- Simoncini, T., A. Hafezi-Moghadam, D.P. Brazil, K. Ley, W.W. Chin, and J.K. Liao. 2000. Interaction of oestrogen receptor with the regulatory subunit of phosphatidylinositol-3-OH kinase. *Nature.* 407:538-541.

- Simpson, E.R. 2003. Sources of estrogen and their importance. *J Steroid Biochem Mol Biol.* 86:225-230.
- Sipido, K.R. 1998. Efficiency of L-type Ca²⁺ current compared to reverse mode Na/Ca exchange or T-type Ca²⁺ current as trigger for Ca²⁺ release from the sarcoplasmic reticulum. *Ann N Y Acad Sci.* 853:357-360.
- Sipido, K.R. 2006. Calcium overload, spontaneous calcium release, and ventricular arrhythmias. *Heart Rhythm.* 3:977-979.
- Sjaastad, I., J.A. Wasserstrom, and O.M. Sejersted. 2003. Heart failure -- a challenge to our current concepts of excitation-contraction coupling. *The Journal of physiology.* 546:33-47.
- Skavdahl, M., C. Steenbergen, J. Clark, P. Myers, T. Demianenko, L. Mao, H.A. Rockman, K.S. Korach, and E. Murphy. 2005. Estrogen receptor-beta mediates male-female differences in the development of pressure overload hypertrophy. *American journal of physiology. Heart and circulatory physiology.* 288:H469-476.
- Spurgeon, H.A., W.H. duBell, M.D. Stern, S.J. Sollott, B.D. Ziman, H.S. Silverman, M.C. Capogrossi, A. Talo, and E.G. Lakatta. 1992. Cytosolic calcium and myofilaments in single rat cardiac myocytes achieve a dynamic equilibrium during twitch relaxation. *The Journal of physiology.* 447:83-102.
- Staessen, J., C.J. Bulpitt, R. Fagard, P. Lijnen, and A. Amery. 1989. The influence of menopause on blood pressure. *J Hum Hypertens.* 3:427-433.
- Statistics Canada. 2011. <http://www.statcan.gc.ca>. Vol. 2012.
- Stice, J.P., L. Chen, S.C. Kim, J.S. Jung, A.L. Tran, T.T. Liu, and A.A. Knowlton. 2011. 17beta-Estradiol, aging, inflammation, and the stress response in the female heart. *Endocrinology.* 152:1589-1598.
- Takagi, G., K. Asai, S.F. Vatner, R.K. Kudej, F. Rossi, A. Peppas, I. Takagi, R.R. Resuello, F. Natividad, Y.T. Shen, and D.E. Vatner. 2003. Gender differences on the effects of aging on cardiac and peripheral adrenergic stimulation in old conscious monkeys. *American journal of physiology. Heart and circulatory physiology.* 285:H527-534.
- Takahashi, A., P. Camacho, J.D. Lechleiter, and B. Herman. 1999. Measurement of intracellular calcium. *Physiol Rev.* 79:1089-1125.
- Teplitz, L., R. Iqic, M.L. Berbaum, and D.W. Schwertz. 2005. Sex differences in susceptibility to epinephrine-induced arrhythmias. *J Cardiovasc Pharmacol.* 46:548-555.

- Thawornkaiwong, A., J. Pantharanontaga, and J. Wattanapermpool. 2007. Hypersensitivity of myofilament response to Ca²⁺ in association with maladaptation of estrogen-deficient heart under diabetes complication. *Am J Physiol Regul Integr Comp Physiol.* 292:R844-851.
- Thompson, S.G., T.W. Meade, and G. Greenberg. 1989. The use of hormonal replacement therapy and the risk of stroke and myocardial infarction in women. *J Epidemiol Community Health.* 43:173-178.
- Trepanier-Boulay, V., C. St-Michel, A. Tremblay, and C. Fiset. 2001. Gender-based differences in cardiac repolarization in mouse ventricle. *Circ Res.* 89:437-444.
- Tsien, R.W., B.P. Bean, P. Hess, J.B. Lansman, B. Nilius, and M.C. Nowycky. 1986. Mechanisms of calcium channel modulation by beta-adrenergic agents and dihydropyridine calcium agonists. *Journal of molecular and cellular cardiology.* 18:691-710.
- Tsien, R.Y. 1981. A non-disruptive technique for loading calcium buffers and indicators into cells. *Nature.* 290:527-528.
- Tunwell, R.E., C. Wickenden, B.M. Bertrand, V.I. Shevchenko, M.B. Walsh, P.D. Allen, and F.A. Lai. 1996. The human cardiac muscle ryanodine receptor-calcium release channel: identification, primary structure and topological analysis. *Biochem J.* 318 (Pt 2):477-487.
- Umetani, K., D.H. Singer, R. McCraty, and M. Atkinson. 1998. Twenty-four hour time domain heart rate variability and heart rate: relations to age and gender over nine decades. *Journal of the American College of Cardiology.* 31:593-601.
- van Eickels, M., C. Grohe, J.P. Cleutjens, B.J. Janssen, H.J. Wellens, and P.A. Doevendans. 2001. 17beta-estradiol attenuates the development of pressure-overload hypertrophy. *Circulation.* 104:1419-1423.
- Vasan, R.S., M.G. Larson, D. Levy, J.C. Evans, and E.J. Benjamin. 1997. Distribution and categorization of echocardiographic measurements in relation to reference limits: the Framingham Heart Study: formulation of a height- and sex-specific classification and its prospective validation. *Circulation.* 96:1863-1873.
- Venetucci, L.A., A.W. Trafford, S.C. O'Neill, and D.A. Eisner. 2008. The sarcoplasmic reticulum and arrhythmogenic calcium release. *Cardiovasc Res.* 77:285-292.
- Vizgirda, V.M., G.M. Wahler, K.L. Sondgeroth, M.T. Ziolo, and D.W. Schwertz. 2002. Mechanisms of sex differences in rat cardiac myocyte response to beta-adrenergic stimulation. *American journal of physiology. Heart and circulatory physiology.* 282:H256-263.

- Volders, P.G., M.A. Vos, B. Szabo, K.R. Sipido, S.H. de Groot, A.P. Gorgels, H.J. Wellens, and R. Lazzara. 2000. Progress in the understanding of cardiac early afterdepolarizations and torsades de pointes: time to revise current concepts. *Cardiovascular research*. 46:376-392.
- Waldron, I. 1985. What do we know about causes of sex differences in mortality? A review of the literature. *Popul Bull UN*:59-76.
- Walker, K.E., E.G. Lakatta, and S.R. Houser. 1993. Age associated changes in membrane currents in rat ventricular myocytes. *Cardiovasc Res*. 27:1968-1977.
- Wallukat, G. 2002. The beta-adrenergic receptors. *Herz*. 27:683-690.
- Wang, S.Q., L.S. Song, E.G. Lakatta, and H. Cheng. 2001. Ca²⁺ signalling between single L-type Ca²⁺ channels and ryanodine receptors in heart cells. *Nature*. 410:592-596.
- Watters, J.J., J.S. Campbell, M.J. Cunningham, E.G. Krebs, and D.M. Dorsa. 1997. Rapid membrane effects of steroids in neuroblastoma cells: effects of estrogen on mitogen activated protein kinase signalling cascade and c-fos immediate early gene transcription. *Endocrinology*. 138:4030-4033.
- Wehrens, X.H., S.E. Lehnart, S.R. Reiken, and A.R. Marks. 2004. Ca²⁺/calmodulin-dependent protein kinase II phosphorylation regulates the cardiac ryanodine receptor. *Circulation research*. 94:e61-70.
- Wei, J.Y., H.A. Spurgeon, and E.G. Lakatta. 1984. Excitation-contraction in rat myocardium: alterations with adult aging. *Am J Physiol*. 246:H784-791.
- Wu, J.M., M.B. Zelinski, D.K. Ingram, and M.A. Ottinger. 2005. Ovarian aging and menopause: current theories, hypotheses, and research models. *Exp Biol Med (Maywood)*. 230:818-828.
- Wu, Q., Z. Zhao, H. Sun, Y.L. Hao, C.D. Yan, and S.L. Gu. 2008. Oestrogen changed cardiomyocyte contraction and beta-adrenoceptor expression in rat hearts subjected to ischaemia-reperfusion. *Exp Physiol*. 93:1034-1043.
- Xiao, L., L. Zhang, W. Han, Z. Wang, and S. Nattel. 2006. Sex-based transmural differences in cardiac repolarization and ionic-current properties in canine left ventricles. *American journal of physiology. Heart and circulatory physiology*. 291:H570-580.
- Xiao, R.P., X. Ji, and E.G. Lakatta. 1995. Functional coupling of the beta 2-adrenoceptor to a pertussis toxin-sensitive G protein in cardiac myocytes. *Mol Pharmacol*. 47:322-329.

- Xiao, R.P., and E.G. Lakatta. 1993. Beta 1-adrenoceptor stimulation and beta 2-adrenoceptor stimulation differ in their effects on contraction, cytosolic Ca²⁺, and Ca²⁺ current in single rat ventricular cells. *Circulation research*. 73:286-300.
- Xiao, R.P., H.A. Spurgeon, F. O'Connor, and E.G. Lakatta. 1994. Age-associated changes in beta-adrenergic modulation on rat cardiac excitation-contraction coupling. *J Clin Invest*. 94:2051-2059.
- Xu, A., and N. Narayanan. 1998. Effects of aging on sarcoplasmic reticulum Ca²⁺-cycling proteins and their phosphorylation in rat myocardium. *The American journal of physiology*. 275:H2087-2094.
- Yarnoz, M.J., and A.B. Curtis. 2008. More reasons why men and women are not the same (gender differences in electrophysiology and arrhythmias). *Am J Cardiol*. 101:1291-1296.
- Zalk, R., S.E. Lehnart, and A.R. Marks. 2007. Modulation of the ryanodine receptor and intracellular calcium. *Annu Rev Biochem*. 76:367-385.
- Zhang, X.P., S.F. Vatner, Y.T. Shen, F. Rossi, Y. Tian, A. Peppas, R.R. Resuello, F.F. Natividad, and D.E. Vatner. 2007. Increased apoptosis and myocyte enlargement with decreased cardiac mass; distinctive features of the aging male, but not female, monkey heart. *Journal of molecular and cellular cardiology*. 43:487-491.
- Zhu, X., B.A. Altschaf, R.J. Hajjar, H.H. Valdivia, and U. Schmidt. 2005. Altered Ca²⁺ sparks and gating properties of ryanodine receptors in aging cardiomyocytes. *Cell Calcium*. 37:583-591.

APPENDIX A: PUBLICATIONS

Portions of this thesis have been published as follows:

Publications

Fares E, Howlett SE. The impact of age on cardiac excitation-contraction coupling. *Clinical and Experimental Pharmacology and Physiology*, 37(1):1-7, January 2010.

Fares E, Parks RJ, MacDonald JK, Egar JM, Howlett SE. Ovariectomy increases the size of calcium sparks and enhances SR calcium release in isolated ventricular myocytes. *J Mol Cell Cardiol*, 52(1):32-42, January 2012.

Parks RJ, **Fares E**, MacDonald JK, Ernst MC, Sinal CJ, Rockwood KJ, Howlett SE. Deficit accumulation in aging mice: Frailty in an animal model of aging. *J Gerontol Biol Sci*, 67(3):217-27, March 2012.

Fares E, Pyle WG, Chen RP, Howlett SE. Long-term ovariectomy enhances intracellular calcium release but reduces myofilament calcium sensitivity in the aging mouse heart. *Am J Physiol Heart Circ Physiol*, submitted, 2012.

Abstracts

Fares E, Howlett SE. Impact of ovariectomy on cardiac contractile function in aged murine ventricular myocytes. *J Mol Cell Cardiol*, 2010.

Fares E, Pyle WG, Chen RP, Howlett SE. Long-term ovariectomy modifies intracellular calcium homeostasis in cardiomyocytes from aging female mice. *J Mol Cell Cardiol*, 2011.

Fares E, Parks RJ, MacDonald JK, Egar JM, Howlett SE. Ovariectomy increases the size of calcium sparks and enhances SR calcium release in ventricular myocytes from sexually-mature female mice. *J Mol Cell Cardiol*, 2011.

Parks RJ, **Fares E**, MacDonald JK, Ernst MC, Sinal CJ, Rockwood KJ, Howlett SE. Deficit accumulation in aging mice: Frailty in an animal model of aging. *Can J Ger*, 2011.

Fares E, Howlett SE. Contractile function declines in cardiomyocytes from male, but not female mice in extreme old age. *J Mol Cell Cardiol*, 2012.

APPENDIX B: COPYRIGHT PERMISSIONS

JOHN WILEY AND SONS LICENSE TERMS AND CONDITIONS

Aug 20, 2012

This is a License Agreement between Elias Fares ("You") and John Wiley and Sons ("John Wiley and Sons") provided by Copyright Clearance Center ("CCC"). The license consists of your order details, the terms and conditions provided by John Wiley and Sons, and the payment terms and conditions.

All payments must be made in full to CCC. For payment instructions, please see information listed at the bottom of this form.

License Number	2973250153747
License date	Aug 20, 2012
Licensed content publisher	John Wiley and Sons
Licensed content publication	Clinical and Experimental Pharmacology and Physiology
Licensed content title	Effect of age on cardiac excitation-contraction coupling
Licensed content author	Elias Fares,Susan E Howlett
Licensed content date	Aug 4, 2009
Start page	1
End page	7
Type of use	Dissertation/Thesis
Requestor type	Author of this Wiley article
Format	Print and electronic
Portion	Full article
Will you be translating?	No
Order reference number	
Total	0.00 USD

**OXFORD UNIVERSITY PRESS LICENSE
TERMS AND CONDITIONS**

Aug 20, 2012

This is a License Agreement between Elias Fares ("You") and Oxford University Press ("Oxford University Press") provided by Copyright Clearance Center ("CCC"). The license consists of your order details, the terms and conditions provided by Oxford University Press, and the payment terms and conditions.

All payments must be made in full to CCC. For payment instructions, please see information listed at the bottom of this form.

License Number	2973251212770
License date	Aug 20, 2012
Licensed content publisher	Oxford University Press
Licensed content publication	Journals of Gerontology - Series A: Biological Sciences and Medical Sciences
Licensed content title	A Procedure for Creating a Frailty Index Based on Deficit Accumulation in Aging Mice:
Licensed content author	Randi J. Parks, Elias Fares, Jennifer K. MacDonald, Matthew C. Ernst, Christopher J. Sinal, Kenneth Rockwood, Susan E. Howlett
Licensed content date	03/01/2012
Type of Use	Thesis/Dissertation
Institution name	
Title of your work	THE IMPACT OF AGING AND OVARECTOMY ON CARDIAC CONTRACTILE FUNCTION IN ISOLATED VENTRICULAR MYOCYTES
Publisher of your work	n/a
Expected publication date	Aug 2012
Permissions cost	0.00 USD
Value added tax	0.00 USD
Total	0.00 USD
Total	0.00 USD

**ELSEVIER LICENSE
TERMS AND CONDITIONS**

Aug 20, 2012

This is a License Agreement between Elias Fares ("You") and Elsevier ("Elsevier") provided by Copyright Clearance Center ("CCC"). The license consists of your order details, the terms and conditions provided by Elsevier, and the payment terms and conditions.

All payments must be made in full to CCC. For payment instructions, please see information listed at the bottom of this form.

Supplier	Elsevier Limited The Boulevard, Langford Lane Kidlington, Oxford, OX5 1GB, UK
Registered Company Number	1982084
Customer name	Elias Fares
Customer address	5850 College Street Halifax, NS B3H 1X5
License number	2973240946008
License date	Aug 20, 2012
Licensed content publisher	Elsevier
Licensed content publication	Journal of Molecular and Cellular Cardiology
Licensed content title	Ovariectomy enhances SR Ca ²⁺ release and increases Caspase-3 amplitudes in isolated ventricular myocytes
Licensed content author	Elias Fares, Randi J. Parks, Jennifer K. MacDonald, Jeanne M.S. Egar, Susan E. Howlett
Licensed content date	January 2012
Licensed content volume number	52
Licensed content issue number	1
Number of pages	11
Start Page	32
End Page	42
Type of Use	reuse in a thesis/dissertation
Portion	full article
Format	both print and electronic

Are you the author of this Elsevier article?	Yes
Will you be translating?	No
Order reference number	
Title of your thesis/dissertation	THE IMPACT OF AGING AND OVARIECTOMY ON CARDIAC CONTRACTILE FUNCTION IN ISOLATED VENTRICULAR MYOCYTES
Expected completion date	Aug 2012
Estimated size (number of pages)	205
Elsevier VAT number	GB 494 6272 12
Permissions price	0.00 USD
VAT/Local Sales Tax	0.0 USD / 0.0 GBP
Total	0.00 USD